Structural Causal Bandits under Markov Equivalence

Min Woo Park¹ Andy Arditi² Elias Bareinboim^{2*} Sanghack Lee^{1*}

¹Seoul National University ²Columbia University alsdn0110@snu.ac.kr ava2123@columbia.edu eb@cs.columbia.edu sanghack@snu.ac.kr

Abstract

In decision-making processes, an intelligent agent with causal knowledge can optimize action spaces to avoid unnecessary exploration. A *structural causal bandit* framework provides guidance on how to prune actions that are unable to maximize reward by leveraging prior knowledge of the underlying causal structure among actions. A key assumption of this framework is that the agent has access to a fully-specified causal diagram representing the target system. In this paper, we extend the structural causal bandits to scenarios where the agent leverages a Markov equivalence class. In such cases, the causal structure is provided to the agent in the form of a *partial ancestral graph* (PAG). We propose a generalized framework for identifying potentially optimal actions within this graph structure, thereby broadening the applicability of structural causal bandits.

1 Introduction

The multi-armed bandit (MAB) [Robbins, 1952, Lai and Robbins, 1985, Lattimore and Szepesvári, 2020] problem is a central topic in decision-making studies, where an agent aims to maximize cumulative rewards by repeatedly choosing actions based on observed reward, balancing the exploration-exploitation trade-off. Traditionally, MAB problems assume independence among the rewards of different arms, meaning that the reward obtained from one arm provides no information about the others, e.g., KL-UCB [Cappé et al., 2013] and Thompson sampling [Thompson, 1933]. Although this independence assumption simplifies the problem, it limits its applicability to real-world scenarios where dependencies among actions are common, e.g., in a movie recommendation system, a user's positive reaction to one genre may indicate a higher likelihood of a positive reaction to similar genres.

Recent research has increasingly recognized the importance of structured dependencies among arms and reward [Li et al., 2010, Abbasi-Yadkori et al., 2011, Cesa-Bianchi and Lugosi, 2012], leading to the development of structured bandits. Concurrently, the integration of causal inference into the MAB framework has opened new avenues for modeling and solving decision problems with richer dependency structures [Bareinboim et al., 2024]. Causal diagrams [Pearl, 1995] have been employed to represent causal relationships among actions, rewards, and other relevant factors. This approach enables agents to make informed decisions by considering how each action causally influences the reward through causal pathways. Existing studies [Bareinboim et al., 2015, Lattimore et al., 2016, Forney et al., 2017] have shown that causality-aware strategies can significantly outperform MAB algorithms that do not account for such underlying causal relationships. Subsequent work has explored various specialized settings by introducing additional structural assumptions, such as the availability of both observational and experimental distributions, or linear mechanisms [Zhang and Bareinboim, 2017, Lu et al., 2020, Bilodeau et al., 2022, Feng and Chen, 2023, Varici et al., 2023].

^{*}Corresponding authors

Specifically, Lee and Bareinboim [2018] formalized the *structural causal bandit* (SCM-MAB) without any parametric assumptions, where causal dependencies between arms are modeled using a structural causal model (SCM) [Pearl, 2000]. They proposed a sound and complete graphical characterization to identify *minimal intervention sets* (MISs) and *possibly-optimal minimal intervention sets* (POMISs), where the former includes only the variables that affect the reward, and the latter refers to actions that could be part of an optimal strategy among MISs, thereby guiding the agent to avoid unnecessary exploration without any actual interaction. Lee and Bareinboim [2019] extended this approach to accommodate scenarios involving non-manipulable variables among all the variables in the graph. Lee and Bareinboim [2020] and Everitt et al. [2021] established SCM-MAB with stochastic policies and Carey et al. [2024] studied the completeness of its graphical characterization.

While SCM-MAB has been established as a general framework, these studies assume that the decision-making agent has perfect access to the entire causal structure. From observational data, only a Markov equivalence class of the true causal diagram over observed variables can be inferred without making a substantial assumption about causal mechanisms such as causal sufficiency [Verma and Pearl, 1990, Spirtes et al., 2001b, Chickering, 2002, Tsamardinos et al., 2006] or a functional assumption [Perry et al., 2022, Peters et al., 2016, Ghassami et al., 2017, Heinze-Deml et al., 2018, Huang et al., 2020, Ghassami et al., 2018, Zeng et al., 2021]. A prominent representation of the equivalence class is known as partial ancestral graphs (PAGs), and any causal diagrams can be uniquely represented by a PAG [Richardson and Spirtes, 2002, Zhang, 2006, 2008a,b, Ali, 2005].

Motivation and Contributions. With observational data, we can only learn a PAG, which encodes a super-exponential number of maximal ancestral graphs (MAGs), each of which, in turn, represents an *infinite* number of causal diagrams over supersets of the observed variables. Therefore, considering all causal diagrams consistent with the PAG is computationally prohibitive. Identifying conditions for MIS and POMIS at the level of ancestral graphs *directly* would allow one to circumvent the issue. Our key contributions are as follows:

- We generalize MIS and develop its graphical criteria in ancestral graphs, enabling an agent to identify and exclude variables that have no effect on the reward (Sec. 3).
- We devise POMIS for ancestral graphs along with its graphical characterization, leading to an action space worth exploring (Secs. 4.1 and 4.2).
- We present an efficient algorithm to determine whether a given intervention set can be a POMIS in the Markov equivalence class represented by a PAG (Sec. 4.3).

Experiments in Sec. 5 and additional ones in Appendix D corroborate our findings. All omitted proofs are provided in Appendix H along with auxiliary results in Appendix G.

2 Preliminaries

We introduce notation and review relevant prior work. Following conventions, we use a capital letter, such as X, to represent a variable, with its corresponding lowercase letter, x, denoting a realization of the variable. Boldface is employed to represent a set of variables or values, denoted by \mathbf{X} or \mathbf{x} . The domain of X is indicated by \mathfrak{X}_X . We use calligraphic letters for graphs and models such as \mathcal{G} and \mathcal{S} .

Graphical notations. We consider a graph \mathcal{G} having vertices \mathbf{V} and edges \mathbf{E} composed of directed (\rightarrow) and bidirected edges (\leftrightarrow) . If there is an edge between two vertices X and Y in \mathcal{G} , we say that the two vertices are *adjacent* in \mathcal{G} , denoted by $Y \in \mathrm{Adj}(X)_{\mathcal{G}}$ or $X \in \mathrm{Adj}(Y)_{\mathcal{G}}$. An ordered sequence of distinct nodes in \mathcal{G} is called a *path* between X and Y in \mathcal{G} if (1) the start node is X and the end node is Y, and (2) there is an edge between any two subsequent variables in the sequence. If a path consists of directed edges with the same orientation, we say the path is *directed*. A variable Z is called a *collider* on the path if the path contains two edges having arrowheads toward Z. We define a path as a *collider path* if all non-endpoint vertices along the path are colliders. A path is *uncovered* (unshielded) if, for every consecutive triple on the path, its endpoints are not adjacent.

A path is *possibly directed* from X to Y if there is no arrowhead on the path pointing towards X. If there is a (possibly) directed path from X to Y, then Y is called a (possible) descendant of X, and X is a (possible) ancestor of Y. A variable Y is referred to as a possible child of X, and X is a possible parent of Y if they are adjacent and the edge is not directed into X. We denote the

ancestors, descendants, parents, and children of a given variable as An, De, Pa, and Ch, respectively. Ancestors and descendants include the variable itself. For a set of variables, we define the ancestral set as $\operatorname{An}(\mathbf{X})_{\mathcal{G}} = \bigcup_{X \in \mathbf{X}} \operatorname{An}(X)_{\mathcal{G}}$, and similarly for other relationships. We add the prefix Poss when referring to possible relationships, such as PossAn.

An *inducing path* relative to $\mathbf L$ is defined as a path where every vertex not in $\mathbf L$ is a collider on the path, and every collider is an ancestor of an endpoint of the path. A directed edge $X \to Y$ is *visible* if there exists no causal diagram in the corresponding equivalence class where there is an inducing path between X and Y that is into X. We refer to any edge that is not visible as *invisible*. The $\mathbf X$ -lower-manipulation of $\mathcal G$ deletes all edges that are visible and are out of variables in $\mathbf X$, and replaces all those edges that are out of variables in $\mathbf X$ but are invisible in $\mathcal G$ with bidirected edges denoted as $\mathcal G_{\mathbf X}$. The $\mathbf X$ -upper-manipulation of $\mathcal G$ deletes all those edges in $\mathcal G$ that are into variables in $\mathbf X$ denoted as $\mathcal G_{\mathbf X}$. We denote the set of variables in $\mathcal G$ by $\mathbf V(\mathcal G)$. A subgraph $\mathcal G[\mathbf V']$, where $\mathbf V' \subseteq \mathbf V(\mathcal G)$ is defined as a vertex-induced subgraph in which all edges among the vertices in $\mathbf V'$ are preserved. We define $\mathcal G \setminus \mathbf X$ as $\mathcal G[\mathbf V(\mathcal G) \setminus \mathbf X]$ for $\mathbf X \subseteq \mathbf V(\mathcal G)$.

Structural Causal Model. We use structural causal model (SCM) [Pearl, 2000] as the semantical framework to represent the underlying environment a decision-maker is deployed. An SCM $\mathcal S$ is a quadruple $\langle \mathbf U, \mathbf V, \mathbf F, P(\mathbf U) \rangle$, where $\mathbf U$ is a set of exogenous variables determined by factors outside the model following a joint distribution $P(\mathbf U)$, and $\mathbf V$ is a set of endogenous variables whose values are determined following a collection of functions $\mathbf F = \{f_i\}_{V_i \in \mathbf V}$ such that $V_i \leftarrow f_i(\mathbf p \mathbf a_i, \mathbf u_i)$ where $\mathbf P \mathbf A_i \subseteq \mathbf V \setminus \{V_i\}$ and $\mathbf U_i \subseteq \mathbf U$. The observational probability $P(\mathbf v)$ is defined as $\sum_{\mathbf u} \prod_{V_i \in \mathbf V} P(v_i \mid \mathbf p \mathbf a_i, \mathbf u_i) P(\mathbf u)$. Every SCM $\mathcal S$ is associated with a causal diagram $\mathcal G = \langle \mathbf V, \mathbf E \rangle$ where a directed edge $V_i \rightarrow V_j \in \mathbf E$ if $V_i \in \mathbf P \mathbf A_j$, and a bidirected edge between V_i and V_j if $\mathbf U_i$ and $\mathbf U_j$ are correlated. The probability of $\mathbf V = \mathbf v$ when $\mathbf X$ is intervened upon to take the value $\mathbf x$ is denoted by $P(\mathbf v \setminus \mathbf x \mid do(\mathbf x))$.

Ancestral graphical structures. Ancestral graphs are designed to capture graph structures without explicitly modeling latent variables. While directed edges between vertices in a causal diagram imply a direct causal effect between them, in ancestral graphs, directed edges instead represent ancestral relationships. Similar to the absence of directed cycles in causal diagrams, ancestral graphs do not permit *almost directed cycle*, which occurs when $X \leftrightarrow Y$ is present while X is an ancestor of Y.

A mixed graph is called a *maximal* ancestral graph (MAG) if (i) it does not contain any directed or almost directed cycles (i.e., ancestral); and (ii) there is no inducing path between any two non-adjacent vertices (i.e., maximal). In general, a MAG represents a set of causal diagrams with the same set of observed variables

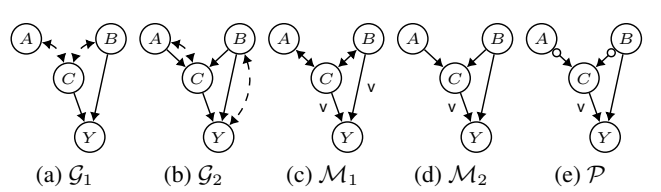


Figure 1: Causal diagrams (a, b) with corresponding (c, d) MAGs and (e) PAG. A visible edge is marked with v.

that entail the same conditional independence and ancestral relations among the observed variables. For each causal diagram, there exists a unique MAG over observed variables which represents its marginal independence relations, as well as its ancestral relations. However, a MAG is not fully testable with observational data since distinct MAGs can encode the same marginal independence relations. To illustrate, consider the causal diagrams \mathcal{G}_1 and \mathcal{G}_2 in Fig. 1. While they yield the same conditional independence relations, they correspond to distinct MAGs, \mathcal{M}_1 and \mathcal{M}_2 , respectively.

A graph is a partial mixed graph (PMG) if it contains three types of marks: tails (-), arrowheads (>), and circles (\circ) . A circle mark implies an uncertain mark that can be either an arrowhead or a tail. In addition, we use an asterisk (*) as a wildcard to denote any possible mark. In a PMG, if every edge mark on a path consists of circles, the path is called a *circle path*, and each edge is called a *circle edge* $(\circ -\circ)$. An edge is a *partially directed edge* $(\circ -)$ if it has both circle and arrowhead. A *circle component* is a subgraph of a PMG in which every edge is a circle edge. We use the ? mark to emphasize a wildcard that represents either a tail (-) or a circle (\circ) , but not an arrowhead (>). Furthermore, $[\mathcal{Q}]$ denotes the set of MAGs represented by the PMG \mathcal{Q} , and similarly $[\mathcal{M}]$ denotes the set of causal diagrams conforming to the MAG \mathcal{M} .

A partial ancestral graph (PAG) denoted by \mathcal{P} , is a PMG such that it represents a Markov equivalence class of MAGs. Every MAG \mathcal{M} represented by a PAG has the same skeleton as \mathcal{P} , and the non-circle marks in \mathcal{P} are identical to those in \mathcal{M} . Every circle in \mathcal{P} corresponds to a variant mark among the

represented MAGs. The PAG \mathcal{P} in Fig. 1e, for instance, encodes every MAG obtained by orienting circle marks incident to A and B as either > or —, including both \mathcal{M}_1 and \mathcal{M}_2 . In our work, we assume the absence of selection bias; therefore, there is no undirected edge in PAGs and MAGs. Moreover, we assume access to the *true* PAG that represents the target underlying system. We refer readers unfamiliar with ancestral graphs to Zhang [2006] and Jaber [2022].

Structural causal bandits. We follow the *structural causal bandit* (SCM-MAB) problem [Lee and Bareinboim, 2018], where an SCM models the target system with which an agent interacts, including a reward variable $Y \in \mathbf{V}$ where $\mathfrak{X}_Y \subseteq \mathbb{R}$. In the SCM-MAB setting, pulling each arm corresponds to intervening on a set of variables $\{\mathbf{x} \in \mathfrak{X}_\mathbf{X} \mid \mathbf{X} \subseteq \mathbf{V} \setminus \{Y\}\}$. The mean reward of an arm is denoted by $\mu_{\mathbf{x}} = \mathbb{E}[Y \mid do(\mathbf{x})]$ and the best expected reward by intervening on \mathbf{X} is $\mu_{\mathbf{x}^*} = \max_{\mathbf{x} \in \mathfrak{X}_\mathbf{X}} \mu_{\mathbf{x}}$. We denote μ^* as the optimal expected reward. The goal of the agent is to minimize the cumulative regret after N rounds, which is given by $\mathrm{Reg}_N = \sum_{\mathbf{x} \in \mathfrak{X}_\mathbf{X}, \mathbf{X} \subseteq \mathbf{V} \setminus \{Y\}} \Delta_{\mathbf{x}} \mathbb{E}[T_{\mathbf{x}}(N)]$ where $T_{\mathbf{x}}(N)$ denotes the number of times the arm \mathbf{x} was played after N rounds, $\Delta_{\mathbf{x}} = \mu^* - \mu_{\mathbf{x}}$ and $\mathfrak{X}_{\mathbf{X}} = \mathbf{X}_{X \in \mathbf{X}} \mathfrak{X}_X$.

MIS and POMIS. A minimal intervention set (MIS) ensures that there is no proper subset that is equivalent to the set with respect to the reward. Lee and Bareinboim [2018] demonstrated that \mathbf{X} is an MIS if and only if $\mathbf{X} \subseteq \operatorname{An}(Y)_{\mathcal{G}_{\overline{\mathbf{X}}}}$. For instance, consider \mathcal{G} in Fig. 2 where $\{A,B\}$ is an MIS since $\{A,B\}\subseteq \operatorname{An}(Y)_{\mathcal{G}_{\overline{\{A,B\}}}}$ holds. In contrast, $\{A,B,C\}$ is *not* an MIS since A is not an ancestor of Y in $\mathcal{G}_{\overline{\{A,B,C\}}}$, as depicted in Fig. 2c.

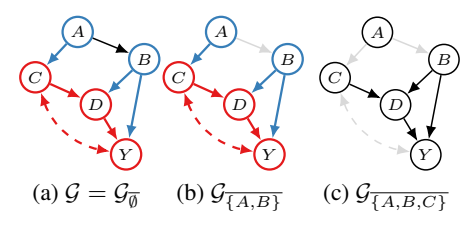


Figure 2: MUCT (red) and IB (blue).

A possibly-optimal minimal intervention set (POMIS) is an MIS such that intervening on any non-POMISs cannot yield a better outcome than the optimal one associated with the POMIS. Therefore, an agent who is aware of POMISs should only explore and exploit actions consistent with those sets. When given a causal diagram \mathcal{G} , minimal unobserved confounders' territory (MUCT) and interventional border (IB) [Lee and Bareinboim, 2018] provide a graphical characterization of POMIS. MUCT is the minimal set of variables that (i) contains the reward variable Y; and (ii) is closed under descendants and bidirected edge connections; and IB consists of the parents of MUCT, excluding MUCT itself. We defer the formal definitions to Appendix B. Intuitively, MUCT is the minimal closed mechanism that conveys all hidden information from unobserved confounders to the downstream reward, while IB consists of the nodes that directly affect this closed mechanism. Let us denote MUCT and IB with respect to $[\![\mathcal{G},Y]\!]$ as $\mathsf{MUCT}(\mathcal{G},Y)$ and $\mathsf{IB}(\mathcal{G},Y)$, respectively. Leveraging these, the authors showed that $\mathsf{IB}(\mathcal{G}_{\overline{X}},Y) = X$ provides a complete characterization of POMISs. For example, Figs. 2a and 2b show MUCT and IB for the subgraphs \mathcal{G}_\emptyset and $\mathcal{G}_{\overline{\{A,B\}}}$. The do-nothing action $(do(\emptyset))$ is not a POMIS since $\mathsf{MUCT}(\mathcal{G}_{\overline{\emptyset}},Y) = \{C,D,Y\}$ implies $\mathsf{IB}(\mathcal{G}_{\overline{\emptyset}},Y) = \{A,B\}$, not \emptyset , while the set $\{A,B\}$ is a POMIS since $\mathsf{MUCT}(\mathcal{G}_{\overline{\emptyset}},Y) = \{C,D,Y\}$, implying $\mathsf{IB}(\mathcal{G}_{\overline{\{A,B\}}},Y) = \{A,B\}$.

3 Generalizing Minimal Intervention Sets

We first generalize minimal intervention set (MIS) to cover not only causal diagrams but also ancestral graphs, aiming to identify all sets that do not include variables irrelevant to the reward by ruling them out, referring to MAGs or PAGs. In the following parts, we first provide complete graphical conditions for MIS in terms of MAGs and PAGs. Surprisingly, we then show in Sec. 3.1 that an MIS may include variables irrelevant to reward when dealing with PAGs. To address this issue, in Sec. 3.2, we propose the concept of *definitely* minimal intervention set (DMIS), which ensures that no further variables can be pruned, thereby aligning with the intuitive notion of minimality.

We use \mathcal{D} to refer to either a causal diagram or an ancestral graph (MAG or PAG) over \mathbf{V} . We denote by $\mathbf{x}[\mathbf{W}]$ the values of \mathbf{x} restricted to the subset of variables in $\mathbf{W} \cap \mathbf{X}$.

Definition 1 (Minimal intervention set (MIS)). Given information $[\![\mathcal{D},Y]\!]$, a set of variables $\mathbf{X}\subseteq\mathbf{V}\setminus\{Y\}$ is called a *minimal intervention set* (MIS) relative to $[\![\mathcal{D},Y]\!]$ if there is no $\mathbf{X}'\subsetneq\mathbf{X}$ such that $\mu_{\mathbf{x}[\mathbf{X}']}=\mu_{\mathbf{x}}$ for every SCM conforming to \mathcal{D} .

Proposition 1. Let \mathcal{M} be a MAG over \mathbf{V} . A set $\mathbf{X} \subseteq \mathbf{V} \setminus \{Y\}$ is an MIS relative to $[\![\mathcal{M},Y]\!]$ if and only if there exists a causal diagram \mathcal{G} conforming to \mathcal{M} such that \mathbf{X} is an MIS relative to $[\![\mathcal{G},Y]\!]$.

The proposition guarantees the existence of a causal diagram $\mathcal G$ where $\mathbf X$ is an MIS relative to $[\![\mathcal G,Y]\!]$, provided that $\mathbf X$ is an MIS relative to $[\![\mathcal M,Y]\!]$ for the given MAG $\mathcal M$. We now proceed to the graphical characterization of MIS for MAGs, in a manner similar to causal diagrams, utilizing the explicit ancestral relations among variables in MAGs and Rule 3 of do-calculus for MAGs, i.e., $\mu_{\mathbf x\mathbf z}=\mu_{\mathbf x}$ if $\mathbf Z$ and Y are m-separated in $\mathcal M_{\overline{\mathbf X}}$ [Zhang, 2008b].

Theorem 1 (Characterization of MIS for MAGs). Let \mathcal{M} be a MAG over \mathbf{V} . Given information $[\![\mathcal{M},Y]\!]$, a set $\mathbf{X} \subseteq \mathbf{V} \setminus \{Y\}$ is an MIS relative to $[\![\mathcal{M},Y]\!]$ if and only if $\mathbf{X} \subseteq \mathtt{An}(Y)_{\mathcal{M}_{\overline{\mathbf{V}}}}$ holds.

For example, consider \mathcal{G}' and \mathcal{M} in Figs. 3a and 3b where $\mathcal{G}' \in [\mathcal{M}]$. A set $\{A, B, C\}$ is an MIS relative to $[\![\mathcal{M}, Y]\!]$ since $\{A, B, C\} \subseteq \mathtt{An}(Y)_{\mathcal{M}_{\overline{\{A,B,C\}}}}$ holds.

Remark 1. Even though a set X is an MIS with respect to [M, Y], there is no guarantee that X is an MIS with respect to [G, Y] for every causal diagram G conforming to M.

The set $\{A, B, C\}$ is also an MIS relative to $[\mathcal{G}', Y]$ in Fig. 3a since $\{A, B, C\} \subseteq \operatorname{An}(Y)_{\mathcal{G}'_{\overline{\{A, B, C\}}}}$ holds. However, while \mathcal{G} in Fig. 2a is also represented by \mathcal{M} , it is *not* an MIS with respect to $[\mathcal{G}, Y]$.

3.1 MIS for PAGs and Its Possible Vacuousness

We proceed to the characterization of MIS for PAGs. Unfortunately, we cannot similarly rely on Rule 3 for PAGs (Jaber et al. [2022]; see Thm. 6 in Appendix B) because the rule is applied when ancestral relations are apparent for *all* represented models, whereas a PAG might involve uncertainty reflected by circle marks—one may easily surmise that $\{X, Z\}$ is not an MIS in a PAG $X \circ - \circ Z \circ - \circ Y$, but Rule 3 remains silent on this case.

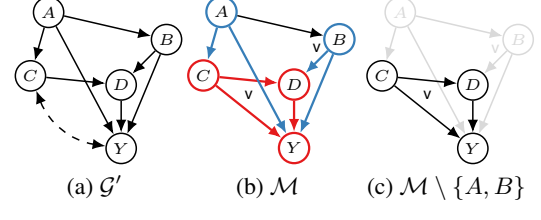


Figure 3: (a) Causal diagram; and (b) MAG representing both causal diagrams \mathcal{G}' and \mathcal{G} in Fig. 2a. (c) Induced graph of \mathcal{M} over $\mathbf{V} \setminus \{A, B\}$.

Hence, we utilize a specific type of path: A *proper* possibly-directed path from $X \in \mathbf{X}$ to Y with respect to \mathbf{X} , where only the first node X is in X

respect to X, where only the first node X is in X. This path is not disturbed by other intervening variables, thus aligning with the characterizations of MISs for causal diagrams and MAGs.

Proposition 2 (Graphical characterization of MIS for PAGs). *Let* \mathcal{P} *be a PAG over the set of variables* \mathbf{V} . A set $\mathbf{X} \subseteq \mathbf{V} \setminus \{Y\}$ is an MIS relative to $[\![\mathcal{P},Y]\!]$ if and only if, for every variable $X \in \mathbf{X}$, there exists a proper possibly-directed path from X to Y with respect to \mathbf{X} in \mathcal{P} .

Possible vacuousness. One might expect that if \mathbf{X} is an MIS relative to $[\![\mathcal{P},Y]\!]$, then it would also be an MIS relative to $[\![\mathcal{M},Y]\!]$ for *some* MAG \mathcal{M} conforming to the PAG \mathcal{P} . However, this is *not* always the case and no SCM may regard \mathbf{X} as an MIS with respect to $[\![\mathcal{M},Y]\!]$.

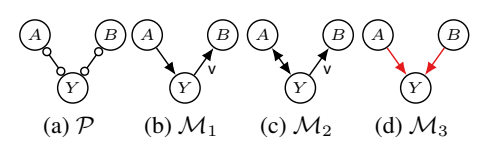


Figure 4: \mathcal{M}_1 and \mathcal{M}_2 are represented by \mathcal{P} . In contrast, \mathcal{M}_3 is not represented by \mathcal{P} .

ables are binary and $\forall_{U_V \in \{U_A, U_Y, U_B\}} P(U_V = 1) = \epsilon \approx 0$. For a proper subset $\mathbf{X}' = \{A\}$, we can construct an SCM \mathcal{S}_1 following that the mechanism for Y in \mathcal{S}_1 is defined as $f_Y = b \oplus u_Y$, and the mechanism for B is $f_B = u_B$ where B denotes the exclusive-or operator. Then, B is B is an Albarian equation of B is B is an Albarian equation of B is B is an Albarian equation of B. This construction can be done for each proper subset of A, which is an Albarian equation of A. However, the remarkable point here is that there is no representative SCM B that satisfies B is an Albarian equation of B is an Albarian equation of B is an Albarian equation of B in the underlying graph equation of B is an Albarian equation of B. This setup would introduce an uncovered collider at B (i.e., $A \to Y \leftarrow B$ and $A \notin Adj(B)$) in the underlying graph

²The inducing path $A \to C \leftrightarrow Y$ in \mathcal{G} appears as $A \to Y$ in \mathcal{M} since C is an ancestor of Y in \mathcal{G} .

of \mathcal{P} , leading to inconsistency with the structure of \mathcal{P} . Therefore, we observe that $\{A, B\}$ is an MIS with respect to $[\mathcal{P}, Y]$, but at least one of A or B is irrelevant to reward Y in all conforming MAGs.

3.2 Definitely MIS and Its Characterization

To address this vacuousness, we propose the concept of *definitely* MIS, which ensures that an MIS in a PAG remains an MIS in some consistent MAG. With the definition of MIS, we first choose $\mathbf{X}' \subseteq \mathbf{X}$, and then check whether $\mu_{\mathbf{x}[\mathbf{X}']} \neq \mu_{\mathbf{x}}$ holds across all SCMs conforming to \mathcal{D} ; here, we first choose an SCM \mathcal{S}^* conforming to \mathcal{D} , then examine whether the inequality holds across all subsets \mathbf{X}' .

Definition 2 (Definitely minimal intervention set). Given information $[\![\mathcal{D},Y]\!]$, a set $\mathbf{X} \subseteq \mathbf{V} \setminus \{Y\}$ is called a *definitely minimal intervention set* (DMIS) relative to $[\![\mathcal{D},Y]\!]$, denoted by $\mathbb{D}_{\mathcal{D},Y}$ if there exists an SCM compatible with \mathcal{D} such that, for every proper subset $\mathbf{X}' \subseteq \mathbf{X}$, $\mu_{\mathbf{x}[\mathbf{X}']} \neq \mu_{\mathbf{x}}$ holds.

Proposition 3. If **X** is a DMIS with respect to $[\![\mathcal{D},Y]\!]$, then **X** is an MIS with respect to $[\![\mathcal{D},Y]\!]$.

Proof. Let S^* be an SCM associated with \mathcal{D} such that $\mu_{\mathbf{x}[\mathbf{X}']} \neq \mu_{\mathbf{x}}$ holds for every $\mathbf{X}' \subsetneq \mathbf{X}$. For all proper subsets, such an S^* certifies that \mathbf{X} satisfies the definition of MIS.

Proposition 4. Let \mathcal{D} be either a causal diagram or a MAG (i.e., not a PAG). If \mathbf{X} is an MIS with respect to $[\![\mathcal{D},Y]\!]$, then \mathbf{X} is a DMIS with respect to $[\![\mathcal{D},Y]\!]$.

Proof sketch. We can construct an SCM \mathcal{S}^* where all mechanisms consist of the sum of the values of their parents, which ensures that **X** is a DMIS.

This equivalence between MIS and DMIS for a causal diagram or a MAG (Props. 3 and 4) is derived from *determined* ancestral relations, $\mathbf{X} \subseteq \mathrm{An}(Y)_{\mathcal{D}_{\overline{\mathbf{X}}}}$. We now move on to discuss DMIS for PAGs, where ancestral relations are *undetermined*, suggesting a notable gap between MIS and DMIS. Recall the PAG \mathcal{P} in Fig. 4a, where $\{A, B\}$ is an MIS but not a DMIS with respect to $[\mathcal{P}, Y]$.

Proposition 5. Let \mathcal{P} be a PAG over \mathbf{V} . A set $\mathbf{X} \subseteq \mathbf{V} \setminus \{Y\}$ is a DMIS relative to $[\mathcal{P}, Y]$ if and only if there exists a MAG \mathcal{M} conforming to \mathcal{P} such that \mathbf{X} is an MIS relative to $[\mathcal{M}, Y]$.

Hence, DMIS provides a *truly* feasible space for actions associated with intervention sets that no longer contain variables to rule out. According to Props. 3 and 4, we focus on establishing the graphical criterion for DMIS only for PAGs. In Fig. 4a, we have observed that $A \circ - \circ Y$ and $B \circ - \circ Y$ cannot both be an ancestor of Y at the same time due to the uncovered path $A \circ - \circ Y \circ - \circ B$. To this end, we devise the notion of *relevance* among edges in a PAG.

Definition 3 (Relevant edges). Let $\mathcal P$ be a PAG. For any edges $e_1(V_1*-*V_2)$ and $e_2(V_{n-1}*-*V_n)$, we say that e_1 is *relevant* to e_2 in $\mathcal P$ if there exists an uncovered path $V_1*-\circ V_2\circ-\circ\cdots\circ-\circ V_{n-1}\circ-*V_n$ with $n\geq 3$ in $\mathcal P$.

Theorem 2 (Graphical characterization of DMIS for PAGs). Let \mathcal{P} be a PAG over the set of variables \mathbf{V} . A set $\mathbf{X} \subseteq \mathbf{V} \setminus \{Y\}$ is a DMIS relative to $[\![\mathcal{P},Y]\!]$ if and only if, for any pair of vertices $X,Z \in \mathbf{X}$, there exist uncovered proper possibly-directed paths from X and Z to Y with respect to \mathbf{X} such that their starting edges are not relevant.

Consider the PAG \mathcal{P} shown in Fig. 5, where $A \circ \multimap C$ and $D \circ \multimap Y$ are relevant in \mathcal{P} because of the path $A \circ \multimap C \circ \multimap Y \circ \multimap D$. The key point here is that all triplets along the path are definite non-colliders so that the end nodes cannot be simultaneously ancestors of non-end nodes. Furthermore, consider any MAGs represented by \mathcal{P} where $A \circ \multimap C$ appears as a directed edge out of A (e.g., \mathcal{M}_1 and \mathcal{M}_2). Clearly, this results in $C \to Y \to D$, as the path is of definite status. In contrast, if any MAG contains $D \to Y$, this

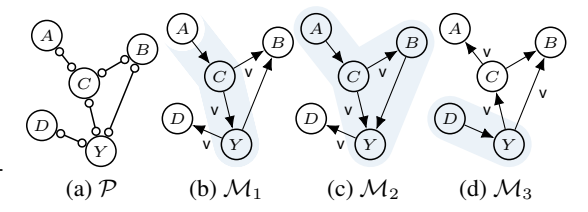


Figure 5: The nodes in the light blue region are the ancestors of Y. The three MAGs are represented by the PAG \mathcal{P} .

leads to $Y \to C \to A$, as in \mathcal{M}_3 . The important observation is that $A \to C$ ensures $D \notin \operatorname{An}(Y)_{\mathcal{M}_1}$, and $D \to Y$ ensures $A \notin \operatorname{An}(Y)_{\mathcal{M}}$ for all MAGs \mathcal{M} represented by \mathcal{P} . This indicates that A and D cannot simultaneously be ancestors of Y in \mathcal{M} , thus $\{A, D\}$ is not a DMIS relative to $[\mathcal{P}, Y]$.

4 Possibly Optimal Minimal Intervention Sets

We now refine the *possibly-optimal minimal intervention set* over DMISs rather than MISs. This refinement guarantees the existence of an underlying SCM compatible with a PAG and implies the following proposition. Note that the refined POMIS exactly matches established studies and serves as a natural extension, as supported by Props. 3 and 4, which state that MIS and DMIS coincide in causal diagrams and MAGs.

Definition 4 (Possibly-optimal minimal intervention set (POMIS)). Let $\mathbf{X} \subseteq \mathbf{V} \setminus \{Y\}$ be a DMIS relative to $[\![\mathcal{D},Y]\!]$. If there exists an SCM conforming to \mathcal{D} such that $\mu_{\mathbf{x}^*} > \forall_{\mathbf{W} \in \mathbb{D}_{\mathcal{D},Y} \setminus \{\mathbf{X}\}} \mu_{\mathbf{w}^*}$, then \mathbf{X} is a *possibly-optimal minimal intervention set* (POMIS) relative to $[\![\mathcal{D},Y]\!]$.

Proposition 6. Let \mathcal{P} be a PAG over \mathbf{V} . A set $\mathbf{X} \subseteq \mathbf{V} \setminus \{Y\}$ is a POMIS relative to $[\![\mathcal{P},Y]\!]$ if and only if there exists a MAG \mathcal{M} conforming to \mathcal{P} such that \mathbf{X} is a POMIS relative to $[\![\mathcal{M},Y]\!]$.

We investigate into the graphical characterization of POMISs for MAGs and PAGs. The main challenge in characterizing POMIS for ancestral graphs lies in the fact that induced paths by latent variables (or UCs) do not explicitly appear, which makes it impossible to directly identify the unobserved confounders' territory as for causal diagrams. Instead, we leverage edge's *visibility* which indicates that the edge is not confounded in any underlying causal diagram (Lem. 2 in Appendix B for details). To generalize the UC-territory, we introduce a *possible c-component*, which provides a necessary condition for nodes to belong to the same c-component in an underlying causal diagram.

Definition 5 (pc-component [Jaber et al., 2018]). Two nodes are in the same *possible c-component* (pc-component) if there is a path between them such that (i) all non-endpoint nodes along the path are colliders, and (ii) none of the edges are visible.

We denote the pc-component of a partial mixed graph (PMG) $\mathcal Q$ containing X as $\mathsf{PC}(X)_{\mathcal Q}$ and $\mathsf{PC}(X)_{\mathcal Q} \triangleq \bigcup_{X \in \mathbf X} \mathsf{PC}(X)_{\mathcal Q}$. For example, A and B are in the same pc-component in $\mathcal P$ of Fig. 1e because they are connected through an invisible colliding path $A \circ \to C \leftarrow B$, i.e., $\mathsf{PC}(A)_{\mathcal P} = \{A, B, C\}$. Furthermore, due to $A \notin \mathsf{PC}(Y)_{\mathcal P} = \{B, Y\}$, A and Y cannot belong to the same c-component in any causal diagrams conforming to $\mathcal P$. We now generalize MUCT and IB for PMGs.

Definition 6 (Unobserved-confounders' territory for PMGs). Given information $[\![\mathcal{Q},Y]\!]$ and intervention set $\mathbf{X} \subseteq \mathbf{V} \setminus \{Y\}$, let $\mathcal{H} = \mathcal{Q}[\mathsf{PossAn}(Y)_{\mathcal{Q}} \setminus \mathbf{X}]$. A set of variables $\mathbf{T} \subseteq \mathsf{PossAn}(Y)_{\mathcal{Q}} \setminus \mathbf{X}$ containing Y is called a *UC-territory* on \mathcal{Q} with respect to Y if $\mathsf{PossDe}(\mathbf{T})_{\mathcal{H}} = \mathbf{T}$ and $\mathsf{PC}(\mathbf{T})_{\mathcal{H}} = \mathbf{T}$. A UC-territory \mathbf{T} is called a *minimal* UC-territory (MUCT) if no $\mathbf{T}' \subseteq \mathbf{T}$ is a UC-territory.

Definition 7 (Interventional border for PMGs). Let **T** be a minimal UC-territory with respect to $[\![Q,Y,X]\!]$. Then $Pa(T)_Q \setminus T$ is called an *interventional border* (IB) with respect to $[\![Q,Y,X]\!]$.

For concreteness, consider \mathcal{M} and $\mathbf{X} = \{A, B\}$ in Fig. 3. Here, we omit Poss, as we discuss in the context of a MAG. Let \mathcal{H} be the induced graph $\mathcal{M}[\operatorname{An}(Y)_{\mathcal{M}} \setminus \mathbf{X}]$. In \mathcal{H} , the nodes C and Y are in the same pc-component, and D is a descendant of C. This implies that $\mathbf{T} = \{C, D, Y\}$ is the minimal closed set for $\operatorname{De}_{\mathcal{H}}$ and $\operatorname{PC}_{\mathcal{H}}$, leading to $\operatorname{IB}(\mathcal{M}, Y, \mathbf{X}) = \{A, B\}^3$, derived from $\operatorname{Pa}(\mathbf{T})_{\mathcal{M}} \setminus \mathbf{T}$.

4.1 Characterization of POMIS for MAGs

With the MUCT and IB for PMGs established, we are now ready to characterize POMISs for MAGs.

Theorem 3 (Graphical characterization of POMIS for MAGs). *Let* \mathcal{M} *be a MAG over the set of variable* \mathbf{V} . *A set* $\mathbf{X} \subseteq \mathbf{V} \setminus \{Y\}$ *is a POMIS relative to* $[\![\mathcal{M},Y]\!]$ *if and only if* $\mathbf{X} = \mathsf{IB}(\mathcal{M},Y,\mathbf{X})$.

For example, consider the MAG \mathcal{M} in Fig. 3c where IB $(\mathcal{M}, Y, \{A, B\}) = \{A, B\}$ holds. Therefore, we get that $\{A, B\}$ is a POMIS with respect to $[\![\mathcal{M}, Y]\!]$. Indeed, as previously shown, \mathcal{G} in Fig. 2 represented by \mathcal{M} and $\{A, B\}$ is a POMIS with respect to $[\![\mathcal{G}, Y]\!]$.

4.2 Characterization of POMIS for PAGs.

The remainder of the main body focuses on characterizing POMIS for PAGs. We first present necessary conditions for a PMG to represent MAGs \mathcal{M} in which \mathbf{X} is a POMIS relative to $[\![\mathcal{M},Y]\!]$.

³We denote MUCT and IB with respect to [Q, Y, X] as MUCT(Q, Y, X) and IB(Q, Y, X), respectively.

```
Algorithm 1: Identify whether a given set is a POMIS for PAG.
```

```
1 function IsPOMIS(\mathcal{P}, Y, \mathbf{X})
    Input: \mathcal{P}: PAG, Y: reward, \mathbf{X}: Intervention set
           if given X does not satisfy Thm. 2 then return False
           Let Q_{\mathbf{X}} be a PMG oriented from \mathcal{P} with \mathbf{X} according to Prop. 7.
           return sublsPOMIS(Q_X, X \cup \{Y\}, Y, X)
5 function sublsPOMIS(Q, A, Y, X)
           if A is empty then return \mathsf{IB}(\mathcal{Q}, Y, \mathbf{X}) = \mathbf{X}
           A \leftarrow \text{Pick a node from } \mathbf{A}.
          \begin{array}{l} \textbf{for each set } \mathbf{C}_A^{\mathcal{Q}} \subseteq \{V \in \mathtt{Adj}(A)_{\mathcal{Q}} \mid A \circ \!\!\!\!-\!\!\!\!+\!\!\!\!+ V\} \textbf{ do} \\ \textbf{ if } \mathbf{C}_A^{\mathcal{Q}} \text{ satisfies Thm. 7 (i.e., check validity of local transformation) and } \\ Y \in \mathtt{PossDe}(A)_{\mathcal{Q} \backslash \mathbf{C}_A^{\mathcal{Q}}} \textbf{ then} \end{array}
 8
                        Let Q' be the PMG obtained by orienting the circle marks around A following \mathbf{C}_{A}^{Q}
10
                          and completing the orientation rules from Q.
                        if sublsPOMIS(Q', A \setminus \{A\}, Y, X) then return True
11
12
           return False
```

Proposition 7. Let Q_X be a PMG representing MAGs where X is a POMIS with respect to Y. Then, the following properties hold in Q_X , for every $X \in X$:

- Every uncovered proper possibly-directed path from X to Y relative to X ends with an arrowhead (>).
- 2. If X is adjacent to Y, then the edge between X and Y is a directed edge $(X \to Y)$.

Put simply, violating these conditions introduces an almost directed cycle or directed cycle. To characterize POMIS for PAGs, we partition $[\mathcal{Q}_{\mathbf{X}}]$ based on the orientation of circle marks incident on $\mathbf{X} \cup \{Y\}$. We refer to a *local transformation* [Wang et al., 2023b] $\mathbf{C}_A^{\mathcal{Q}} \subseteq \{V \in \mathtt{Adj}(A)_{\mathcal{Q}} \mid A \circ -*V\}$ as the vertices whose edges with a circle at A (i.e., $A \circ -*V$ in \mathcal{Q}) will be oriented with arrowheads at A (i.e., $A \leftarrow *V$); all remaining edges $A \circ -*V'$ will be oriented as A -*V'.

Proposition 8. For every MAG $\mathcal{M} \in [\mathcal{Q}_{\mathbf{X}}]$, if \mathbf{X} is a POMIS relative to $[\![\mathcal{M}, Y]\!]$, then there exists a PMG $\mathcal{Q}_{\mathbf{X}}^i$ representing \mathcal{M} such that the following conditions are satisfied:

- 1. Every circle mark around $\mathbf{X} \cup \{Y\}$ in $\mathcal{Q}_{\mathbf{X}}$ is oriented as either a tail (-) or an arrowhead (>) in $\mathcal{Q}_{\mathbf{X}}^i$ according to valid local transformations⁴.
- 2. Every $X \in \mathbf{X}$ is an ancestor of Y in $\mathcal{Q}_{\mathbf{X}}^i$.
- 3. $Q_{\mathbf{X}}^{i}$ is closed under orientation rules.⁵

In words, $\mathcal{Q}_{\mathbf{X}}^{i}$ is a *more* oriented PMG instance derived from $\mathcal{Q}_{\mathbf{X}}$ by applying the valid local transformations for circle marks around $\mathbf{X} \cup \{Y\}$, along with the orientation rules, while confirming that \mathbf{X} is an ancestor of Y in all MAGs $\mathcal{M} \in [\mathcal{Q}_{\mathbf{X}}^{i}]$. For clarity, recall the PAG \mathcal{P} in Fig. 5a with a DMIS $\mathbf{X} = \{C\}$. Here, every MAG $\mathcal{M} \in [\mathcal{P}]$ satisfying that $\{C\}$ is a POMIS conforms to $\mathcal{Q}_{\{C\}}$ in Fig. 6a. Each $\mathcal{Q}_{\{C\}}^{1}$ (Fig. 6b; corresponding to $\mathbf{C}_{Y}^{\mathcal{Q}_{\{C\}}} = \{B\}$ and $\mathbf{C}_{C}^{\mathcal{Q}_{\{C\}}} = \{B\}$) and $\mathcal{Q}_{\{C\}}^{2}$ (Fig. 6c;

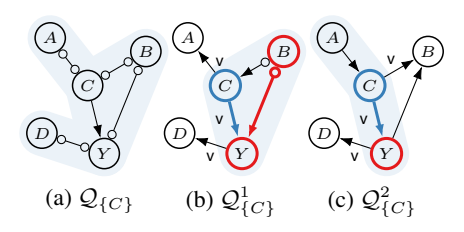


Figure 6: The light blue region indicates possible ancestors of Y.

corresponding to $\mathbf{C}_Y^{\mathcal{Q}_{\{C\}}} = \emptyset$ and $\mathbf{C}_C^{\mathcal{Q}_{\{C\}}} = \{A\}$) illustrates a PMG where local transformations for C and Y are oriented, and both graphs are closed under the orientation rules.

⁴For example, $\mathbf{C}_Y^{\mathcal{Q}_{\{C\}}} = \emptyset$ with $\mathbf{C}_C^{\mathcal{Q}_{\{C\}}} = \{B\}$ is invalid local transformation, as it implies $Y \to B \circ \to C \to Y$ which introduces either an directed or almost directed cycle. The complete graphical criterion of the validity of proposed by Wang et al. [2023b] is presented in Thm. 7 of Appendix B.

⁵The orientation rules refer to $\mathcal{R}_1 - \mathcal{R}_3$, \mathcal{R}_4' , $\mathcal{R}_8 - \mathcal{R}_{10}$ and \mathcal{R}_{SB} . $\mathcal{R}_5 - \mathcal{R}_7$ are not considered since we assume no selection bias. Further details regarding the orientation rules are provided in Appendix B.

Theorem 4 (Characterization of POMIS for PAGs). A set $X \subseteq V \setminus \{Y\}$ is a POMIS relative to $[\![P,Y]\!]$ if and only if there exists \mathcal{Q}_X^i satisfying Props. 7 and 8 such that $\mathsf{IB}(\mathcal{Q}_X^i,Y,X)=X$.

The key observation is that local transformations restricted to $\mathbf{X} \cup \{Y\}$ are sufficient for this determination, thereby circumventing the need to enumerate all MAGs represented by the given PAG. To witness, consider $\mathcal{Q}^1_{\{C\}}$ with $\mathbf{X} = \{C\}$ in Fig. 6b where $\mathsf{IB}(\mathcal{Q}^1_{\{C\}}, Y, \mathbf{X}) = \mathbf{X}$ holds, and it follows that $\{C\}$ is a POMIS with respect to $[\![\mathcal{P},Y]\!]$. Indeed, we can find a MAG instance \mathcal{M} by orienting the circle marks around B in $\mathcal{Q}^1_{\{C\}}$ as tails, in which $\mathsf{IB}(\mathcal{M},Y,\mathbf{X}) = \mathbf{X}$ (Thm. 3) also holds.

4.3 Algorithmic Approach: Enumerating POMISs

We now present an algorithm IsPOMIS (Alg. 1), through which we can determine whether a given set **X** is a POMIS relative to [P, Y] based on our theoretical results (Thms. 2 and 4).

Theorem 5 (Soundness and completeness). *The algorithm IsPOMIS* (Alg. 1) returns True if and only if there exists a MAG \mathcal{M} conforming to \mathcal{P} such that \mathbf{X} is a POMIS relative to $[\mathcal{M}, Y]$.

The algorithm begins by checking whether the given set X is a DMIS (Line 2). If X is identified as a DMIS, it then infuses the necessary condition in Prop. 7 (Line 3). Subsequently, the local transformations for $X \cup \{Y\}$ are oriented recursively within sublsPOMIS. During each recursion, it evaluates the validity of a local transformation around a vertex and the ancestral relations between the vertex and the reward Y (Line 9). The PMG is updated based on local transformations and orientation rules (Lines 10–11). Finally, in the base case (Line 6), the algorithm checks whether the fully-oriented PMG \mathcal{Q}_X^i satisfies $\mathsf{IB}(\mathcal{Q}_X^i, Y, X) = X$ based on Thm. 4.

Runtime analysis. In the algorithm, Line 2 runs in $\mathcal{O}(|\mathbf{V}|^5)$ time, using standard reachability algorithm. Each local transformation (Line 8) requires $\mathcal{O}(2^p)$ space, where $p < |\mathbf{V}|$ denotes the number of circle marks around the current vertex. Both the validation of local transformations and the check for ancestral relations (Line 9) take $\mathcal{O}(|\mathbf{V}|^3)$ [Wang et al., 2023b].

Identifying all POMIS sets requires checking all subsets of $V \setminus \{Y\}$ using IsPOMIS (Alg. 1), and thus the size of the search space grows exponentially. However, since all non-DMIS sets are filtered out in Line 2, the enumeration process effectively depends only on the number of DMISs⁶.

A naive approach is to enumerate all possible MAGs \mathcal{M} that conform to a given PAG, and verify whether $\mathsf{IB}(\mathcal{M},Y,\mathbf{X})=\mathbf{X}$ holds for each \mathcal{M} . However, this method presents analytical challenges in terms of complexity—the enumeration process may generate many duplicate MAGs, and it is difficult to determine when the transformation should terminate. Even under optimistic assumptions—namely, that no duplicate MAGs are produced and that an oracle informs us when all MAGs consistent with the PAG have been generated—the number of such MAGs remains super-exponentially large [Zhang, 2012, Wang et al., 2023a]. Even when adopting MAGLIST [Wang et al., 2024a], which systematically enumerates MAGs via local transformations, its worst-case complexity remains higher than ours, as it performs transformations over the entire set \mathbf{V} , whereas IsPOMIS constructs only distinct PMGs $\mathcal{Q}_{\mathbf{X}}^i$ oriented through local transformations around $\mathbf{X} \cup \{Y\} \subseteq \mathbf{V}$ for a DMIS \mathbf{X} .

5 Experiments

We evaluate the cumulative regrets (CR) of SCM-MAB under different strategies to assess the effect of employing POMIS for PAGs (Fig. 7). The number of trials is set to 10,000 for Tasks 1 and 2, and 5,000 for Task 3, which is sufficient to observe performance differences. Each simulation is repeated 1,000 times to obtain consistent results. We compare three arm-selection strategies: POMISs (pink), DMISs (purple), and Brute-force (BF; green), each combined with two prominent solvers: Thompson Sampling (TS) and KL-UCB. In the Brute-force strategy (i.e., without causal knowledge), all possible combinations of arms are evaluated; that is, the number of possible intervention sets of BF is $2^{|\mathbf{V}|-1}$ and the total number of corresponding arms is $\sum_{i=0}^{|\mathbf{V}|-1} {|\mathbf{V}|-1 \choose i} K^i = (K+1)^{|\mathbf{V}|-1}$ where K denotes the cardinality. We assume that all variables are binary for simplicity (K=2).

⁶Although Lee and Bareinboim [2018] provided an efficient algorithm for enumerating all POMISs in a causal diagram by leveraging a topological order, such an approach is *not* applicable to PAGs, where the topological order is not determined.

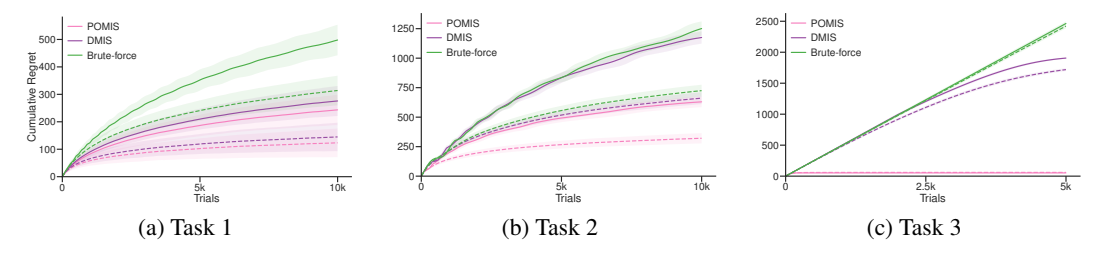


Figure 7: Cumulative regrets for the corresponding KL-UCB (solid) and TS (dashed) under distinct strategies. We plot the average cumulative regrets along with their standard deviations.

The underlying model mechanisms are randomly generated by combining binary logical operations, and the exogenous variables are set to follow Bernoulli distributions whose parameters are randomly selected over (0,1). Additional details and experiments are provided in Appendix D.

Task 1. The deployed agent can only access the PAG $\mathcal P$ in Fig. 5a to obtain DMISs and POMISs. The environment in which an agent interacts is consistent with $\mathcal P$. Using three strategies (BF: 81 arms, DMIS: 25 arms, POMIS: 19 arms), the POMIS-based TS and KL-UCB achieve CRs of 123.4 and 243.4, which correspond to $\mathbf{39.3}\%$ and $\mathbf{48.9}\%$, respectively, of CR for BF.

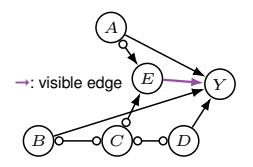


Figure 8: Six variables.

Task 2. We consider the PAG in Fig. 8 to validate our result. Using three strategies (BF: 243 arms, DMIS: 195 arms, POMIS: 85 arms), the POMIS-based TS and KL-UCB achieve CRs of 320.9 and 629.9, which correspond to 44.3% and 50.4%, respectively, of CR for BF.

Task 3. We consider a more involved scenario (Fig. 9) to validate our result. Using three strategies (BF: 19683 arms, DMIS: 2025 arms, POMIS: 54 arms), the POMIS-based TS and KL-UCB achieve CRs of 60.3 and 52.0, which correspond to only **2.5**% and **2.1**%, respectively, of CR for BF. Notably, the size of the POMIS arms accounts for only $\frac{54}{19683}$ =**0.27**% of that of the BF. We observe that the superiority of POMIS remains consistent regardless of the solvers used. All CRs and the numbers of sets and arms are provided in Tables 1 and 2 in Appendix D. These results demonstrate that refining arms by taking into account the Markov equivalence class represented by a PAG enhances the efficiency of agents.

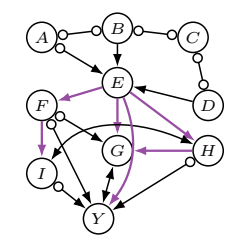


Figure 9: Ten variables.

6 Conclusion

We proposed a novel structured causal bandit strategy (SCM-MAB) in the context of ancestral graphs. We first provided a graphical characterization of MIS for MAGs and PAGs. We then demonstrated the *vacuousness* of MIS, i.e., that some MISs for a PAG are not MISs of any MAG consistent with that PAG. To address this, we introduced the notion of a *definitely* minimal intervention set (DMIS), which guarantees the existence of an underlying SCM, thereby aligning with the general intuition behind the concept of MIS. Finally, we refined the concept of POMIS over DMIS from MIS and provided a complete characterization of POMIS for MAGs and PAGs, along with an algorithm for enumerating all POMISs given a PAG. We believe these results have practical implications for the design of intelligent agents, providing a foundation for optimizing the action space when the environment is not fully accessible but is abstracted as a Markov equivalence class.

Acknowledgments and Disclosure of Funding

This work was supported in part by the NSF, ONR, AFOR, DOE, Amazon, JP Morgan, and The Alfred P. Sloan Foundation. Min Woo Park and Sanghack Lee were partly supported by the IITP (RS-2022-II220953/25%, RS-2025-02263754/25%) and NRF (RS-2023-00211904/25%, RS-2023-00222663/25%) grant funded by the Korean government.

References

- Yasin Abbasi-Yadkori, Dávid Pál, and Csaba Szepesvári. Improved algorithms for linear stochastic bandits. *Advances in neural information processing systems*, 24, 2011.
- Virginia Aglietti, Xiaoyu Lu, Andrei Paleyes, and Javier González. Causal bayesian optimization. In *International Conference on Artificial Intelligence and Statistics*, pages 3155–3164. PMLR, 2020.
- Shipra Agrawal and Navin Goyal. Analysis of thompson sampling for the multi-armed bandit problem. In *Conference on learning theory*, pages 39.1–39.26. JMLR Workshop and Conference Proceedings, 2012.
- R Ayesha Ali. Towards characterizing Markov equivalence classes for directed acyclic graph models with latent variables. In *Proc. Conf. on Uncertainty in Artificial Intelligence (UAI-05)*, pages 10–17, 2005.
- Bryan Andrews, Peter Spirtes, and Gregory F Cooper. On the completeness of causal discovery in the presence of latent confounding with tiered background knowledge. In *International Conference on Artificial Intelligence and Statistics*, pages 4002–4011. PMLR, 2020.
- Alexander Balke and Judea Pearl. Counterfactuals and policy analysis in structural models. In *Proceedings of the Eleventh conference on Uncertainty in artificial intelligence*, pages 11–18, 1995.
- Elias Bareinboim, Andrew Forney, and Judea Pearl. Bandits with unobserved confounders: A causal approach. In *Proceedings of the 28th Annual Conference on Neural Information Processing Systems*, pages 1342–1350, 2015.
- Elias Bareinboim, Sanghack Lee, and Junzhe Zhang. An introduction to causal reinforcement learning. Technical Report R-65, Causal Artificial Intelligence Lab, Columbia University, Dec 2024. URL https://causalai.net/r65.pdf.
- Alexis Bellot. Towards bounding causal effects under markov equivalence. In *The 40th Conference on Uncertainty in Artificial Intelligence*, 2024.
- Alexis Bellot and Silvia Chiappa. Towards estimating bounds on the effect of policies under unobserved confounding. Advances in Neural Information Processing Systems, 37:104556–104594, 2024.
- Shriya Bhatija, Paul-David Zuercher, Jakob Thumm, and Thomas Bohné. Multi-objective causal bayesian optimization. *arXiv preprint arXiv:2502.14755*, 2025.
- Blair Bilodeau, Linbo Wang, and Dan Roy. Adaptively exploiting d-separators with causal bandits. *Advances in Neural Information Processing Systems*, 35:20381–20392, 2022.
- Olivier Cappé, Aurélien Garivier, Odalric-Ambrym Maillard, Rémi Munos, and Gilles Stoltz. Kullback-leibler upper confidence bounds for optimal sequential allocation. *The Annals of Statistics*, pages 1516–1541, 2013.
- Ryan Carey, Sanghack Lee, and Robin J Evans. Toward a complete criterion for value of information in insoluble decision problems. *Transactions on Machine Learning Research*, 2024.
- Nicolo Cesa-Bianchi and Gábor Lugosi. Combinatorial bandits. *Journal of Computer and System Sciences*, 78(5):1404–1422, 2012.
- Olivier Chapelle and Lihong Li. An empirical evaluation of thompson sampling. *Advances in neural information processing systems*, 24, 2011.
- David Maxwell Chickering. Optimal structure identification with greedy search. *Journal of machine learning research*, 3(Nov):507–554, 2002.
- Davin Choo and Kirankumar Shiragur. Adaptivity complexity for causal graph discovery. In *Uncertainty in Artificial Intelligence*, pages 391–402. PMLR, 2023.

- Diego Colombo, Marloes H Maathuis, Markus Kalisch, and Thomas S Richardson. Learning high-dimensional directed acyclic graphs with latent and selection variables. *The Annals of Statistics*, pages 294–321, 2012.
- Arnoud De Kroon, Joris Mooij, and Danielle Belgrave. Causal bandits without prior knowledge using separating sets. In *Conference on Causal Learning and Reasoning*, pages 407–427. PMLR, 2022.
- Gabriel Andrew Dirac. On rigid circuit graphs. In *Abhandlungen aus dem Mathematischen Seminar der Universität Hamburg*, volume 25, pages 71–76. Springer, 1961.
- Wen-Bo Du, Tian Qin, Tian-Zuo Wang, and Zhi-Hua Zhou. Avoiding undesired future with minimal cost in non-stationary environments. *Advances in Neural Information Processing Systems*, 37: 135741–135769, 2024.
- Wen-Bo Du, Hao-Yi Lei, Lue Tao, Tian-Zuo Wang, and Zhi-Hua Zhou. Enabling optimal decisions in rehearsal learning under care condition. In *Forty-second International Conference on Machine Learning*, 2025.
- Muhammad Qasim Elahi, Mahsa Ghasemi, and Murat Kocaoglu. Partial structure discovery is sufficient for no-regret learning in causal bandits. *arXiv* preprint arXiv:2411.04054, 2024a.
- Muhammad Qasim Elahi, Lai Wei, Murat Kocaoglu, and Mahsa Ghasemi. Adaptive online experimental design for causal discovery. *arXiv preprint arXiv:2405.11548*, 2024b.
- Tom Everitt, Ryan Carey, Eric D Langlois, Pedro A Ortega, and Shane Legg. Agent incentives: A causal perspective. In *Proceedings of the AAAI Conference on Artificial Intelligence*, volume 35, pages 11487–11495, 2021.
- Shi Feng and Wei Chen. Combinatorial causal bandits. In *Proceedings of the AAAI Conference on Artificial Intelligence*, volume 37, pages 7550–7558, 2023.
- Shi Feng, Nuoya Xiong, and Wei Chen. Combinatorial causal bandits without graph skeleton. *arXiv* preprint arXiv:2301.13392, 2023.
- Andrew Forney, Judea Pearl, and Elias Bareinboim. Counterfactual data-fusion for online reinforcement learners. In Doina Precup and Yee Whye Teh, editors, *Proceedings of the 34th International Conference on Machine Learning*, volume 70 of *Proceedings of Machine Learning Research*, pages 1156–1164. PMLR, 06–11 Aug 2017. URL https://proceedings.mlr.press/v70/forney17a.html.
- Aurélien Garivier and Olivier Cappé. The kl-ucb algorithm for bounded stochastic bandits and beyond. In *Proceedings of the 24th annual conference on learning theory*, pages 359–376. JMLR Workshop and Conference Proceedings, 2011.
- AmirEmad Ghassami, Saber Salehkaleybar, Negar Kiyavash, and Kun Zhang. Learning causal structures using regression invariance. *Advances in Neural Information Processing Systems*, 30, 2017.
- AmirEmad Ghassami, Negar Kiyavash, Biwei Huang, and Kun Zhang. Multi-domain causal structure learning in linear systems. *Advances in neural information processing systems*, 31, 2018.
- Martin Charles Golumbic. Algorithmic graph theory and perfect graphs. Elsevier, 2004.
- Kristjan Greenewald, Dmitriy Katz, Karthikeyan Shanmugam, Sara Magliacane, Murat Kocaoglu, Enric Boix Adsera, and Guy Bresler. Sample efficient active learning of causal trees. *Advances in Neural Information Processing Systems*, 32, 2019.
- Michel Habib, Ross Mac Connell, Christophe Paul, and Laurent Viennot. Lex-bfs a partition refining technique, application to transitive orientation and consecutive 1's testing. *Theoretical Computer Science*, 234, 2000.
- Alain Hauser and Peter Bühlmann. Characterization and greedy learning of interventional markov equivalence classes of directed acyclic graphs. *The Journal of Machine Learning Research*, 13(1): 2409–2464, 2012.

- Christina Heinze-Deml, Jonas Peters, and Nicolai Meinshausen. Invariant causal prediction for nonlinear models. *Journal of Causal Inference*, 6(2), 2018.
- Biwei Huang, Kun Zhang, Jiji Zhang, Joseph Ramsey, Ruben Sanchez-Romero, Clark Glymour, and Bernhard Schölkopf. Causal discovery from heterogeneous/nonstationary data. *Journal of Machine Learning Research*, 21(89):1–53, 2020.
- Inwoo Hwang, Yunhyeok Kwak, Suhyung Choi, Byoung-Tak Zhang, and Sanghack Lee. Fine-grained causal dynamics learning with quantization for improving robustness in reinforcement learning. In *International Conference on Machine Learning*, pages 20842–20870. PMLR, 2024.
- Amin Jaber. Causal Reasoning in Equivalence Classes. PhD thesis, Purdue University Graduate School, 2022.
- Amin Jaber, Jiji Zhang, and Elias Bareinboim. Causal identification under Markov equivalence. In *Proceedings of the 34th Conference on Uncertainty in Artificial Intelligence*, 2018.
- Amin Jaber, Adele Ribeiro, Jiji Zhang, and Elias Bareinboim. Causal identification under Markov equivalence: calculus, algorithm, and completeness. *Advances in Neural Information Processing Systems*, 35:3679–3690, 2022.
- Yonghan Jung and Alexis Bellot. Efficient policy evaluation across multiple different experimental datasets. *Advances in Neural Information Processing Systems*, 37:136361–136392, 2024.
- Yonghan Jung, Min Woo Park, and Sanghack Lee. Complete graphical criterion for sequential covariate adjustment in causal inference. *Advances in Neural Information Processing Systems*, 37: 19813–19838, 2024.
- Emilie Kaufmann, Nathaniel Korda, and Rémi Munos. Thompson sampling: An asymptotically optimal finite-time analysis. In *International conference on algorithmic learning theory*, pages 199–213. Springer, 2012.
- Murat Kocaoglu, Karthikeyan Shanmugam, and Elias Bareinboim. Experimental design for learning causal graphs with latent variables. *Advances in Neural Information Processing Systems*, 30, 2017.
- Mikhail Konobeev, Jalal Etesami, and Negar Kiyavash. Causal bandits without graph learning. *arXiv* preprint arXiv:2301.11401, 2023.
- Tze Leung Lai and Herbert Robbins. Asymptotically efficient adaptive allocation rules. *Advances in applied mathematics*, 6(1):4–22, 1985.
- Finnian Lattimore, Tor Lattimore, and Mark D Reid. Causal bandits: Learning good interventions via causal inference. *Advances in neural information processing systems*, 29, 2016.
- Tor Lattimore and Csaba Szepesvári. Bandit algorithms. Cambridge University Press, 2020.
- Sanghack Lee and Elias Bareinboim. Structural causal bandits: Where to intervene? *Advances in neural information processing systems*, 31, 2018.
- Sanghack Lee and Elias Bareinboim. Structural causal bandits with non-manipulable variables. In *Proceedings of the AAAI Conference on Artificial Intelligence*, pages 4164–4172, 2019.
- Sanghack Lee and Elias Bareinboim. Characterizing optimal mixed policies: Where to intervene and what to observe. *Advances in neural information processing systems*, 33:8565–8576, 2020.
- Lihong Li, Wei Chu, John Langford, and Robert E Schapire. A contextual-bandit approach to personalized news article recommendation. In *Proceedings of the 19th international conference on World wide web*, pages 661–670, 2010.
- Yangyi Lu, Amirhossein Meisami, Ambuj Tewari, and William Yan. Regret analysis of bandit problems with causal background knowledge. In *Conference on Uncertainty in Artificial Intelligence*, pages 141–150. PMLR, 2020.
- Yangyi Lu, Amirhossein Meisami, and Ambuj Tewari. Causal bandits with unknown graph structure. *Advances in Neural Information Processing Systems*, 34:24817–24828, 2021.

- Marloes H Maathuis and Diego Colombo. A generalized back-door criterion. *The Annals of Statistics*, 43(3):1060–1088, 2015.
- Marloes H Maathuis, Markus Kalisch, and Peter Bühlmann. Estimating high-dimensional intervention effects from observational data. *The Annals of Statistics*, pages 3133–3164, 2009.
- Alan Malek, Virginia Aglietti, and Silvia Chiappa. Additive causal bandits with unknown graph. In *International Conference on Machine Learning*, pages 23574–23589. PMLR, 2023.
- Judea Pearl. Causal diagrams for empirical research. Biometrika, 82(4):669-710, 1995.
- Judea Pearl. Causality: Models, Reasoning, and Inference. Cambridge University Press, New York, 2000. 2nd edition, 2009.
- Judea Pearl and James Robins. Probabilistic evaluation of sequential plans from causal models with hidden variables. In *Proceedings of the Eleventh conference on Uncertainty in artificial intelligence*, pages 444–453, 1995a.
- Judea Pearl and James Robins. Probabilistic evaluation of sequential plans from causal models with hidden variables. In *Proceedings of the 11th Conference on Uncertainty in Artificial Intelligence*, pages 444–453. Morgan Kaufmann Publishers Inc., 1995b.
- Emilija Perkovic, Johannes Textor, Markus Kalisch, Marloes H Maathuis, et al. Complete graphical characterization and construction of adjustment sets in Markov equivalence classes of ancestral graphs. *Journal of Machine Learning Research*, 18(220):1–62, 2018.
- Ronan Perry, Julius Von Kügelgen, and Bernhard Schölkopf. Causal discovery in heterogeneous environments under the sparse mechanism shift hypothesis. *Advances in Neural Information Processing Systems*, 35:10904–10917, 2022.
- Jonas Peters, Peter Bühlmann, and Nicolai Meinshausen. Causal inference by using invariant prediction: identification and confidence intervals. *Journal of the Royal Statistical Society: Series B (Statistical Methodology)*, 78(5):947–1012, 2016.
- Tian Qin, Tian-Zuo Wang, and Zhi-Hua Zhou. Rehearsal learning for avoiding undesired future. *Advances in Neural Information Processing Systems*, 36:80517–80542, 2023.
- Tian Qin, Tian-Zuo Wang, and Zhi-Hua Zhou. Gradient-based nonlinear rehearsal learning with multivariate alterations. In *Proceedings of the AAAI Conference on Artificial Intelligence*, volume 39, pages 26859–26867, 2025.
- Amy Richardson, Michael G Hudgens, Peter B Gilbert, and Jason P Fine. Nonparametric bounds and sensitivity analysis of treatment effects. *Statistical Science*, pages 596–618, 2014.
- Thomas Richardson and Peter Spirtes. Ancestral graph Markov models. *The Annals of Statistics*, 30 (4):962–1030, 2002.
- Herbert Robbins. Some aspects of the sequential design of experiments. *Bull. Amer. Math. Soc.*, 58 (5):527–535, 1952.
- Raanan Y Rohekar, Shami Nisimov, Yaniv Gurwicz, and Gal Novik. Iterative causal discovery in the possible presence of latent confounders and selection bias. *Advances in Neural Information Processing Systems*, 34:2454–2465, 2021.
- Raanan Yehezkel Rohekar, Shami Nisimov, Yaniv Gurwicz, and Gal Novik. From temporal to contemporaneous iterative causal discovery in the presence of latent confounders. In *International Conference on Machine Learning*, pages 39939–39950. PMLR, 2023.
- Donald J Rose, R Endre Tarjan, and George S Lueker. Algorithmic aspects of vertex elimination on graphs. *SIAM Journal on computing*, 5(2):266–283, 1976.

- Peter Spirtes and Thomas S. Richardson. A polynomial time algorithm for determining dag equivalence in the presence of latent variables and selection bias. In David Madigan and Padhraic Smyth, editors, *Proceedings of the Sixth International Workshop on Artificial Intelligence and Statistics*, volume R1 of *Proceedings of Machine Learning Research*, pages 489–500. PMLR, 04–07 Jan 1997. URL https://proceedings.mlr.press/r1/spirtes97b.html. Reissued by PMLR on 30 March 2021.
- Peter Spirtes, Clark Glymour, and Richard Scheines. *Causation, prediction, and search*. MIT press, 2001a.
- Peter Spirtes, Clark N Glymour, and Richard Scheines. Causation, Prediction, and Search. MIT Press, 2nd edition, 2001b. ISBN 9780262194402.
- Chandler Squires, Sara Magliacane, Kristjan Greenewald, Dmitriy Katz, Murat Kocaoglu, and Karthikeyan Shanmugam. Active structure learning of causal dags via directed clique trees. *Advances in Neural Information Processing Systems*, 33:21500–21511, 2020.
- Lue Tao, Tian-Zuo Wang, Yuan Jiang, and Zhi-Hua Zhou. Avoiding undesired future with sequential decisions. pages 6245–6253, 09 2025. doi: 10.24963/ijcai.2025/695.
- William R Thompson. On the likelihood that one unknown probability exceeds another in view of the evidence of two samples. *Biometrika*, 25(3-4):285–294, 1933.
- Jin Tian and Judea Pearl. A general identification condition for causal effects. In *Proceedings of the 18th National Conference on Artificial Intelligence*, pages 567–573, 2002.
- Ioannis Tsamardinos, Laura E Brown, and Constantin F Aliferis. The max-min hill-climbing bayesian network structure learning algorithm. *Machine learning*, 65:31–78, 2006.
- Burak Varici, Karthikeyan Shanmugam, Prasanna Sattigeri, and Ali Tajer. Causal bandits for linear structural equation models. *Journal of Machine Learning Research*, 24(297):1–59, 2023.
- Aparajithan Venkateswaran and Emilija Perković. Towards complete causal explanation with expert knowledge. *arXiv preprint arXiv:2407.07338*, 2024.
- Thomas Verma and Judea Pearl. Equivalence and synthesis of causal models. In *Proceedings of the Sixth Annual Conference on Uncertainty in Artificial Intelligence*, pages 255–270, 1990.
- Tian-Zuo Wang, Tian Qin, and Zhi-Hua Zhou. Sound and complete causal identification with latent variables given local background knowledge. *Advances in Neural Information Processing Systems*, 35:10325–10338, 2022.
- Tian-Zuo Wang, Tian Qin, and Zhi-Hua Zhou. Estimating possible causal effects with latent variables via adjustment. In Andreas Krause, Emma Brunskill, Kyunghyun Cho, Barbara Engelhardt, Sivan Sabato, and Jonathan Scarlett, editors, *Proceedings of the 40th International Conference on Machine Learning*, volume 202 of *Proceedings of Machine Learning Research*, pages 36308–36335. PMLR, 23–29 Jul 2023a. URL https://proceedings.mlr.press/v202/wang23ag.html.
- Tian-Zuo Wang, Tian Qin, and Zhi-Hua Zhou. Sound and complete causal identification with latent variables given local background knowledge. *Artificial Intelligence*, 322:103964, 2023b.
- Tian-Zuo Wang, Wen-Bo Du, and Zhi-Hua Zhou. An efficient maximal ancestral graph listing algorithm. In *Forty-first International Conference on Machine Learning*, 2024a.
- Tian-Zuo Wang, Lue Tao, and Zhi-Hua Zhou. New rules for causal identification with background knowledge, 2024b. URL https://arxiv.org/abs/2407.15259.
- Tian-Zuo Wang, Wen-Bo Du, and Zhi-Hua Zhou. Polynomial-delay mag listing with novel locally complete orientation rules. In *Forty-second International Conference on Machine Learning*, 2025a.
- Tian-Zuo Wang, Lue Tao, Tian Qin, and Zhi-Hua Zhou. Estimating possible causal effects with latent variables via adjustment and novel rule orientation. *Artificial Intelligence*, page 104387, 2025b.

- Lai Wei, Muhammad Qasim Elahi, Mahsa Ghasemi, and Murat Kocaoglu. Approximate allocation matching for structural causal bandits with unobserved confounders. *Advances in Neural Information Processing Systems*, 36:68810–68832, 2023.
- Marcel Wienöbst, Max Bannach, and Maciej Liśkiewicz. A new constructive criterion for Markov equivalence of MAGs. In *Proceedings of the Thirty-Eighth Conference on Uncertainty in Artificial Intelligence*, volume 180 of *Proceedings of Machine Learning Research*, pages 2107–2116. PMLR, 2022. URL https://proceedings.mlr.press/v180/wienobst22a.html.
- Zirui Yan and Ali Tajer. Linear causal bandits: Unknown graph and soft interventions. *Advances in Neural Information Processing Systems*, 37:23939–23987, 2024.
- Yan Zeng, Shohei Shimizu, Ruichu Cai, Feng Xie, Michio Yamamoto, and Zhifeng Hao. Causal discovery with multi-domain lingam for latent factors. In *Causal Analysis Workshop Series*, pages 1–4. PMLR, 2021.
- Jiji Zhang. Causal inference and reasoning in causally insufficient systems. PhD thesis, Citeseer, 2006.
- Jiji Zhang. On the completeness of orientation rules for causal discovery in the presence of latent confounders and selection bias. *Artificial Intelligence*, 172(16):1873–1896, 2008a. ISSN 0004-3702. doi: https://doi.org/10.1016/j.artint.2008.08.001. URL https://www.sciencedirect.com/science/article/pii/S0004370208001008.
- Jiji Zhang. Causal reasoning with ancestral graphs. *Journal of Machine Learning Research*, 9: 1437–1474, 2008b.
- Jiji Zhang. A characterization of markov equivalence classes for directed acyclic graphs with latent variables. *arXiv preprint arXiv:1206.5282*, 2012.
- Junzhe Zhang and Elias Bareinboim. Transfer learning in multi-armed bandit: a causal approach. In *Proceedings of the 16th Conference on Autonomous Agents and MultiAgent Systems*, pages 1778–1780, 2017.
- Junzhe Zhang and Elias Bareinboim. Designing optimal dynamic treatment regimes: A causal reinforcement learning approach. In *International conference on machine learning*, pages 11012–11022. PMLR, 2020.
- Junzhe Zhang and Elias Bareinboim. Bounding causal effects on continuous outcome. In *Proceedings of the AAAI Conference on Artificial Intelligence*, volume 35, pages 12207–12215, 2021.
- Junzhe Zhang and Elias Bareinboim. Online reinforcement learning for mixed policy scopes. *Advances in Neural Information Processing Systems*, 35:3191–3202, 2022.
- Junzhe Zhang, Jin Tian, and Elias Bareinboim. Partial counterfactual identification from observational and experimental data. In *International conference on machine learning*, pages 26548–26558. PMLR, 2022.
- Hui Zhao, Zhongguo Zheng, and Baijun Liu. On the Markov equivalence of maximal ancestral graphs. *Science in China Series A: Mathematics*, 48:548–562, 2005.
- Zihan Zhou, Muhammad Qasim Elahi, and Murat Kocaoglu. Characterization and learning of causal graphs from hard interventions. *arXiv preprint arXiv:2505.01037*, 2025.

Contents

1	Introduction						
2	Preliminaries	2					
3	Generalizing Minimal Intervention Sets						
	3.1 MIS for PAGs and Its Possible Vacuousness	5					
	3.2 Definitely MIS and Its Characterization	6					
4	Possibly Optimal Minimal Intervention Sets	7					
	4.1 Characterization of POMIS for MAGs	7					
	4.2 Characterization of POMIS for PAGs	7					
	4.3 Algorithmic Approach: Enumerating POMISs	9					
5	Experiments	9					
6	Conclusion	10					
A	Related Works	18					
В	Additional Preliminaries and Background Results						
	B.1 Additional Preliminaries	19					
	B.2 Background Results	23					
	B.2.1 Background Results in Zhang [2006, 2008a]	23					
	B.2.2 Background Results in Maathuis and Colombo [2015]	24					
	B.2.3 Background Results in Perkovic et al. [2018]	24					
	B.2.4 Background Results in Jaber et al. [2018, 2022]	24					
	B.2.5 Background Results in Wang et al. [2023b, 2024a]	25					
C	Assumptions	26					
D	Experimental Details and Additional Results	26					
E	Discussions	29					
	E.1 Partial Mixed Graphs Obtained from Local Transformation	29					
	E.2 Adaptive Learning: Simultaneous Discovery and Regret Minimization	30					
	E.3 Comparison with Elahi et al. [2024a]	30					
F	Limitations and Future Works	31					
G	Auxiliary Results	32					
Н	Proofs	34					

Appendix for "Structural Causal Bandits under Markov Equivalence"

A Related Works

The integration of causal inference into the MAB framework has opened new avenues for modeling and solving decision problems with richer dependency structures [Bareinboim et al., 2024]. Causal diagrams [Pearl, 1995] have been employed to represent causal relationships among actions, rewards, and other relevant factors. This approach enables agents to make informed decisions by considering how each action causally influences the reward through causal pathways. Existing studies [Bareinboim et al., 2015, Lattimore et al., 2016, Forney et al., 2017] have shown that causality-aware strategies can significantly outperform MAB algorithms that do not account for such underlying causal relationships. Subsequent work has explored various specialized settings by introducing additional structural assumptions, such as the availability of both observational and experimental distributions, or linear mechanisms [Zhang and Bareinboim, 2017, Lu et al., 2020, Bilodeau et al., 2022, De Kroon et al., 2022, Feng and Chen, 2023, Varici et al., 2023].

Lu et al. [2021] were the first to study causal bandits without assuming access to the full causal diagram. Their approach targets the atomic setting in which the reward variable has only a single parent, reducing the problem to identifying that parent for optimal intervention. They further assume that the agent instead observes the skeleton of the true causal diagram. Extending this line of work, Konobeev et al. [2023] eliminated the need for prior knowledge of the graph skeleton. However, their setting remains restricted to the same atomic case. More recently, Feng et al. [2023] considered causal bandits in which each action corresponds to an intervention on a set of variables. Yan and Tajer [2024] considered actions as soft interventions on variables, i.e., changing the conditional distribution $P(v_i \mid \mathbf{pa}_i)$ to $Q(v_i \mid \mathbf{pa}_i)$. Despite this generalization, all these approaches assumed causal sufficiency and thus do not account for the presence of latent variables. Malek et al. [2023] provided some results for settings with unknown graph structures, the authors initially highlight the challenge posed by the exponentially large number of arms in causal bandit problems under unknown graphs, and assumed that no confounding exists between the reward variable and its ancestors.

Lee and Bareinboim [2018] formalized the structural causal bandit (SCM-MAB) framework, in which a bandit instance is structured by an SCM, and each action corresponds to an intervention on a subset of variables. They proposed a sound and complete graphical characterization to identify minimal intervention sets (MISs) and possibly-optimal minimal intervention sets (POMISs), where the former includes only the variables that affect the reward, and the latter refers to actions that could be part of an optimal strategy among MISs, thereby guiding the agent to avoid unnecessary exploration, without any actual interaction. Lee and Bareinboim [2019] extended this approach to accommodate scenarios involving non-manipulable variables among all the variables in the graph. Lee and Bareinboim [2020] established the framework under stochastic policies and demonstrated the informativeness of such policies. Everitt et al. [2021] and Carey et al. [2024] further investigated the completeness of the graphical characterization of optimal policy spaces, although the general completeness remains an open problem. Wei et al. [2023] proposed a parameterization-based approach to incorporate shared information among possibly-optimal actions. Elahi et al. [2024a] extended the SCM-MAB framework to settings where no causal graph is assumed to be accessible, requiring their algorithm to perform causal discovery—i.e., constructing the causal structure—during online interaction. In contrast, our work investigates a graphical approach that eliminates unnecessary actions a priori, given a partial ancestral graph, before the interaction begins. A detailed comparison between our work and Elahi et al. [2024a] is presented in Appendix E.3.

Building on this line of work, causal Bayesian optimization (CBO; Aglietti et al. [2020]) leverages the systematic characterization of MIS and POMIS for structural pruning in continuous action spaces, and Bhatija et al. [2025] extend it to a multi-outcome variant incorporating Pareto optimality.

B Additional Preliminaries and Background Results

In this section, we provide additional preliminaries from previous works (B.1) and background results relevant to our study (B.2).

B.1 Additional Preliminaries

Definite status. Let p be any path in a PMG, and $\langle X, Z, Y \rangle$ be any consecutive triple along p. We say that Z is a *definite collider* on p if both edges are directed into Z. If one of the edges is out of Z, or both edges have a circle mark at Z (i.e., $X * \multimap Z \multimap * Y$) and there is no edge between X and Z, then we say that Z is a *definite non-collider* on p. A path is said to have a *definite status* if every non-endpoint node along it is either a definite collider or a definite non-collider.

Markov equivalence class. Multiple MAGs can entail the same m-separation⁷ relationships. Such MAGs constitute a Markov equivalence class (MEC). The Markov equivalence class of MAGs can be uniquely represented by a PMG which we refer to as a PAG.

Definition 8 (Markov equivalence [Zhang, 2012]). Two MAGs \mathcal{M}_1 , \mathcal{M}_2 with $\mathbf{V}(\mathcal{M}_1) = \mathbf{V}(\mathcal{M}_2)$ are Markov equivalent if for any three disjoint sets of vertices \mathbf{X} , \mathbf{Y} , \mathbf{Z} , \mathbf{X} and \mathbf{Y} are m-separated by \mathbf{Z} in \mathcal{M}_1 if and only if \mathbf{X} and \mathbf{Y} are m-separated by \mathbf{Z} in \mathcal{M}_2 .

A path between X and Y, $p = \langle X, \dots, W, Z, Y \rangle$, is a discriminating path for Z if (i) p includes at least three edges; (ii) Z is a non-endpoint vertex on p, and is adjacent to Y on p; and (iii) X is not adjacent to Y, and every vertex between X and Z is a collider on p and is a parent of Y.

For two MAGs to be in the same Markov equivalence class, discriminating paths must either be present in both graphs or none of the graphs, as well as the same skeleton and unobserved colliders.

Lemma 1 (Graphical characterization of MEC [Spirtes and Richardson, 1997, Zhang, 2012]). Two MAGs \mathcal{M}_1 and \mathcal{M}_2 with $\mathbf{V}(\mathcal{M}_1) = \mathbf{V}(\mathcal{M}_2)$ are Markov equivalent if and only if

- (i) they have the same adjacencies;
- (ii) they have the same uncovered colliders; and
- (iii) if some path is a discriminating path for a vertex V in both graphs \mathcal{M}_1 and \mathcal{M}_2 , then V is a collider on the path in \mathcal{M}_1 if and only if it is a collider on the path in \mathcal{M}_2 .

A collider path $\langle V_1, \dots, V_k \rangle$ is called a *minimal collider path* if V_1 is not adjacent to V_k , and no subsequence of the path is also a collider path.

The two conditions (ii) and (iii) can be expressed as a condition for two MAGs to share the same minimal colliding paths [Zhao et al., 2005]. Identifying Markov equivalence of a pair of MAGs is tractable with worst-case runtime $\mathcal{O}(|\mathbf{V}|^3)$ [Wienöbst et al., 2022].

Visible edges. A directed edge $X \to Y$ is *visible* if there exists no causal diagram in the corresponding equivalence class where there is an inducing path between X and Y that is into X. We refer to any edge that is not visible as *invisible*.

Lemma 2 (Graphical characterization of visibility [Zhang, 2006, Maathuis and Colombo, 2015]). A directed edge $X \to Y$ is visible if

- (i) there is a vertex Z not adjacent to Y, such that there is an edge between Z and X that is into X ($Z*\to X$); or
- (ii) there is a collider path between Z and X that is into X ($Z * \rightarrow \cdot \leftrightarrow \cdot \cdot \leftrightarrow X$) and every vertex on the path except Z is a parent of Y.

⁷M-separation [Richardson and Spirtes, 2002] refers to an extension of d-separation [Pearl and Robins, 1995b] for ancestral graphs.

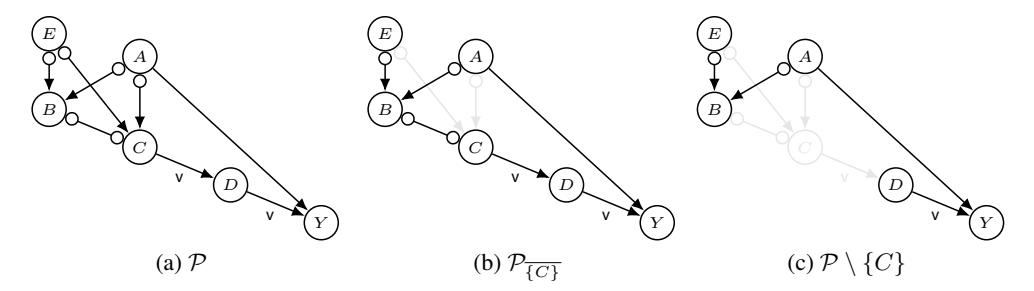


Figure 10: (a) PAG \mathcal{P} , (b) $\{C\}$ -upper-manipulated graph, and (c) induced graph over $\mathbf{V}(\mathcal{P}) \setminus \{C\}$. In MAGs and PAGs, the visibility is preserved from \mathcal{P} (see Lem. 15). For example, although there is no edge oriented into D in $\mathcal{P} \setminus \{C\}$, the directed edge $D \to Y$ remains visible.

It is important to note that (i) an invisible edge $X \to Y$ does not necessarily imply that X and Y are confounded in every underlying causal graph; and (ii) invisible edges should not be considered independently. To witness, consider a scenario where we have $X \leftarrow Y \to Z$ in a MAG \mathcal{M} , and X and Z are not adjacent. Since both edges, $X \leftarrow Y$ and $Y \to Z$, are invisible, causal diagrams can include at most one of the following structures added to \mathcal{M} : $X \leftarrow L_1 \leftarrow \cdots \rightarrow L_n \to Y$ or $Y \leftarrow L_1 \leftarrow \cdots \rightarrow L_n \to Z$ ($X \leftrightarrow Y$, or $Y \leftrightarrow Z$). Adding any one of these does not introduce a new collider between X and X, thereby maintaining conformity with M. However, if both are added simultaneously, a new collider is introduced at Y, resulting in a causal diagram that is not represented by M.

Manipulations. Given a causal diagram \mathcal{G} and a set of variables X therein, the X-lower-manipulation of \mathcal{G} deletes all edges in \mathcal{G} that are out of the variables in X. The resulting graph is denoted by $\mathcal{G}_{\underline{X}}$. The X-upper-manipulation of \mathcal{G} deletes all edges in \mathcal{G} that are into variables in X. The resulting graph is denoted by $\mathcal{G}_{\overline{X}}$.

Given a PMG $\mathcal Q$ and a set of variables $\mathbf X$ therein, the $\mathbf X$ -lower-manipulation of $\mathcal Q$ deletes all those edges that are visible in $\mathcal Q$ and are out of variables in $\mathbf X$ and replaces all those edges that are out of variables in $\mathbf X$ but are invisible in $\mathcal Q$ with bidirected edges. The resulting graph is denoted as $\mathcal Q_{\overline{\mathbf X}}$. The $\mathbf X$ -upper-manipulation of $\mathcal Q$ deletes all edges in $\mathcal Q$ that are into variables in $\mathbf X$, and otherwise keeps $\mathcal Q$ as it is.

The manipulated graphs play a crucial role in the derivation of do-calculus.

Do-calculus. Pearl [1995] devised *do-calculus* which acts as a bridge between observational and interventional distributions from a causal diagram without relying on any parametric assumptions. Zhang [2008b] proposed the do-calculus for MAGs and PAGs (also known as Zhang's calculus). Jaber et al. [2022] noted that there are cases where Pearl's do-calculus rules are applicable to every causal diagram within a given PAG, but Zhang's calculus cannot be applied to the same PAG. To address this, Jaber et al. [2022] proposed a refined version of do-calculus for PAGs and demonstrated that whenever the proposed rule is not applicable given a PAG, then the corresponding rule in Pearl's calculus is not applicable for some causal diagram in the Markov equivalence class represented by the PAG.

Here, we present do-calculus for PAGs, which encompasses that for MAGs.

Definition 9 (Definite m-connecting path [Jaber et al., 2022]). In a PAG, a path p between X and Y is a *definite m-connecting path* relative to a set of nodes \mathbf{Z} if p is definite status, every definite non-collider on p is not a member of \mathbf{Z} , and every collider on p is a ancestor of some member of \mathbf{Z} . X and Y are *m-separated* by \mathbf{Z} if there is no definite m-connecting path between them relative to \mathbf{Z} .

Theorem 6 (Do-calculus for PAGs [Jaber et al., 2022]). Let \mathcal{P} be the PAG over V, and X, Y, W, Z be disjoint subsets of V. The following rules are valid, in the sense that if the antecedent of the rule holds, then the consequent holds in every MAG and consequently every causal diagrams represented by \mathcal{P} .

Rule 1. $P(y \mid do(w), x, z) = P(y \mid do(w), z)$ if **X** and **Y** are m-separated by $\mathbf{W} \cup \mathbf{Z}$ in $\mathcal{P}_{\overline{\mathbf{W}}}$

```
Rule 2. P(\mathbf{y} \mid do(\mathbf{w}), do(\mathbf{x}), \mathbf{z}) = P(\mathbf{y} \mid do(\mathbf{w}), \mathbf{x}, \mathbf{z}) if \mathbf{X} and \mathbf{Y} are m-separated by \mathbf{W} \cup \mathbf{Z} in \mathcal{P}_{\overline{\mathbf{W}}, \underline{\mathbf{X}}}

Rule 3. P(\mathbf{y} \mid do(\mathbf{w}), do(\mathbf{x}), \mathbf{z}) = P(\mathbf{y} \mid do(\mathbf{w}), \mathbf{z}) if \mathbf{X} and \mathbf{Y} are m-separated by \mathbf{W} \cup \mathbf{Z} in \mathcal{P}_{\overline{\mathbf{W}}, \overline{\mathbf{X}}(\overline{\mathbf{Z}})}

where \mathbf{X}(\mathbf{Z}) \triangleq \mathbf{X} \setminus \text{PossAn}(\mathbf{Z})_{\mathcal{P}[\mathbf{V} \setminus \mathbf{W}]}.
```

Induced graph. A subgraph $\mathcal{Q}[\mathbf{A}]$ is defined as a vertex-induced subgraph in which all the edges among the vertices in $\mathbf{A} \subseteq \mathbf{V}(\mathcal{Q})$ are preserved while maintaining the visibility from \mathcal{Q} (see Fig. 10).

Chordal graph. We also introduce some useful graph theory and terminology, excerpted from Maathuis et al. [2009] and Wang et al. [2023a]. A graph is *chordal* if any cycle of length four or more has a chord, which refers to an edge joining two vertices that are not adjacent in the cycle. If a graph $\mathcal{G} = \langle \mathbf{V}, \mathbf{E} \rangle$ is chordal, then its subgraphs are also chordal. A vertex Z in \mathbf{V} is called *simplicial* if $\mathcal{G}[\mathrm{Adj}(Z)_{\mathcal{G}}]$ induces a complete graph. As shown by Dirac [1961] and Golumbic [2004], there are at least two non-adjacent simplicial vertices in any non-complete chordal graph with more than one vertex. A *perfect elimination order* of a graph \mathcal{G} is an ordering $\sigma = (V_1, \cdots, V_{|\mathbf{V}|})$ of its vertices, so that each vertex V_i is a simplicial vertex in the subgraph $\mathcal{G} \setminus \{V_1, \cdots, V_{i-1}\}$. It is always possible to transform any circle component in a PAG into a *directed acyclic graph* (DAG) without introducing new unshielded colliders, as the circle component is chordal and every chordal graph has a perfect elimination order [Rose et al., 1976, Habib et al., 2000].

Orientation rules. Fast Causal Inference (FCI) [Spirtes et al., 2001a] is a causal discovery algorithm for identifying PAGs from conditional independence relationships derived from an observable distribution that follows underlying model. We present the complete orientation rules proposed by Zhang [2008a], omitting rules \mathcal{R}_5 – \mathcal{R}_7 due to the absence of selection bias.

- \mathcal{R}_0 For each uncovered triple $\langle X, Z, Y \rangle$ in \mathcal{P} , orient it as a collider $X * \to Z \leftarrow *Y$ if and only if Z is not in $\mathsf{Sepset}(X,Y)^8$.
- \mathcal{R}_1 If $X * \to Z \circ *Y$, and X and Y are not adjacent, then orient $Z \circ *Y$ as $Z \to Y$.
- \mathcal{R}_2 If $X \to Z *\to Y$ or $X *\to Z \to Y$, and $X *\multimap Y$, then orient $X *\multimap Y$ as $X *\to Y$.
- \mathcal{R}_3 If $X * \to Z \leftarrow *Y$, $X * \multimap W \circ \multimap *Y$, X and Y are not adjacent, and $W * \multimap Z$, then orient $W * \multimap Z$ as $W * \to Z$.
- \mathcal{R}_4 If $\langle X, \cdots, W, Z, Y \rangle$ is a discriminating path between X and Y for Z, and $Z \circ -*Y$; then if $Z \in \mathsf{Sepset}(X,Y)$, orient $Z \circ -*Y$ as $Z \to Y$; Otherwise orient the triple $\langle W, Z, Y \rangle$ as $W \leftrightarrow Z \leftrightarrow Y$.
- \mathcal{R}_8 If $X \to Z \to Y$, and $X \circ \to Y$, orient $X \circ \to Y$ as $X \to Y$.
- \mathcal{R}_9 If $X \circ \to Y$, and $p = \langle X, Z, W, \cdots, Y \rangle$ is an uncovered possibly directed path from X to Y such that Z and Y are not adjacent, then orient $X \circ \to Y$ as $X \to Y$.
- \mathcal{R}_{10} Suppose $X \circ \to Y$, $Z \to Y \leftarrow W$, p_1 is an uncovered possibly directed path from X to Z, and p_2 is an uncovered possibly directed path from X to W. Let U be the vertex adjacent to X on p_1 (U could be Z), and V be the vertex adjacent to X on p_2 (V could be W). If U and V are distinct, and not adjacent, then orient $X \circ \to Y$ as $X \to Y$.

Incorporating background knowledge. Andrews et al. [2020] demonstrated that the ten rules $\mathcal{R}_1 - \mathcal{R}_{10}$ are complete for incorporating *tiered background knowledge*, which refers to background knowledge where the variables in a PAG can be partitioned into distinct groups with an explicit causal order defined among them.

Wang et al. [2022, 2023b] proposed that the rules $\mathcal{R}_1 - \mathcal{R}_3$, \mathcal{R}_4' , $\mathcal{R}_8 - \mathcal{R}_{10}$ and \mathcal{R}_{SB} are complete for orienting a PAG when *local background knowledge* (i.e., *all* marks around a vertex) is available. The second additional rule \mathcal{R}_{SB} naturally follows from the absence of selection bias.

⁸A set $\mathbb{Z} \in \mathsf{Sepset}(X,Y)$ if X and Y are independent given \mathbb{Z} .

⁹Wang et al. [2024a] proved that rules $\mathcal{R}_1 - \mathcal{R}_{10}$ with one additional rule are sound and complete to incorporate local background knowledge to scenarios where selection bias is present.

 \mathcal{R}_4' If $\langle X, \cdots, W, Z, Y \rangle$ is a discriminating path between X and Y for Z, and $Z \circ -*Y$; then orient $Z \circ -*Y$ as $Z \to Y$.

$$\mathcal{R}_{SB}$$
 If $X \multimap Y$, then orient $X \multimap Y$ as $X \to Y$.

Furthermore, they built the necessary and sufficient conditions for validating local background knowledge (referred to here as *local transformation* in the context of our paper), which can be determined in $\mathcal{O}(|\mathbf{V}|^3)$.

Theorem 7 (Theorem 3 in Wang et al. [2023b]). Denote $\mathcal Q$ the obtained PMG after some valid local transformations from a PAG $\mathcal P$ with orientation rules $\mathcal R_1 - \mathcal R_3$, $\mathcal R'_4$, $\mathcal R_8 - \mathcal R_{10}$ and $\mathcal R_{\mathit{SB}}$. Given a set $\mathbf C_X^Q \subseteq \{V \in \operatorname{Adj}(X)_{\mathcal Q} \mid X \circ -\!\!\!\!-\!\!\!\!-\!\!\!\!+ V\}$, there exists a MAG $\mathcal M$ consistent to $\mathcal Q$ with $X \leftarrow \!\!\!\!\!\!+ V$ for all $V \in \mathbf C_X^Q$, and $X \to V$ for all $V \in \{V \in \operatorname{Adj}(X)_{\mathcal Q} \mid X \circ -\!\!\!\!\!\!\!+ V\} \setminus \mathbf C_X^Q$ if and only if $\mathbf C_X^Q$ satisfies the following conditions:

- $1. \ \operatorname{PossDe}(X)_{\mathcal{Q} \backslash \mathbf{C}_X^Q} \cap \operatorname{Pa}(\mathbf{C}_X^Q)_{\mathcal{Q}} = \emptyset;$
- 2. $\mathcal{Q}[\mathbf{C}_X^Q]$ is a complete graph;
- 3. Orient the subgraph $\mathcal{Q}[\mathsf{PossDe}(X)_{\mathcal{Q}\backslash \mathbf{C}_X^{\mathcal{Q}}}]$ as follows until no feasible updates: For any vertices V_l and V_j such that $V_l \circ \multimap V_j$, orient it as $V_l \circ \rightarrowtail V_j$ if
 - (i) $\mathcal{F}_{V_l} \setminus \mathcal{F}_{V_j} \neq \emptyset$, or;
 - (ii) $\mathcal{F}_{V_l} = \mathcal{F}_{V_j}$ as well as there is a vertex $V_m \in \mathsf{PossDe}(X)_{\mathcal{Q} \backslash \mathbf{C}_X^{\mathcal{Q}}}$ not adjacent to V_j such that $V_m \to V_l \circ \neg \circ V_j$

where $\mathcal{F}_{V_l} = \{V \in \mathbf{C}_X^Q \cup \{X\} \mid V * \multimap V_l \in \mathcal{Q}\}$. Then, no new uncovered colliders are introduced.

The PMG incorporating local transformations satisfies desirable properties as follows.

Theorem 8 (Theorem 1 in Wang et al. [2023b]). Let Q be a PMG obtained from some valid local transformations from a PAG P and orientation rules $\mathcal{R}_1 - \mathcal{R}_3$, \mathcal{R}'_4 , $\mathcal{R}_8 - \mathcal{R}_{10}$ and \mathcal{R}_{SB} . Then Q satisfies the following properties.

(Closed). Q is closed under the orientation rules.

(*Invariant*). The arrowheads (>) and tails (-) in Q are invariant in all the MAGs consistent with Q.

(*Chordal*). The circle component in Q is chordal.

(Balanced). For any three nodes A, B, C in Q, if $A * \rightarrow B \circ - * C$, then there is an edge between A and C with an arrowhead at C, namely, $A * \rightarrow C$. Furthermore, if the edge between A and B is $A \rightarrow B$, then the edge between A and C is either $A \rightarrow C$ or $A \circ \rightarrow C$ (i.e., it is not $A \leftrightarrow C$).

(Complete). For each circle at vertex A on any edge $A \circ -*B$ in \mathcal{Q} , there exist MAGs \mathcal{M}_1 and \mathcal{M}_2 consistent with \mathcal{Q} such that $A \leftarrow *B$ in \mathcal{M}_1 and $A \rightarrow B$ in \mathcal{M}_2 .

Recently, Venkateswaran and Perković [2024], Wang et al. [2024b, 2025a] devised additional rules for more general type of background knowledge. However, the completeness of the orientations in the resulting PMG after applying these rules remains an open problem.

Wang et al. [2023a] leveraged the PMG incorporating local background knowledge to determine whether a given set of variables can be an adjustment set in some MAG consistent with the PMG, and Wang et al. [2024b, 2025b] demonstrated that the additional rules can improve this process.

Soundness and completeness of orientations. To eliminate ambiguity, we provide a formal description of soundness and completeness in the context of orientation within a PMG. Let Q be a PMG. We say that orientations in Q are *sound* if there is at least one MAG \mathcal{M} conforming to Q such

that invariant edge marks in \mathcal{Q} are a subset of edge marks in \mathcal{M} . We say that the orientations in \mathcal{Q} are complete if for every $A \circ -* B$ edge in \mathcal{H} , there are two MAGs \mathcal{M}_1 and \mathcal{M}_2 represented by \mathcal{Q} containing the edges $A \to B$ and $A \leftarrow *B$, respectively, such that \mathcal{M}_1 and \mathcal{M}_2 conforming to \mathcal{Q} .

Structural causal bandit. We review the notion of minimal intervention set (MIS) and possibly optimal minimal intervention set (POMIS) as well as their graphical characterizations for causal diagram by Lee and Bareinboim [2018]. Let \mathcal{G} be a causal diagram and $CC(X)_{\mathcal{G}}$ be the *c-component* [Tian and Pearl, 2002] of \mathcal{G} that contains X where a c-component is a maximal set of vertices connected with bidirected edges. We denote $CC(X)_{\mathcal{G}} = \bigcup_{X \in X} CC(X)_{\mathcal{G}}$. Let $MUCT(\mathcal{G}, Y)$ and $B(\mathcal{G}, Y)$ be the MUCT and $B(\mathcal{G}, Y)$, respectively.

Definition 10 (MIS [Lee and Bareinboim, 2018]). Given information $[\![\mathcal{G},Y]\!]$, a set of variables $\mathbf{X} \subseteq \mathbf{V} \setminus \{Y\}$ is said to be a *minimal intervention set* (MIS) with respect to $[\![\mathcal{G},Y]\!]$, denoted by $\mathbb{M}_{\mathcal{G},Y}$ if there is no $\mathbf{X}' \subseteq \mathbf{X}$ such that $\mu_{\mathbf{x}[\mathbf{X}']} = \mu_{\mathbf{x}}$ for every SCM conforming to the causal diagram \mathcal{G} .

Proposition 9 (Proposition 1 in Lee and Bareinboim [2018]). Let \mathcal{G} be a causal diagram over the set of variables \mathbf{V} . A set $\mathbf{X} \subseteq \mathbf{V} \setminus \{Y\}$ is an MIS relative to $[\mathcal{G}, Y]$ if and only if $\mathbf{X} \subseteq \mathrm{An}(Y)_{\mathcal{G}_{\mathbf{X}}}$.

MIS leverages Rule 3 of do-calculus [Pearl, 1995] to eliminate variables that are irrelevant to the reward. Intuitively, an MIS can be understood as a set X in which there exists a directed path from any variable $X \in X$ to Y, ensuring that each X can influence Y.

Definition 11 (POMIS [Lee and Bareinboim, 2018]). Let $\mathbf{X} \subseteq \mathbf{V} \setminus \{Y\}$ be an MIS with respect to $[\![\mathcal{G},Y]\!]$. If there exists an SCM conforming to \mathcal{G} such that $\mu_{\mathbf{X}^*} > \forall_{\mathbf{W} \in \mathbb{M}_{\mathcal{G},Y} \setminus \{\mathbf{X}\}} \mu_{\mathbf{W}^*}$, then \mathbf{X} is a possibly-optimal minimal intervention set (POMIS) with respect to $[\![\mathcal{G},Y]\!]$.

Definition 12 (Unobserved-confounders' territory). Given information $[\![\mathcal{G},Y]\!]$, let $\mathcal{H}=\mathcal{G}[\operatorname{An}(Y)_{\mathcal{G}}]$. A set of variables $\mathbf{T}\subseteq\mathbf{V}(\mathcal{H})$ containing Y is called a UC-territory on \mathcal{G} with respect to Y if $\operatorname{De}(\mathbf{T})_{\mathcal{H}}=\mathbf{T}$ and $\operatorname{CC}(\mathbf{T})_{\mathcal{H}}=\mathbf{T}$. A UC-territory \mathbf{T} is said to be *minimal* if no $\mathbf{T}'\subsetneq\mathbf{T}$ is a UC-territory (MUCT).

Definition 13 (Interventional border). Let T be a minimal UC-territory on causal diagram \mathcal{G} with respect to Y. Then $\mathbf{W} = \operatorname{Pa}(\mathbf{T})_{\mathcal{G}} \setminus \mathbf{T}$ is called an *interventional border* (IB) for \mathcal{G} with respect to Y.

When given a causal diagram \mathcal{G} , MUCT and IB provide a graphical characterization of POMIS. In words, MUCT is the minimal set of variables that is closed under descendants and connected by a bidirected edge; and IB consists of the parents of MUCT, excluding MUCT itself. Intuitively, MUCT is the minimal closed mechanism that conveys all hidden information from unobserved confounders to the downstream reward, while IB consists of the nodes that directly affect this closed mechanism.

Theorem 9 (Theorem 6 in Lee and Bareinboim [2018]). Let \mathcal{G} be a causal diagram over the set of variables \mathbf{V} . A set $\mathbf{X} \subseteq \mathbf{V} \setminus \{Y\}$ is a POMIS if and only if it holds $\mathsf{IB}(\mathcal{G}_{\overline{\mathbf{X}}}, Y) = \mathbf{X}$.

B.2 Background Results

We present useful results established in existing works.

B.2.1 Background Results in Zhang [2006, 2008a]

Lemma 3 (Lemma 0, as used in the proof of Lemma 5.1.7 in Zhang [2006]). Let X and Y be distinct nodes in a MAG M. If $p = \langle X, \dots, Z, V, Y \rangle$ is a discriminating path from X to Y for V in a MAG M, and the corresponding subpath between X and V in P is (also) a collider path, then the path corresponding to p in Q is also a discriminating path for V.

Lemma 4 (Lemma A.1 in Zhang [2008a] & Lemma 5 in Jaber et al. [2018]). Let \mathcal{P} be a PAG over V, and let $\mathcal{P}[A]$ be the subgraph of \mathcal{P} induced by $A \subseteq V$. For any three nodes A, B, C, if $A*\to B\circ -*C$, then there is an edge between A and C with an arrowhead at C, namely, $A*\to C$. Furthermore, if the edge between A and B is $A\to B$, then the edge between A and C is either $A\to C$ or $A\circ\to C$ (i.e., it is not $A\leftrightarrow C$).

Lemma 5 (Lemma 3.3.2 in Zhang [2006]). In a PAG \mathcal{P} , for any two nodes A and B, if there is a circle path, then following holds:

- 1. If there is an edge between A and B, the edge is not into A or B;
- 2. For any other node C, $C*\to A$ if and only if $C*\to B$. Furthermore, $C\leftrightarrow A$ if and only if $C\leftrightarrow B$.

Lemma 6 (Theorem 2 in Zhang [2008a]). Let \mathcal{P} be a PAG. Let \mathcal{M} be the graph resulting from the following procedure applied to a \mathcal{P} .

- Step 1. Replace all partially directed edges $(\circ \rightarrow)$ in \mathcal{P} with directed edges (\rightarrow) .
- Step 2. Orient the circle component of \mathcal{P} into a DAG with no unshielded colliders.

Then, the result graph \mathcal{M} conforms to \mathcal{P} .

Lemma 7 (Lemma B.1 in Zhang [2008a]). Let A and B be two distinct nodes in a PAG P. If p is a possibly directed path from A to B in a PAG P, then some subsequence of p forms an uncovered possibly directed path from A to B in P.

Lemma 8 (Lemma B.2 in Zhang [2008a]). Let A and B be two distinct nodes in a PAG \mathcal{P} . If $p = \langle V_0(=A), \cdots V_n(=B) \rangle, n \geq 2$, is an uncovered possibly directed path from A to B in \mathcal{P} , and $V_{i-1} * \rightarrow V_i$ for some $i \in \{1, \cdots, n\}$, then $V_{j-1} \rightarrow V_j$ for all $j \in \{i+1, \cdots, n\}$.

Lemma 9 (Lemma B.4 in Zhang [2008a]). In a PAG \mathcal{P} , if there is a possibly directed path from A to B, then the edge between A and B, if any, is not into A.

Lemma 10 (Lemma B.5 in Zhang [2008a]). In a PAG \mathcal{P} , let A and B be two distinct nodes in a PAG \mathcal{P} . If there is a possibly directed path from A to B that is into B, then every uncovered possibly directed path from A to B is into B.

Lemma 11 (Lemma B.7 in Zhang [2008a]). In a PAG \mathcal{P} , if there is a circle path between two adjacent vertices in \mathcal{P} , then the edge between the two vertices is a circle edge (\circ – \circ).

B.2.2 Background Results in Maathuis and Colombo [2015]

Lemma 12 (Lemma 7.6 in Maathuis and Colombo [2015]). Let \mathcal{P} be a PAG with k edges into X, $k \geq 0$. Then there exists at least one MAG \mathcal{M} in the Markov equivalence class represented by \mathcal{P} that has k edges into X.

B.2.3 Background Results in Perkovic et al. [2018]

B.2.4 Background Results in Jaber et al. [2018, 2022]

Lemma 14 (Proposition 1 in Jaber et al. [2018]). Let \mathcal{P} be a PAG over \mathbf{V} , and \mathcal{G} be any causal diagram in the equivalence class represented by \mathcal{P} . Let $X \neq Y$ be two nodes in $\mathbf{A} \subseteq \mathbf{V}$. If X is an ancestor of Y in $\mathcal{G}[\mathbf{A}]$, then X is a possible ancestor of Y in $\mathcal{P}[\mathbf{A}]$.

Lemma 15 (Lemma 4 in Jaber et al. [2018]). Let \mathcal{P} be a PAG over \mathbf{V} . For every directed edge $X \to Y$ in induced subgraph $\mathcal{P}[\mathbf{A}]$ with $\mathbf{A} \subseteq \mathbf{V}$, if it is visible in \mathcal{P} , then it is also visible in $\mathcal{P}[\mathbf{A}]$.

Lemma 16 (Proposition 2 in Jaber et al. [2018]). Let \mathcal{P} be a PAG over \mathbf{V} , and \mathcal{G} be any causal diagram in the equivalence class represented by \mathcal{P} . Let $X \neq Y$ be two nodes in $\mathbf{A} \subseteq \mathbf{V}$. If X and Y are in the same c-component in $\mathcal{G}[\mathbf{A}]$, then X and Y are in the same pc-component in $\mathcal{P}[\mathbf{A}]$.

Algorithm 2: Partial Topological Order PTO [Jaber et al., 2018]

Input: \mathcal{P} , $\mathbf{A} \subseteq \mathbf{V}(\mathcal{P})$

Output: Partial Topological Order over $\mathcal{P}[\mathbf{A}]$

- 1 while there exists a bucket B in $\mathcal{P}[A]$ with only arrowheads incident on it do
- 2 Extract **B** from $\mathcal{P}[\mathbf{A}]$
- $\mathbf{A} \leftarrow \mathbf{A} \setminus \mathbf{B}$
- 4 end
- 5 The partial order is $\mathbf{B}^1 \prec \cdots \prec \mathbf{B}^m$ in reverse order of the bucket extraction, i.e., \mathbf{B}^1 is the last bucket extracted and \mathbf{B}^m is the first.

Lemma 17 (Proposition 4 in Jaber et al. [2018]). Let \mathcal{P} be a PAG over V, and let $\mathcal{P}[A]$ be the subgraph of \mathcal{P} induced by $A \subseteq V$. Then, Alg. 2 is sound over $\mathcal{P}[A]$, in the sense that the partial order is valid with respect to $\mathcal{G}[A]$, for every causal diagram \mathcal{G} in the equivalence class represented by \mathcal{P} . 10

Lemma 18 (Lemma 6 in Jaber et al. [2018]). *In* $\mathcal{M}[\mathbf{A}]$, *where* \mathcal{M} *is a MAG over* \mathbf{V} *and* $\mathbf{A} \subseteq \mathbf{V}$, *the following property holds:*

For any three vertices A, B, C, if $A*\to B\to C$ and both edges are invisible, then we have $A*\to C$ and the edge is invisible.

Lemma 19 (Lemma 18 in Jaber et al. [2022]). Let \mathcal{P} be a PAG over V, and let $\mathcal{P}[A]$ be the subgraph of \mathcal{P} induced by $A \subseteq V$. In $\mathcal{P}[A]$, the following property holds:

For any three vertices A, B, C, if $A*\to B^?\to C$ and both edges are invisible, then we have $A*\to C$ and the edge is invisible.

B.2.5 Background Results in Wang et al. [2023b, 2024a]

Lemma 20 (Lemma 2 in Wang et al. [2023b]). Let Q be a PMG obtained from some valid local transformations from a PAG \mathcal{P} and the orientation rules. If p is a possibly directed path from A to B in Q, then some subsequence of p is an uncovered possibly directed path from A to B in Q.

Lemma 21 (Lemma 3 in Wang et al. [2023b]). Let Q be a PMG obtained from some valid local transformations from a PAG P and the orientation rules. In a PMG Q, for any two nodes A and B, if there is a circle path, then following holds:

- 1. If there is an edge between A and B, the edge is not into A or B;
- 2. For any other node C, $C*\to A$ if and only if $C*\to B$. Furthermore, $C\leftrightarrow A$ if and only if $C\leftrightarrow B$.

Lemma 22 (Lemma 4 in Wang et al. [2023b]). Let \mathcal{Q} be a PMG obtained from some valid local transformations from a PAG \mathcal{P} and the orientation rules. Suppose a MAG \mathcal{M} consistent to \mathcal{Q} and the local transformation $\mathbf{C}_X^{\mathcal{Q}}$. Then $Y \in \mathsf{PossDe}(X)_{\mathcal{Q} \setminus \mathbf{C}_X^{\mathcal{Q}}}$ if and only if $Y \in \mathsf{De}(X)_{\mathcal{M}}$.

Lemma 23 (Lemma 16.1 in Wang et al. [2023b]). Let Q be a PMG obtained from some valid local transformations from a PAG P and the orientation rules. The MAG oriented according to Lem. 6 conforms to Q.

Lemma 24 (Lemma 2 in Wang et al. [2024a]). Let Q be a PMG obtained from some valid local transformations from a PAG \mathcal{P} and the orientation rules. If there is an uncovered circle path $p = \langle V_1, V_2, \cdots, V_n \rangle, n \geq 3$ in Q, then any two non-consecutive vertices are not adjacent (minimal circle path).

¹⁰A *bucket* refers to the closure of nodes connected with circle paths.

	Total trials	Task 1 10k	Task 2 10k	Task 3 5k	Task 4* 10k	Task 5* 2k	Task 6 * 2k
T	POMIS BF	$123.4 \pm 52.2 (39.3\%) \\ 144.9 \pm 51.9 \\ 314.0 \pm 54.1$	$320.9 \pm 43.7 (44.3\%) \\ 661.1 \pm 50.6 \\ 724.8 \pm 50.3$	$60.3 \pm 3.9 (2.5\%)$ 1719.6 ± 23.1 2421.3 ± 35.5	$85.9 \pm 43.1 (9.7\%)$ 335.9 ± 48.3 889.1 ± 59.5	$51.9 \pm 2.3 (14.5\%)$ 108.2 ± 4.7 357.9 ± 16.2	$203.3 \pm 3.9 (23.8\%) \\ 805.6 \pm 20.2 \\ 854.5 \pm 20.3$
KL-L	POMIS ICB DMIS BF	$243.4 \pm 55.5 (48.9\%) 275.9 \pm 54.9 497.9 \pm 55.7$	$629.9 \pm 45.1 (50.4\%)$ 1175.3 ± 52.3 1250.9 ± 60.5		$195.1 \pm 45.7 (12.9\%) 705.5 \pm 55.6 1518.4 \pm 71.0$		

Table 1: Mean and standard deviation of cumulative regret (CR). The asterisk (*) indicates additional experiments. The percentages (red) represent the ratio $\frac{\text{CR for POMIS}}{\text{CR for BF}} \times 100(\%)$.

C Assumptions

In this paper, we assume that there is *no selection bias* in the SCM-MAB system; that is, the PAG representing our causal diagrams of interest contains no undirected edges. Since our work focuses on a graphical perspective of the structured bandit system in terms of PAGs, we assume access to the *true* PAG representing the causal diagram corresponding to the target bandit instance.

D Experimental Details and Additional Results

This section provides details on the specific SCMs used in all bandit instances presented in the experiments (Sec. 5) and additional experiments. Simulations are repeated 1,000 times to obtain consistent results. The simulations were conducted on a Linux server equipped with an Intel Xeon Gold 5317 processor running at 3.0 GHz and 64 GB of RAM. No GPUs were used during the simulations.

We consider three strategies for selecting arms: POMISs, DMISs, and Brute-force (BF), combined with two prominent MAB solvers: Thompson Sampling (TS) [Thompson, 1933, Chapelle and Li, 2011, Agrawal and Goyal, 2012, Kaufmann et al., 2012] and KL-UCB [Garivier and Cappé, 2011, Cappé et al., 2013]. In the Brute-force strategy, all possible combinations of arms $\bigcup_{\mathbf{X} \subseteq \mathbf{V} \setminus \{Y\}} \mathfrak{X}_{\mathbf{X}}$ are evaluated. The number of trials is set to 10,000 for Tasks 1, 2, and 4; 5,000 for Task 3; and 2,000 for Tasks 5 and 6, which is sufficient to observe performance differences among action spaces. The number of trials is selected such that the cumulative regret with respect to POMIS stabilizes across 1000 repeated runs. Our experimental setup closely follows those of Lee and Bareinboim [2018] and Wei et al. [2023]. Tables 1 and 2 summarize our simulation results.

These results demonstrate that refining arms by considering the Markov equivalence class into account enhances the efficiency of agents when interacting with the underlying environment.

Details of the Causal Models for Bandit Instances

We denote the exclusive-or operation by \oplus , and use Bern to represent a Bernoulli distribution. We *randomly* generate structural functions **F** using binary logical operations $(\land, \lor, \oplus, \neg)$, and the parameters of the exogenous variable distributions are also *randomly* selected.

Task 1. The bandit instance is associated with an SCM S_1 where

$$S_{1} = \begin{cases} \mathbf{U} &= \{U_{A}, U_{B}, U_{C}, U_{D}, U_{Y}, U_{BY}, U_{AC}\} \\ \mathbf{V} &= \{A, B, C, D, Y\} \\ &= \begin{cases} f_{A} = u_{A} \wedge u_{AC}, f_{B} = c \vee ((1 - u_{B}) \wedge u_{BY}), \\ f_{C} = a \vee ((1 - u_{C}) \wedge u_{AC}), f_{D} = y \wedge u_{D}, \\ f_{Y} = \{(1 - b) \vee \{(1 - c) \wedge (1 - u_{BY})\}\} \wedge u_{Y} \end{cases}$$

$$P(\mathbf{U}) = \begin{cases} U_{A} &= \mathbf{Err}(0.41), U_{B} \sim \mathbf{Err}(0.41), U_{C} \sim \mathbf{Err}(0.41), \\ U_{D} \sim \mathbf{Err}(0.59), U_{Y} \sim \mathbf{Err}(0.66), U_{BY} \sim \mathbf{Err}(0.28), \\ U_{AC} \sim \mathbf{Err}(0.77). \end{cases}$$

$$(1)$$

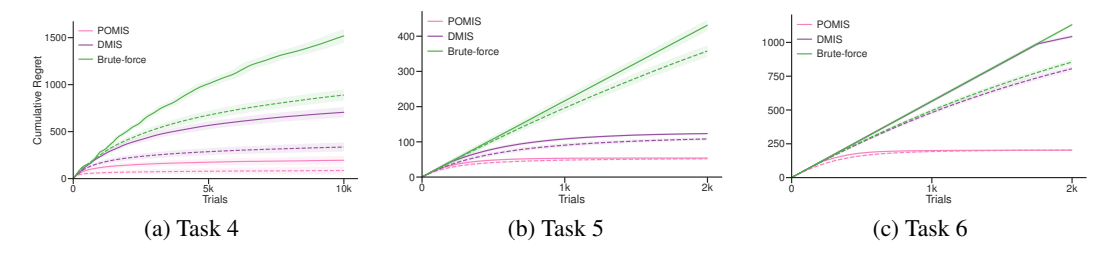


Figure 11: Cumulative regrets for the corresponding KL-UCB (solid) and TS (dashed) for additional experiments (Task 4–6) under distinct strategies. We plot the average cumulative regrets along with their standard deviations.

Task 2. The bandit instance is associated with an SCM S_2 where

$$S_{2} = \begin{cases} \mathbf{U} &= \{U_{A}, U_{B}, U_{C}, U_{D}, U_{E}, U_{Y}, U_{AY}, U_{BY}\} \\ \mathbf{V} &= \{A, B, C, D, E, Y\} \\ f_{A} = u_{A} \oplus u_{AY}, f_{B} = u_{b} \oplus u_{BY}, f_{C} = u_{C} \oplus b, \\ f_{D} = u_{D} \oplus c, f_{E} = \{(1 - u_{E}) \oplus (1 - a)\} \wedge c, \\ f_{Y} = u_{Y} \vee \{\{(1 - e) \oplus (u_{AY} \wedge u_{BY})\} \wedge d\} \\ U_{A} \sim \operatorname{Bern}(0.47), U_{B} \sim \operatorname{Bern}(0.59), U_{C} \sim \operatorname{Bern}(0.37), \\ U_{D} \sim \operatorname{Bern}(0.61), U_{E} \sim \operatorname{Bern}(0.55), U_{Y} \sim \operatorname{Bern}(0.21), \\ U_{AY} \sim \operatorname{Bern}(0.54), U_{BY} \sim \operatorname{Bern}(0.36). \end{cases}$$
 (2)

Task 3. The bandit instance is associated with an SCM S_3 where

$$S_{3} = \begin{cases} \mathbf{U} &= \{U_{A}, U_{B}, U_{C}, U_{D}, U_{E}, U_{F}, U_{G}, U_{H}, U_{I}, U_{Y}, U_{AB}, U_{BE}, U_{FG}, U_{HI}, U_{IY} \} \\ \mathbf{V} &= \{A, B, C, D, E, F, G, H, I, Y \} \\ &= \begin{cases} f_{A} = u_{A} \oplus U_{AB}, f_{B} = (u_{BE} \oplus u_{AB}) \wedge (a \vee u_{b}), \\ f_{C} = u_{C} \oplus b, f_{D} = u_{D} \oplus c, \\ f_{E} = ((1 - u_{E}) \oplus (1 - d)) \wedge u_{BE}, \\ f_{F} = ((1 - u_{F}) \oplus (1 - e)) \wedge u_{FG}, \\ f_{G} = (u_{FG} \oplus h) \wedge (e \vee u_{G}), \\ f_{H} = ((1 - u_{H}) \oplus (1 - e)) \wedge u_{HI}, \\ f_{I} = (u_{IY} \oplus u_{HI}) \wedge (f \vee u_{I}), \\ f_{Y} = u_{Y} \vee (((1 - h) \oplus (i \wedge u_{IY})) \wedge f) \\ &= \begin{cases} U_{A} \sim \text{Bern}(0.47), U_{B} \sim \text{Bern}(0.59), U_{C} \sim \text{Bern}(0.37), \\ U_{D} \sim \text{Bern}(0.61), U_{E} \sim \text{Bern}(0.55), U_{F} \sim \text{Bern}(0.21), \\ U_{G} \sim \text{Bern}(0.54), U_{H} \sim \text{Bern}(0.36), U_{I} \sim \text{Bern}(0.45), \\ U_{Y} \sim \text{Bern}(0.37), U_{AB} \sim \text{Bern}(0.29), U_{BE} \sim \text{Bern}(0.53), \\ U_{FG} \sim \text{Bern}(0.62), U_{HI} \sim \text{Bern}(0.46), U_{IY} \sim \text{Bern}(0.67). \end{cases}$$

$$(3)$$

As an additional experiment, we evaluate the cumulative regrets (CR) of SCM-MAB using the PAGs illustrated in Fig. 12. The corresponding plots are shown in Fig. 11.

Task 4. We consider the PAG in Fig. 12a to validate our result. Using three strategies, the POMIS-based TS and KL-UCB achieve CRs of 85.9 and 195.1, which correspond to 9.7% and 12.9%,

		Task 1	Task 2	Task 3	Task 4*	Task 5*	Task 6*
IS	POMIS	7 (43.75%)	18 (56.3%)	8 (1.56%)	6 (37.5%)	16 (12.5%)	40 (31.3%)
	DMIS	9	30	152	14	32	120
	BF	16	32	512	16	128	128
Arms	POMIS	19 (23.5%)	89 (36.6%)	54 (0.27%)	15 (6.17%)	81 (3.70%)	231 (10.7%)
	DMIS	25	195	2025	57	189	1755
	BF	81	243	19683	243	2187	2187

Table 2: For each task, the number of intervention sets (IS; shown above) and the corresponding number of arms (shown below) are reported. The percentages (red) indicate the ratio $\frac{\text{\# POMIS}}{\text{\# BF}} \times 100(\%)$, and the corresponding ratio for the number of arms.

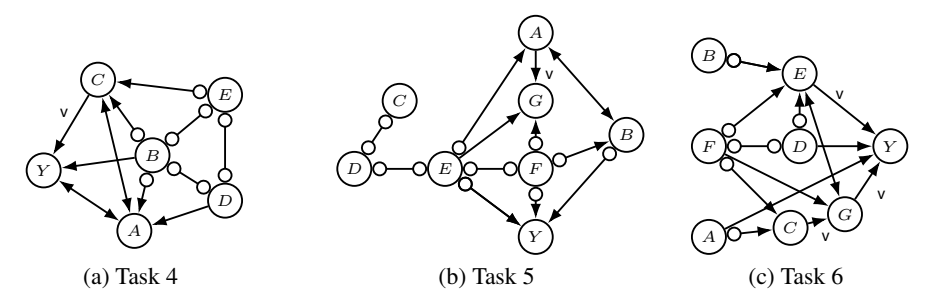


Figure 12: Each PAG represents a target bandit mechanism that the deployment agent interacts with.

respectively, of CR for BF. The bandit instance is associated with an SCM S_4 where

$$S_{4} = \begin{cases} \mathbf{U} &= \{U_{A}, U_{B}, U_{C}, U_{D}, U_{E}, U_{Y}, U_{AC}, U_{AY}, U_{BY}\} \\ \mathbf{V} &= \{A, B, C, D, E, Y\} \\ f_{A} = u_{A} \vee \{\{(1 - d) \oplus (u_{AY} \wedge u_{AC})\} \wedge b\}, \\ f_{B} = u_{B} \oplus u_{BY}, \\ f_{C} = (u_{AC} \oplus E) \wedge (B \vee u_{C}), f_{D} = u_{D} \oplus b, \\ f_{E} = \{(1 - u_{E}) \oplus (1 - b)\} \wedge d, \\ f_{Y} = u_{Y} \vee \{\{(1 - c) \oplus (u_{AY} \wedge u_{BY})\} \wedge b \\ U_{A} \sim \text{Bern}(0.47), \{U_{B} \sim \text{Bern}(0.59), U_{C} \sim \text{Bern}(0.37), \\ U_{D} \sim \text{Bern}(0.61), U_{E} \sim \text{Bern}(0.55), U_{Y} \sim \text{Bern}(0.21), \\ U_{AC} \sim \text{Bern}(0.36), U_{AY} \sim \text{Bern}(0.54), U_{BY} \sim \text{Bern}(0.45). \end{cases}$$

Task 5. We consider the PAG in Fig. 12b to validate our result. Using three strategies, the POMISbased TS and KL-UCB achieve CRs of 51.9 and 54.1, which correspond to 14.5% and 12.7%, respectively, of CR for BF. The bandit instance is associated with an SCM S_5 where

$$S_{5} = \begin{cases} \mathbf{U} &= \{U_{A}, U_{B}, U_{C}, U_{D}, U_{E}, U_{F}, U_{G}, U_{Y}, U_{AB}, U_{BY}, U_{CD}, U_{FG} \} \\ \mathbf{V} &= \{A, B, C, D, E, F, G, Y \} \\ &= \begin{cases} f_{A} = (1 - u_{A}) \vee \{(1 - u_{AB}) \oplus e \}, \\ f_{B} = \{1 - \{u_{BY} \vee (1 - u_{B})\}\} \oplus (u_{AB} \oplus f), \\ f_{C} = u_{CD} \oplus u_{C}, f_{D} = (1 - u_{D}) \vee \{(1 - u_{CD}) \oplus c \}, \\ f_{E} = d \oplus u_{E}, f_{F} = (1 - u_{F}) \vee \{(1 - u_{FG}) \oplus e \}, \\ f_{G} = \{1 - \{u_{FG} \vee (1 - u_{G})\}\} \oplus (e \oplus a), \\ f_{Y} = f \oplus \{\{(1 - u_{BY}) \oplus u_{Y}\}\} \oplus (b \oplus a) \end{cases} \\ &= \begin{cases} U_{A} \sim \text{Bern}(0.29), U_{B} \sim \text{Bern}(0.73), U_{C} \sim \text{Bern}(0.36), \\ U_{D} \sim \text{Bern}(0.45), U_{E} \sim \text{Bern}(0.38), U_{F} \sim \text{Bern}(0.36), \\ U_{C} \sim \text{Bern}(0.55), U_{Y} \sim \text{Bern}(0.57), U_{FG} \sim \text{Bern}(0.36), \\ U_{AB} \sim \text{Bern}(0.37), U_{BY} \sim \text{Bern}(0.35), U_{CD} \sim \text{Bern}(0.4). \end{cases}$$

Task 6. We consider the PAG in Fig. 12c to validate our result. Using three strategies, the POMIS-based TS and KL-UCB achieve CRs of 203.3 and 202.9, which correspond to 23.8% and 17.9%, respectively, of CR for BF. The bandit instance is associated with an SCM S_6 where

$$S_{6} = \begin{cases} \mathbf{U} &= \{U_{A}, U_{B}, U_{C}, U_{D}, U_{E}, U_{F}, U_{G}, U_{Y}, U_{AY}, U_{EF}, U_{FG}\} \\ \mathbf{V} &= \{A, B, C, D, E, F, G, Y\} \end{cases}$$

$$= \begin{cases} f_{A} = u_{A} \oplus u_{AY}, f_{B} = u_{B}, \\ f_{C} = ((1 - u_{C}) \wedge f) \vee a, f_{D} = f \wedge u_{D}, \\ f_{E} = ((1 - b) \vee ((1 - u_{EF}) \wedge (1 - d))) \wedge u_{E}, \\ f_{F} = ((1 - u_{F}) \wedge u_{FG}) \vee u_{EF}, \\ f_{G} = ((1 - u_{G}) \wedge u_{FG}) \vee g, \\ f_{Y} = e \wedge ((1 - d) \vee (((1 - u_{Y}) \wedge g) \vee u_{AY})) \end{cases}$$

$$P(\mathbf{U}) = \begin{cases} U_{A} \sim \text{Bern}(0.59), U_{B} \sim \text{Bern}(0.42), U_{C} \sim \text{Bern}(0.77), \\ U_{D} \sim \text{Bern}(0.59), U_{E} \sim \text{Bern}(0.72), U_{F} \sim \text{Bern}(0.48), \\ U_{G} \sim \text{Bern}(0.68), U_{Y} \sim \text{Bern}(0.51), U_{AY} \sim \text{Bern}(0.61), \\ U_{EF} \sim \text{Bern}(0.63), U_{FG} \sim \text{Bern}(0.55). \end{cases}$$

$$(6)$$

E Discussions

In this section, we discuss circle mark transformations from the perspective of orientation completeness and complexity of enumerating all POMISs for PAGs.

E.1 Partial Mixed Graphs Obtained from Local Transformation

Let $\widetilde{\mathcal{Q}_{\mathbf{X}}}$ be a PMG that satisfies (1) the two conditions in Prop. 7 and (2) is closed under orientation rules $\mathcal{R}_1 - \mathcal{R}_3$, $\widetilde{\mathcal{R}}_4$, $\mathcal{R}_8 - \mathcal{R}_{10}$, and $\mathcal{R}_{\mathtt{SB}}$ with additional Rules provided by Wang et al. [2024b], Venkateswaran and Perković [2024], Wang et al. [2025a]. It is important to note that the completeness of $\widetilde{\mathcal{Q}_{\mathbf{X}}}$ remains an open problem. Therefore, $\widetilde{\mathcal{Q}_{\mathbf{X}}}$ is inadequate to completely characterize POMIS for PAGs.

Remark 2. Every $Q_{\mathbf{X}}^i$ is complete for orientations; for any $A \circ -* B$ in $Q_{\mathbf{X}}^i$, there are two MAGs \mathcal{M}_1 and \mathcal{M}_2 represented by $Q_{\mathbf{X}}^i$ containing $A \to B$ and $A \leftarrow *B$ respectively.

Moreover, even though we have access to $\mathcal{Q}_{\mathbf{X}}^*$ —a PMG that satisfies (1) the two conditions in Prop. 7 and (2) the orientation completeness— $\mathcal{Q}_{\mathbf{X}}^*$ is still insufficient to ensure $\mathbf{X} \subseteq \mathrm{An}(Y)_{\mathcal{Q}_{\mathbf{X}}^*}$. To witness, consider a PAG \mathcal{P} in Fig. 5 with $\mathbf{X} = \{A\}$.

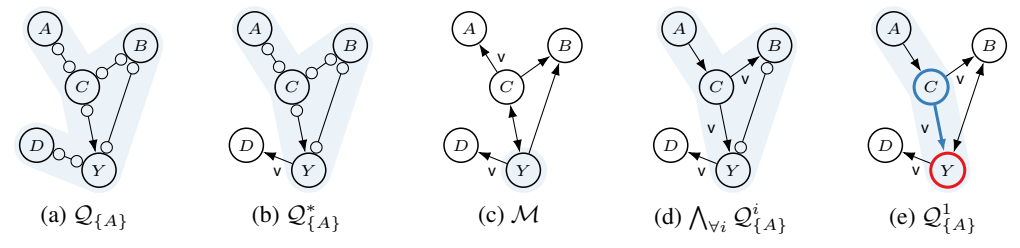


Figure 13: The light blue region indicates possible ancestors of Y. (a) PMG incorporating necessary conditions (Prop. 7) and (b) the PMG with orientation completeness. (c) MAG represented by $\mathcal{Q}_{\{A\}}$ while $A \notin \operatorname{An}(Y)_{\mathcal{M}}$. (d) PMG representing sound and complete orientations over MAGs satisfying that $\{A\}$ is an MIS. (e) PMG with $\mathbf{C}_{\{A\}}^{\mathcal{Q}_{\{A\}}} = \emptyset$ and $\mathbf{C}_{\{Y\}}^{\mathcal{Q}_{\{A\}}} = \{B\}$.

Then $C \circ \multimap Y$ in \mathcal{P} corresponds to $C \circ \multimap Y$ in $\mathcal{Q}_{\mathbf{X}}^*$, according to the first condition in Prop. 7 supported by the uncovered proper possibly directed path $A \circ \multimap C \circ \multimap Y$. Moreover, $Y \to D$ is oriented by \mathcal{R}_1 , and all remaining circle marks can vary across the underlying MAGs represented by $\mathcal{Q}_{\mathbf{X}}^*$. Here, we can find a MAG \mathcal{M} where $\mathbf{X} \notin \operatorname{An}(Y)_{\mathcal{M}}$ by orienting $C \circ \multimap Y$ as $C \leftrightarrow Y$, suggesting that additional information (orientation) is necessary.

Furthermore, neither $\mathcal{Q}_{\mathbf{X}}^*$ nor $\widetilde{\mathcal{Q}_{\mathbf{X}}}$ guarantees the *balanced property* (Lems 4 and 31). To witness, refer to $\mathcal{Q}_{\{C\}}^*$ (identical to $\widetilde{\mathcal{Q}_{\{C\}}}$). We can observe that there is $C \to Y \circ -\circ B$ while $C \circ -\circ B$, which violates the balanced property.

One might surmise that $\mathbf{X} = \mathsf{IB}(\mathcal{P}, Y, \mathbf{X})$ is an appropriate characterization of POMIS for PAGs. However, this approach does *not* hold. For illustration, consider the PAG \mathcal{P} in Fig. 5a and a set $\mathbf{X} = \{A\}$, which is a DMIS with respect to $[\![\mathcal{P},Y]\!]$. Moreover, we can simply derive $\mathsf{IB}(\mathcal{P},Y,\mathbf{X}) = \{A\}$, and thus $\mathbf{X} = \mathsf{IB}(\mathcal{P},Y,\mathbf{X})$ holds. For \mathbf{X} to be an MIS for a MAG \mathcal{M} represented by \mathcal{P} , the edge $A \circ - \circ C$ should correspond to $A \to C$ in \mathcal{M} , implying the visible edges $C \to B$ and $C \to Y$, as these are non-definite colliders (see \mathcal{M}_1 and \mathcal{M}_2 in Figs. 5b and 5c with Fig. 13d). Regardless of the edge orientation of $B \circ - \circ Y$, we find $\mathsf{IB}(\mathcal{M},Y,\mathbf{X}) = \{C\}$, as in Fig. 13e. Thus, $\mathbf{X} = \{A\}$ is not a POMIS with respect to $[\![\mathcal{M},Y]\!]$ for all $\mathcal{M} \in [\mathcal{P}]$. Therefore, $\mathsf{IB}(\mathcal{P},Y,\mathbf{X})$ fails to characterize POMIS.

E.2 Adaptive Learning: Simultaneous Discovery and Regret Minimization

A natural question is why we do not pursue adaptive discovery from online information. We address this point, beginning with relevant literature on *causal discovery with interventions*.

Offline discovery from interventions. In offline or non-adaptive setting, interventions are predetermined before algorithm execution. Hauser and Bühlmann [2012] studied the problem of learning graph structures from interventions under the assumption of no unobserved confounders, while Kocaoglu et al. [2017] explored experimental design for learning causal diagrams from interventions. Recently, Zhou et al. [2025] investigated learning PAGs from interventions.

Online discovery from interventions. While those offline causal discovery researches require access to infinite interventions, there has been intensive works that adaptively selects interventions from an online learning. Squires et al. [2020] and Choo and Shiragur [2023] applied interventions sequentially, with adaptively chosen targets at each step, still necessitating access to interventional distributions. Although Greenewald et al. [2019] and Elahi et al. [2024b] worked with finite interventions, it is applicable only when the underlying causal structure has no unobserved confounders. Notably, designing adaptive discovery algorithms that work with finite interventions and allow for unobserved confounders remains an open problem.

It may possible to incorporate online causal discovery into the decision-making process. For example, at each step, an agent can choose interventions aimed at improving structural knowledge, while also expecting that those arms could be valuable for minimizing regret. However, designing algorithms that effectively balance exploration for structure learning and for regret minimization poses substantial additional challenges, as these two objectives—structure discovery and regret minimization—are not naturally aligned.

Furthermore, Wang et al. [2022, 2023b] adaptively refine a PAG by resolving circle marks through targeted interventions. In this sense, interventions on nodes involved in circle marks can be useful for structural refinement. However, as noted in Wang et al. [2024a], obtaining a closed-form characterization of the number of MAGs compatible with a PAG—given a particular orientation of a circle mark—remains an open problem, implying that determining which circle marks to prioritize for learning is itself a challenging problem. As such, designing reliable algorithms that exploit structural uncertainty during learning involves solving nontrivial structure learning problems and remains an active area of research.

E.3 Comparison with Elahi et al. [2024a]

Elahi et al. [2024a] demonstrated that it is not necessary to learn the full causal diagram to identify all POMISs, and specified the extent of graphical structure that must be discovered to do so. Building on this insight, their work flow proceeds as follows: In the first phase, the method learns the induced subgraph of the ancestors of the reward node in an online manner, through interventions; Using the learned graph, they identify POMISs following the method of Lee and Bareinboim [2018]; Finally, they run standard independent MAB solvers with the identified POMISs.

In contrast, our work does not focus on causal discovery, but instead assumes access to a PAG (e.g., obtained via FCI [Spirtes et al., 2001b, Zhang, 2008a]) and aims to identify POMISs directly from this PAG. That is, given a PAG derived from purely observations, our algorithm prunes suboptimal arms *a priori*, without requiring any interventions for causal discovery. From a practical perspective, interventional data is often more costly and risk-prone than observational data. This suggests that our approach first discovering a PAG from observational data and then identifying POMISs may offer substantial advantages in resource-constrained or high-risk domains, compared to methods that rely on extensive intervention for graph discovery.

Since both our method and Elahi et al. [2024a] ultimately reduce the problem to standard bandits over a set of POMISs, their regret bounds in both approaches depend critically on the size of the resulting POMIS set (each denoted by $\mathcal{I}_{\mathcal{P}}$ and $\mathcal{I}_{\mathcal{G}}$). In Elahi et al. [2024a], the regret bound consists of a discovery term and a minimization: $\mathcal{O}(f(d_{\max}, \delta, \varepsilon)) + \mathcal{O}(\sum_{\mathbf{x} \in \mathcal{I}_{\mathcal{G}}} \Delta_{\mathbf{x}}(1 + \frac{\log T}{\Delta_{\mathbf{x}}^2}))^{11}$, whereas our regret bound contains only the minimization term: $\mathcal{O}(\sum_{\mathbf{x} \in \mathcal{I}_{\mathcal{P}}} \Delta_{\mathbf{x}}(1 + \frac{\log T}{\Delta_{\mathbf{x}}^2}))$. Since our approach avoids online causal discovery, our regret does not include the additional discovery term. However, because PAGs contain structural uncertainty (e.g., circle marks), the number of POMISs derived from a PAG is typically larger than that from a fully specified causal diagram. As a result, the bandit term of Elahi et al. [2024a] is usually smaller than ours. Therefore, although a direct comparison is difficult due to the different settings, the trade-off can be summarized as eliminating the online discovery cost at the expense of starting with a larger initial action space.

F Limitations and Future Works

In this section, we present limitations of our work and outline promising directions.

Modeling bandit instances in the form of SCMs. Structural Causal Models (SCMs) are a versatile and expressive framework that provides a principled way to represent and reason about causal relationships. Their generality makes them applicable across a wide range of domains. However, SCMs come with certain limitations, such as the assumption of a well-defined set of variables and a fixed causal structure, which may not adequately capture the complexity of dynamic, high-dimensional, or partially observed systems. Nonetheless, our work addresses a fundamental problem within the SCM framework. We believe it provides a solid foundation for future research, such as extending causal bandits to more complex or less structured environments.

Known partial ancestral graphs. We make the standard assumption that the deployment-phase learner has access to the true PAG representing the underlying causal diagram. In practice, while several causal discovery methods in the presence of latent confounders have been proposed [Spirtes et al., 2001a, Zhang, 2008a, Colombo et al., 2012, Rohekar et al., 2021, 2023], these techniques typically rely on accurate estimation of conditional independence (CI) relations. This would be especially true for constrained-based algorithms like FCI, where the exact PAG recovery would require many empirical conditional-independence tests to work perfectly. Therefore, our work implicitly assumes that the decision-maker possesses sufficient domain knowledge and statistical capability for reliable CI testing.

PAG misspecification. It is of great practical interest to study how MIS, DMIS and POMIS are affected given PAG misspecification. Notably, the edges in a PAG are governed by structural constraints and logical dependencies such as the balanced property and chordality. Due to the structured entanglements, it is indeed difficult to expect that computing POMISs on an incorrect PAG would yield robust results. Although our work is primarily theoretical and assumes access to the true PAG, we acknowledge that developing robust methodologies that account for such issues is a promising direction for future research.

¹¹where $d_{\rm max}$ denotes a constant greater than the maximal in-degree in the true causal diagram, and δ , ε represent some parameters. See Appendix A.13 of Elahi et al. [2024a] for further details.

Future work. In future research, given the availability of an observational distribution, it becomes possible to identify specific causal effects and eliminate suboptimal arms [Jaber et al., 2022]. Moreover, integrating this approach with partial identification [Balke and Pearl, 1995, Richardson et al., 2014, Zhang and Bareinboim, 2020, 2021, Zhang et al., 2022, Bellot, 2024], enables the exclusion of arms where the upper bound is less than the lower bound of another arm, as proposed by Zhang and Bareinboim [2017]. One can account for uncertainty in identification or bounds caused by a finite sample, which will lead to more robust analyzes [Bellot and Chiappa, 2024, Jung and Bellot, 2024]. Beyond causal bandits, we believe that ancestral graphical modeling offers practical value by integrating with causal reinforcement learning [Zhang and Bareinboim, 2022, Hwang et al., 2024, Bareinboim et al., 2024], rehearsal learning [Qin et al., 2023, 2025, Du et al., 2024, 2025, Tao et al., 2025] and sequential planning [Pearl and Robins, 1995a, Jung et al., 2024].

G Auxiliary Results

In this section, we provide auxiliary results utilized throughout the paper.

Lemma 25. Let \mathcal{P} be a PAG over \mathbf{V} , and let $\mathcal{P}[\mathbf{A}]$ be the subgraph of \mathcal{P} induced by $\mathbf{A} \subseteq \text{PossAn}(Y)_{\mathcal{P}} \subseteq \mathbf{V}$. If X and Z belong to different buckets over $\mathcal{P}[\mathbf{A}]$, then the starting edges of any uncovered proper possibly directed paths from X and Z to Y with respect to \mathbf{X} are not relevant.

Proof. Since X and Z are not in the same bucket, there is no circle path connecting the two nodes. Consequently, X and Z are not relevant.

Lemma 26. Let \mathcal{P} be a PAG over the set of variables \mathbf{V} . If a set $\mathbf{X} \subseteq \mathbf{V} \setminus \{Y\}$ is a DMIS relative to $[\![\mathcal{P},Y]\!]$, then there exists a MAG \mathcal{M} such that every $X \in \mathbf{X}$ has a proper directed path to Y with respect to \mathbf{X} in \mathcal{M} .

Proof. According to Prop. 5 and thm. 1, there exists a MAG \mathcal{M} such that $\mathbf{X} \subseteq \operatorname{An}(Y)_{\mathcal{M}_{\overline{\mathbf{X}}}}$. For the sake of contradiction, suppose that $\mathbf{X} \subseteq \operatorname{An}(Y)_{\mathcal{M}_{\overline{\mathbf{X}}}}$ holds while there is no proper directed path from $X \in \mathbf{X}$ to Y with respect to \mathbf{X} in \mathcal{M} . This implies that every directed path from X to Y must contain some node $Z \in \mathbf{X} \setminus \{X\}$. Consequently, such paths would be cut by the \mathbf{X} -lower manipulation, resulting in $X \notin \operatorname{An}(Y)_{\mathcal{M}_{\overline{\mathbf{X}}}}$. This contradicts the assumption that $\mathbf{X} \subseteq \operatorname{An}(Y)_{\mathcal{M}_{\overline{\mathbf{X}}}}$.

Lemma 27. Let Q be a PMG obtained from some valid local transformations from a PAG P and the orientation rules. In Q, the following property holds:

If $A \to B$ is visible, then every $A \to C$ is also visible for every C connected as circle path with B.

Proof. For the sake of contradiction, assume that there exists a node C such that $A \to C$ is invisible while connected as circle path with B.

First, let $D*\to A$ be an arbitrary edge that makes $A\to B$ visible. Since $A\to C$ is invisible, D and C must be adjacent and the edge is into C by the orientation rule \mathcal{R}_2 (i.e., $D*\to C$). According to Lem. 31, this implies the existence of $D*\to B$, which contradicts the assumption that $A\to B$ is visible.

Next, consider the path $D * \to V_1 \leftrightarrow \cdots \leftrightarrow V_n \leftrightarrow A$ with $n \geq 1$ where V_i is a parent of B. By Lem. 31, we get that there exist edges $V_i ? \to C$ for all V_i . Furthermore, these edges must take the form $V_i \to C$, because if any edges $V_i \circ \to C$ existed, \mathcal{R}'_4 would be triggered, resulting in $V_i \to C$. Therefore, $A \to C$ is also visible, leading to a contradiction for the assumption that $A \to C$ is invisible. This concludes the proof.

Lemma 28. Let Q be a PMG obtained from some valid local transformations from a PAG $\mathcal P$ and the orientation rules, and $\mathcal G$ be any causal diagram in the equivalence class represented by $\mathcal Q$. Let $X \neq Y$ be two nodes in $\mathbf A \subseteq \mathbf V(\mathcal Q)$. If X is an ancestor of Y in $\mathcal G[\mathbf A]$, then X is a possible ancestor of Y in $\mathcal G[\mathbf A]$.

Proof. The lemma follows the proof of Lem. 14 (Prop. 1 in Jaber et al. [2018]). If X is an ancestor of Y in $\mathcal{G}[\mathbf{A}]$, then there exists a directed path $X \to \cdots \to Y$ in $\mathcal{G}[\mathbf{A}]$. This path is also present in \mathcal{G} , and consequently in the corresponding MAG \mathcal{M} . Hence, the path corresponds to a possibly directed path in \mathcal{Q} . Since all nodes along the path are in \mathbf{A} , they are also present in $\mathcal{Q}[\mathbf{A}]$, implying X is a possible ancestor of Y in $\mathcal{Q}[\mathbf{A}]$.

Lemma 29. Let Q be a PMG obtained from some valid local transformations from a PAG \mathcal{P} and the orientation rules, and \mathcal{G} be any causal diagram in the equivalence class represented by Q. Let $X \neq Y$ be two nodes in $\mathbf{A} \subseteq \mathbf{V}(Q)$. For every $X \to Y$ in $Q[\mathbf{A}]$, if it is visible in Q, then it remains visible in $Q[\mathbf{A}]$.

Proof. The proof follows the argument of Lem. 15 (Lem 4. in Jaber et al. [2018]). Let \mathcal{G} defined over $\mathbf{V}(\mathcal{Q}) \cup \mathbf{L}$. Let $X \to Y$ be a visible edge in \mathcal{Q} where X and Y are in \mathbf{A} . Then, there is no inducing path between X and Y relative to \mathbf{L} that is into X in \mathcal{G} . It follows that no such inducing path (relative to the latent nodes in $\mathcal{G}[\mathbf{A}]$) exists in the subgraph $\mathcal{G}[\mathbf{A}]$.

Lemma 30. Let Q be a PMG obtained from some valid local transformations from a PAG P and the orientation rules, and G be any causal diagram in the equivalence class represented by Q. Let $X \neq Y$ be two nodes in $A \subseteq V(Q)$. If X and Y are in the same C-component in G[A], then X and Y are in the same C-component in C[A].

Proof. The proof follows the argument of Lem. 16 (Prop. 2 in Jaber et al. [2018]). If X and Y are in the same c-component in $\mathcal{G}[\mathbf{A}]$, then there is a bidirected path p in $\mathcal{G}[\mathbf{A}]$.

Lemma I (Lemma 6 in Jaber et al. [2018]). Let \mathcal{M} be a MAG over \mathbf{V} and \mathcal{G} be a causal diagram represented by \mathcal{M} . For any X and Y in \mathbf{V} , if there is a bidirected path p between X and Y in \mathcal{G} , then there is a path p' between X and Y in \mathcal{M} over a subsequence of p such that (1) all the non-endpoint nodes are colliders, and (2) all directed edges on p' are invisible.

Lemma II (Lemma 7 in Jaber et al. [2018]). Let \mathcal{M} be a MAG over V and \mathcal{P} be a PAG representing \mathcal{M} . For any X and Y in V, if there is a path p between X and Y in \mathcal{M} such that (1) all non-endpoint nodes are colliders and (2) all directed edges, if any, are not visible, then there is a path p^* between X and Y in \mathcal{P} over a subsequence of p such that (1) all non-endpoint nodes along the path are definite colliders, and (2) none of the edges are visible.

According to Lemma I, we choose a path p', which is the shortest subsequence of p between X and Y in \mathcal{M} , corresponding to p^* in \mathcal{P} , such that (1) all non-endpoint nodes along the path are colliders, and (2) none of the directed edges are visible. By Lemma II, the path p^* is a definite colliding path between X and Y, and none of the directed edges along the path are visible in \mathcal{P} . For contradiction, assume that p^{\dagger} in \mathcal{Q} , which is corresponding to p^* in \mathcal{P} , includes a visible edge out of X. Then, the visible edge would have to appear in all MAGs represented by \mathcal{Q} . However, the edge along p' is invisible in \mathcal{M} , leading to a contradiction. Therefore, p^{\dagger} is also of definite status, containing no visible edges, which implies that X and Y are in the same pc-component in \mathcal{Q} . Since all nodes along p^{\dagger} are in \mathbf{A} , p^{\dagger} is also present in $\mathcal{Q}[\mathbf{A}]$, ensuring that X and Y are in the same pc-component in $\mathcal{Q}[\mathbf{A}]$.

Lemma 31. Let \mathcal{Q} be a PMG obtained from some valid local transformations from a PAG \mathcal{P} and the orientation rules, and $\mathcal{Q}[\mathbf{A}]$ be the induced graph over $\mathbf{A} \subseteq \mathbf{V}(\mathcal{Q})$. For any three nodes A, B, C in \mathcal{Q} , if $A*\to B \circ -*C$, then there is an edge between A and C with an arrowhead at C, namely, $A*\to C$. Furthermore, if the edge between A and B is $A\to B$, then the edge between A and C is either $A\to C$ or $A\circ\to C$ (i.e., it is not $A\leftrightarrow C$).

Proof. The balanced property holds in the PMG with local transformations as shown in Thm. 8 (Theorem 1 in Wang et al. [2023b]). By the definition of an induced graph, this property is preserved in Q[A].

Lemma 32. Let Q be a PMG obtained from some valid local transformations from a PAG P and the orientation rules. In a PMG Q, for any two nodes A and B, if there is a circle path, then following holds:

- 1. If there is an edge between A and B, the edge is not into A or B;
- 2. For any other node C, $C*\to A$ if and only if $C*\to B$. Furthermore, $C\leftrightarrow A$ if and only if $C\leftrightarrow B$.

Proof. The proof follows the argument of Lem. 5 (Lem 3.3.2 in Zhang [2006]). The properties depend on the balanced property in Lem. 4, which holds in Q as demonstrated in Thm. 8 and lem. 31.

Lemma 33. Let Q be a PMG obtained from some valid local transformations from a PAG P and the orientation rules. PTO (Alg. 2) is also sound over Q[A], in the sense that the partial order is valid with respect to G[A], for every causal diagram G in the equivalence class represented by Q.

Proof. The proof follows the argument of Lem. 17 (Prop. 4 in Jaber et al. [2018]). By Lem. 28, the possible-ancestral relations in $\mathcal{Q}[\mathbf{A}]$ subsume those in $\mathcal{G}[\mathbf{A}]$. Hence, a partial topological order that is valid with respect to $\mathcal{Q}[\mathbf{A}]$ is also valid with respect to $\mathcal{G}[\mathbf{A}]$. The correctness of Alg. 2 relies solely on the balanced property, which is satisfied in the PMG with local transformations as per Thm. 8 and lem. 31. Thus, the algorithm is also sound with respect to $\mathcal{Q}[\mathbf{A}]$.

H Proofs

In this section, we provide detailed proofs of the propositions and theorems presented in the main body of the paper. For readability, we restate all of them.

Theorem 1 (Characterization of MIS for MAGs). Let \mathcal{M} be a MAG over \mathbf{V} . Given information $[\![\mathcal{M},Y]\!]$, a set $\mathbf{X} \subseteq \mathbf{V} \setminus \{Y\}$ is an MIS relative to $[\![\mathcal{M},Y]\!]$ if and only if $\mathbf{X} \subseteq \mathtt{An}(Y)_{\mathcal{M}_{\overline{\mathbf{v}}}}$ holds.

Proof. (**If**) Suppose that **X** is *not* an MIS relative to $[\![\mathcal{M},Y]\!]$. This implies that there exists some $\mathbf{X}' \subsetneq \mathbf{X}$ such that $\mu_{\mathbf{x}[\mathbf{X}']} = \mu_{\mathbf{x}}$ for every SCM conforming to the MAG \mathcal{M} . For the sake of contradiction, assume that $\mathbf{X} \subseteq \operatorname{An}(Y)_{\mathcal{M}_{\overline{\mathbf{X}}}}$. To derive a contradiction, it suffices to construct a SCM such that $\mu_{\mathbf{x}[\mathbf{X}']} \neq \mu_{\mathbf{x}}$. Consider the causal diagram \mathcal{G} generated by the following procedure:

Step 1. If $A \to B$ in M, then add a directed edge $A \to B$ to G.

Step 2. If $A \leftrightarrow B$ in \mathcal{M} , then add a bidirected edge $A \leftrightarrow B$ to \mathcal{G} .

From this construction, it is clear that the causal diagram \mathcal{G} corresponds to \mathcal{M} . Furthermore, we have $\mathbf{X} \subseteq \operatorname{An}(Y)_{\mathcal{G}_{\overline{\mathbf{X}}}}$ since \mathcal{G} and \mathcal{M} have the exact same edges.

Now consider the following SCM associated with \mathcal{G} : Each variable in $V_i \in \mathbf{V}(\mathcal{G})$ is associated with a unique latent variable U_i and the function of each endogenous variable in $\mathbf{V}(\mathcal{G})$ is the sum of the

value of its parents. Since $\mathbf{X} \subseteq \mathrm{An}(Y)_{\mathcal{G}_{\overline{\mathbf{X}}}}$ holds, there exist directed paths from $\mathbf{X} \setminus \mathbf{X}'$ to Y without passing through \mathbf{X}' . Let $\mathbf{W} = \mathbf{X} \setminus \mathbf{X}'$. Then, setting \mathbf{W} to $\mathbb{E}[\mathbf{W} \mid do(\mathbf{x}')] + 1$ results in a larger outcome value for Y, i.e., $\mu_{\mathbf{x}} = \mu_{\mathbf{w},\mathbf{x}'} > \mu_{\mathbf{x}[\mathbf{X}']}$, which leads to a contradiction.

(**Only if**) Suppose that $\mathbf{X} \not\subseteq \operatorname{An}(Y)_{\mathcal{M}_{\overline{\mathbf{X}}}}$ holds. This indicates that there exists a nonempty subset $\mathbf{Z} \triangleq \mathbf{X} \setminus \operatorname{An}(Y)_{\mathcal{M}_{\overline{\mathbf{X}}}}$. Let $\mathbf{X}' = \mathbf{X} \setminus \mathbf{Z}$. Our goal is to show that Y and \mathbf{Z} are m-separated by \mathbf{X}' in $\mathcal{M}_{\overline{\mathbf{X}}}$. Once established, we can apply Rule 3 of do-calculus for MAGs [Zhang, 2008b] to derive $\mu_{\mathbf{X}'} = \mu_{\mathbf{X}',\mathbf{Z}}$.

For contradiction, assume that there exists some variable $Z \in \mathbf{Z}$ such that Z and Y are m-connected conditioning on \mathbf{X}' in $\mathcal{M}_{\overline{\mathbf{X}}}$. This means the existence of a m-connected path p between Z and Y. Since Z has its incoming edges removed, p must start with an edge outgoing from Z. If there were any collider along the path, it would be m-separated, as the collider cannot be an ancestor of a conditioned node \mathbf{X}' . However, if the path p begins with an outgoing edge from Z and has no colliders, then it must be a directed path from Z to Y. This implies that $Z \in \operatorname{An}(Y)_{\mathcal{M}_{\overline{\mathbf{X}}}}$ holds, thus \mathbf{Z} and Y are not m-separated by \mathbf{X}' in $\mathcal{M}_{\overline{\mathbf{X}}}$, leading to a contradiction. Consequently, we have that \mathbf{X} is not an MIS relative to $[\![\mathcal{M},Y]\!]$.

Proposition 1. Let \mathcal{M} be a MAG over \mathbf{V} . A set $\mathbf{X} \subseteq \mathbf{V} \setminus \{Y\}$ is an MIS relative to $[\![\mathcal{M},Y]\!]$ if and only if there exists a causal diagram \mathcal{G} conforming to \mathcal{M} such that \mathbf{X} is an MIS relative to $[\![\mathcal{G},Y]\!]$.

Proof. (**If**) Let **X** be an MIS relative to $[\![\mathcal{G},Y]\!]$ for some causal diagram \mathcal{G} conforming to \mathcal{M} . By the definition of MIS for causal diagrams in Def. 10, there is no $\mathbf{X}' \subseteq \mathbf{X}$ such that for all SCM conforming to \mathcal{G} , $\mu_{\mathbf{x}[\mathbf{X}']} = \mu_{\mathbf{x}}$. In other words, for every $\mathbf{X}' \subseteq \mathbf{X}$, there exists an SCM \mathcal{S} conforming to \mathcal{G} such that $\mu_{\mathbf{x}[\mathbf{X}']} \neq \mu_{\mathbf{x}}$. Since any SCM conforming to \mathcal{G} also conforms to \mathcal{M} , we know that \mathcal{S} also conforms to \mathcal{M} . Thus, for any proper subset $\mathbf{X}' \subseteq \mathbf{X}$, there exists an SCM associated with \mathcal{M} in which $\mu_{\mathbf{x}[\mathbf{X}']} = \mu_{\mathbf{x}}$ holds.

(**Only if**) Let **X** be an MIS relative to $[\![\mathcal{M},Y]\!]$. The causal diagram \mathcal{G} constructed in the same manner as in the proof of thm. 1 conforms to \mathcal{M} and satisfies $\mathbf{X} \subseteq \operatorname{An}(Y)_{\mathcal{G}_{\overline{\mathbf{X}}}}$. Therefore, we can conclude that **X** is an MIS relative to $[\![\mathcal{G},Y]\!]$ supported by Prop. 9.

Proposition 2 (Graphical characterization of MIS for PAGs). *Let* \mathcal{P} *be a PAG over the set of variables* \mathbf{V} . A set $\mathbf{X} \subseteq \mathbf{V} \setminus \{Y\}$ is an MIS relative to $[\![\mathcal{P},Y]\!]$ if and only if, for every variable $X \in \mathbf{X}$, there exists a proper possibly-directed path from X to Y with respect to \mathbf{X} in \mathcal{P} .

Proof. (If) Suppose that \mathbf{X} is *not* an MIS relative to $[\![\mathcal{P},Y]\!]$, which implies that there exists some proper subset $\mathbf{X}' \subsetneq \mathbf{X}$ such that $\mu_{\mathbf{x}[\mathbf{X}']} = \mu_{\mathbf{x}}$ for every SCM conforming to \mathcal{P} . For contradiction, suppose that for all $X \in \mathbf{X}$, there exist proper possibly-directed paths from X to Y with respect to \mathbf{X} in \mathcal{P} . Let $\mathbf{W} = \mathbf{X} \setminus \mathbf{X}'$ and W be a vertex in \mathbf{W} . Suppose that p is an uncovered proper possibly-directed path from W to Y with respect to \mathbf{X} in \mathcal{P} . Let $\mathcal{M} \in [\mathcal{P}]$ be a MAG constructed by the following procedure:

- Step 1. Orient all edges along p as directed edges.
- Step 2. Orient the remaining edges according to Lem. 6.

Then, p corresponds to a proper directed path from W to Y with respect to \mathbf{X} in \mathcal{M} . Thus, $W \in \operatorname{An}(Y)_{\mathcal{M}_{\overline{\mathbf{X}}}}$ holds. We can then use the same construction in the proof of Thm. 1. In the constructed causal diagram $\mathcal{G}, W \in \operatorname{An}(Y)_{\mathcal{G}_{\overline{\mathbf{X}}}}$ holds. Furthermore, we know there exists an SCM \mathcal{S} in which W has a positive causal effect on Y which is not mediated by any variable in \mathbf{X} . Thus, setting \mathbf{W} to $\mathbb{E}[\mathbf{W} \mid do(\mathbf{x}')] + 1$ will result in a larger outcome for Y, i.e., $\mu_{\mathbf{x}} = \mu_{\mathbf{w},\mathbf{x}'} > \mu_{\mathbf{x}[\mathbf{X}']}$, meaning $\mu_{\mathbf{x}} \neq \mu_{\mathbf{x}[\mathbf{X}']}$, which contradicts the statement: $\mu_{\mathbf{x}[\mathbf{X}']} = \mu_{\mathbf{x}}$ for every SCM conforming to \mathcal{D}

(Only if) Suppose that for some $Z \in \mathbf{X}$, there is no proper possibly directed path from Z to Y with respect to \mathbf{X} in \mathcal{P} . Let $\mathbf{X}' = \mathbf{X} \setminus \{Z\}$. We aim to show that $P(y \mid do(\mathbf{x}')) = P(y \mid do(\mathbf{x}', z))$,

which would imply $\mu_{\mathbf{x}'} = \mu_{\mathbf{x}',z}$. Unfortunately, we cannot apply Rule 3 of do-calculus for PAGs, since it is not guaranteed that X and Y are definitely m-separated by \mathbf{X}' in $\mathcal{P}_{\overline{\mathbf{X}}}$. However, we can reason over the MAGs in the Markov equivalence class represented by \mathcal{P} .

All paths from Z to Y in $\mathcal P$ which do not pass through $\mathbf X$ must not be a directed path due to our assumption, i.e., they all contain an arrowhead pointing towards Z. Let $\mathcal M$ be a MAG conforming to $\mathcal P$. Then, all paths from Z to Y in $\mathcal M$ which do not pass through $\mathbf X$ must also be non-directed. Thus, using similar reasoning as in the proof of Thm. 1, Z and Y are m-separated by $\mathbf X'$ in $\mathcal M_{\overline{\mathbf X}}$. This is because any path out of Z to Y must contain a collider node, which must be blocked, since it cannot be an ancestor of any conditioned node. Therefore, we conclude that $P(y \mid do(\mathbf x')) = P(y \mid do(\mathbf x', z))$. Since this argument holds for every MAG conforming to $\mathcal P$, it holds for all SCMs conforming to $\mathcal P$.

Proposition 4. Let \mathcal{D} be either a causal diagram or a MAG (i.e., not a PAG). If \mathbf{X} is an MIS with respect to $[\![\mathcal{D},Y]\!]$, then \mathbf{X} is a DMIS with respect to $[\![\mathcal{D},Y]\!]$.

Proof. Without loss of generality, assume that all nodes in \mathcal{D} are ancestors of Y. For contradiction, assume that \mathbf{X} is an MIS but *not* a DMIS relative to $[\![\mathcal{D},Y]\!]$. By Thm. 1 and prop. 9, we have $\mathbf{X} \subseteq \mathrm{An}(Y)_{\mathcal{D}_{\overline{\mathbf{X}}}}$. Then, we can consider an SCM \mathcal{S}^* compatible with \mathcal{D} , where all mechanisms consist of the sum of the values of their parents, i.e., $f_V = \sum_{|\mathbf{pa}_V|} \mathbf{pa}_V + \mathbf{u}_V$. Let \mathbf{X}' be an arbitrary proper subset of \mathbf{X} , and \mathbf{W} denote $\mathbf{X} \setminus \mathbf{X}'$. Such a model \mathcal{S}^* always ensures that setting \mathbf{W} as $\mathbb{E}[\mathbf{W} \mid do(\mathbf{x}')] + 1$ results in $\mu_{\mathbf{x}} = \mu_{\mathbf{w},\mathbf{x}'} > \mu_{\mathbf{x}[\mathbf{X}']}$ for any proper subset \mathbf{X}' since there exist directed paths from each $W \in \mathbf{W}$ to Y without passing through \mathbf{X}' . The existence of \mathcal{S}^* leads to a contradiction.

Proposition 5. Let \mathcal{P} be a PAG over \mathbf{V} . A set $\mathbf{X} \subseteq \mathbf{V} \setminus \{Y\}$ is a DMIS relative to $[\mathcal{P}, Y]$ if and only if there exists a MAG \mathcal{M} conforming to \mathcal{P} such that \mathbf{X} is an MIS relative to $[\mathcal{M}, Y]$.

Proof. (If) Suppose $\mathbf{X} \subseteq \mathbf{V} \setminus \{Y\}$ be an MIS relative to $[\![\mathcal{P},Y]\!]$, and there exists a MAG \mathcal{M} conforming to \mathcal{P} where \mathbf{X} is an MIS relative to $[\![\mathcal{M},Y]\!]$. By Prop. 4, \mathbf{X} is a DMIS relative to $[\![\mathcal{M},Y]\!]$. Hence, there exists an SCM \mathcal{S} such that for any proper subset \mathbf{X}' , $\mu_{\mathbf{x}[\mathbf{X}']} \neq \mu_{\mathbf{x}}$ holds. Since \mathcal{S} conforms to \mathcal{M} , it also conforms to \mathcal{P} , thus concluding proof for this direction.

(**Only if**) Suppose $\mathbf{X} \subseteq \mathbf{V} \setminus \{Y\}$ be a DMIS relative to $[\![\mathcal{P},Y]\!]$. By the definition of DMIS (2), there exists an SCM \mathcal{S} associated with \mathcal{P} such that, for every $\mathbf{X}' \subsetneq \mathbf{X}$, $\mu_{\mathbf{x}[\mathbf{X}']} \neq \mu_{\mathbf{x}}$ holds. Therefore, \mathbf{X} is an MIS, since for any proper subset \mathbf{X}' , $\mu_{\mathbf{x}[\mathbf{X}']} \neq \mu_{\mathbf{x}}$ holds under the SCM \mathcal{S} .

Theorem 2 (Graphical characterization of DMIS for PAGs). Let \mathcal{P} be a PAG over the set of variables \mathbf{V} . A set $\mathbf{X} \subseteq \mathbf{V} \setminus \{Y\}$ is a DMIS relative to $[\![\mathcal{P},Y]\!]$ if and only if, for any pair of vertices $X,Z \in \mathbf{X}$, there exist uncovered proper possibly-directed paths from X and Z to Y with respect to \mathbf{X} such that their starting edges are not relevant.

Proof. (If) Let p_X denote an uncovered proper possibly-directed path from X to Y with respect to X in \mathcal{P} . Suppose that X is *not* a DMIS, implying that, for all MAGs $\mathcal{M} \in [\mathcal{P}]$, it holds that $Z \notin \operatorname{An}(Y)_{\mathcal{M}_{\overline{X}}}$ and $X \in \operatorname{An}(Y)_{\mathcal{M}_{\overline{X}}}$ without loss of generality. In other words, if orienting p_X as $X \to \cdots \to Y$ is valid, it follows that orienting any possibly directed path from Z to Y as $Z \to \cdots \to Y$ is invalid in all MAGs conforming to \mathcal{P} . We will show that the starting edge of p_X is relevant to the starting edge of any uncovered possibly-directed path from Z to Y in \mathcal{P} .

Let p_Z be an arbitrary uncovered proper possibly-directed path from Z to Y with respect to X in \mathcal{P} . Note that such a path always exists, as established by Lem. 7. We know that the path p_Z must begin with one of the following edges: $\circ - \circ$, $\circ - \rightarrow$, or \rightarrow . We will show that p_Z can *only* start with a circle edge $(\circ - \circ)$.

(p_Z only starts with a circle edge (\circ - \circ)). Suppose p_Z starts with $^?$ \rightarrow . Then, the path must take the form Z $^?$ $\rightarrow \cdot \rightarrow \cdots \rightarrow Y$ in \mathcal{P} by Lem. 8. In this case, we can construct a valid \mathcal{M} by orienting any

circle marks (\circ) along the path as tails (-) following Lem. 6. This contradicts the assumption that there is no MAG conforming \mathcal{P} in which p_Z is a directed path from Z to Y. Therefore, we conclude that p_Z only can be $Z \circ - \circ \cdots * - *Y$.

For the sake of contradiction, assume $e_X(X*-*X')$ is not relevant to $e_Z(Z'\circ -\circ Z)$ where each denotes the starting edges of p_X and p_Z respectively; Then, we consider the following two cases separately: ① X and Z are *not* in the same bucket, or ② they are in the same bucket, and every circle path including e_X and e_Z is not uncovered, i.e., they are *not* relevant.

- (① X and Z do not belong to the same bucket). Consider the orientation according to Lem. 6. In the second step of the construction, we always have a MAG $\mathcal M$ containing $Z \to Z'$ by the completeness of orientation in PAGs, which indicates p_Z corresponds to a directed path from Z to Y in $\mathcal M$, as it is uncovered. Therefore, we can construct a valid $\mathcal M$ according to Lem. 6, contradicting the assumption that $Z \notin \operatorname{An}(Y)_{\mathcal M_{\overline{\mathbf x}}}$ for all MAGs $\mathcal M \in [\mathcal P]$.
- (② X and Z are in the same bucket). Suppose that X and Z are in the same bucket. Let $V_1(=X) \circ \multimap V_2(=X') \circ \multimap \cdots \circ \multimap V_{n-1}(=Z') \circ \multimap V_n(=Z)$ be an arbitrary non-uncovered circle path between X and Z in \mathcal{P} . By the definition of an uncovered circle path, such a path must include at least one non-uncovered triple $\langle V_i, V_{i+1}, V_{i+2} \rangle$ on the circle path. The existence of an edge between $V_i \circ \multimap V_{i+2}$ would induce an uncovered circle path $V_1 \circ \multimap \circ V_i \circ \multimap V_{i+2} \circ \multimap \circ \multimap \circ V_n$. To avoid this, X and X must be adjacent, and furthermore, the edge connecting X and X must appear as a circle edge $X \circ \multimap Z$ by Lem. 11.

The existence of the edge $X \circ \multimap Z$ implies that there must be edges $X \circ \multimap V_i$ for all $3 \le i \le n-1$, or $Z \circ \multimap V_i$ for all $2 \le i \le n-2$ by chordality. In the former case, we orient the subgraph of $\mathcal P$ over $\{V_1, \cdots, V_n\}$ following a similar approach to the proof of Lemma 7.6 in Maathuis and Colombo [2015]. We begin by selecting a vertex V_2 and orient all edges incident to V_2 as directed into V_2 . Since the subgraph is chordal and V_2 is simplicial, this orientation does not create any uncovered colliders in the subgraph. We then remove V_2 and the oriented edges from the subgraph. The resulting graph remains chordal and therefore again choose a vertex V_3 , and orient any edges incident to V_3 into V_3 . We continue this procedure until all edges are oriented. The constructed subgraph does not create any directed cycle, almost directed cycle, or uncovered collider, thus it is valid orientations. Since $X \to X' \to \cdots \to Y$ is valid, we have a directed path $Z \to Z' \to \cdots \to X' \to \cdots \to Y$ which leads to a contradiction.

In the latter case, we can similarly orient the edges, starting from V_{n-1} and proceeding to V_2 . Furthermore, this procedure can also be extended to cases where the graph takes on a superimposed form.

(**Only if**) Suppose that e_X is relevant to e_Z in \mathcal{P} . It follows that $V_1(=X) \circ \multimap V_2(=X') \circ \multimap \cdots \circ \multimap V_{n-1}(=Z') \circ \multimap V_n(=Z)$ is an uncovered circle path. For the sake of contradiction, assume that \mathbf{X} is a DMIS relative to $[\![\mathcal{P},Y,]\!]$. Then, there exists a MAG \mathcal{M} conforming to \mathcal{P} such that both p_X and p_Z are proper directed paths with respect to \mathbf{X} in \mathcal{M} . Therefore, we can orient $V_1 \circ \multimap V_2$ as $V_1 \to V_2$, and $V_n \circ \multimap V_{n-1}$ as $V_n \to V_{n-1}$ to construct \mathcal{M} from \mathcal{P} . Furthermore, since the circle path is uncovered, $V_i \circ \multimap V_{i+1}$ must be oriented $V_i \to V_{i+1}$ for $i=2,\cdots,n-2$. However, this orientation introduces a new uncovered collider $V_{n-2} \to V_{n-1} \leftarrow V_n$, which leads to a contradiction. \square

Theorem 3 (Graphical characterization of POMIS for MAGs). Let \mathcal{M} be a MAG over the set of variable \mathbf{V} . A set $\mathbf{X} \subseteq \mathbf{V} \setminus \{Y\}$ is a POMIS relative to $[\![\mathcal{M},Y]\!]$ if and only if $\mathbf{X} = \mathsf{IB}(\mathcal{M},Y,\mathbf{X})$.

Proof. (Only if) We will show contrapositive, i.e., if $\mathbf{X} = \mathsf{IB}(\mathcal{M}, Y, \mathbf{X})$ does not hold, then \mathbf{X} is not a POMIS relative to $[\![\mathcal{M}, Y]\!]$. We denote $\mathbf{W} = \mathsf{IB}(\mathcal{M}, Y, \mathbf{X})$ and $\mathbf{T} = \mathsf{MUCT}(\mathcal{M}, Y, \mathbf{X})$, assuming $\mathbf{X} \neq \mathbf{W}$. Let $\mathbf{W}' \triangleq \mathbf{W} \setminus \mathbf{X}$. Before proceeding with the main proof, we first establish that the following conditional independence statement holds:

Claim 1.
$$(Y \perp \!\!\! \perp \mathbf{W}' \mid \mathbf{X})$$
 holds in $\mathcal{M}_{\overline{\mathbf{X}}\mathbf{W}'}^{12}$.

¹²Note that lower-manipulation has a higher priority than upper-manipulation so that $\mathcal{Q}_{\overline{X}\underline{Y}}$ or $\mathcal{Q}_{\underline{Y}\overline{X}}$ denotes the graph resulting from applying the **X**-upper-manipulation to the **Y**-lower-manipulated graph of \mathcal{Q} .

Proof. Suppose that the negation of this statement holds: $(Y \not\perp \mathbf{W}' \mid \mathbf{X})$ in $\mathcal{M}_{\overline{\mathbf{X}}\mathbf{W}'}$. This would imply that there exists an m-connected path from some $W \in \mathbf{W}'$ to Y given \mathbf{X} in $\mathcal{M}_{\overline{\mathbf{X}}\mathbf{W}'}$. For the m-connected path to exist, there must be no colliders, as no node along the path can be an ancestor of X due to all incoming edges to X being cut in $\mathcal{M}_{\overline{\mathbf{X}}}$. Moreover, as all outgoing edges from W' are cut in $\mathcal{M}_{W'}$, the path cannot begin with an edge going out of W. Therefore, we get that the m-connected path must be of the following form: $W \leftarrow W_1 \leftarrow \cdots \leftarrow W_n \leftrightarrow R_1 \rightarrow \cdots \rightarrow R_1 \rightarrow R_1 \rightarrow R_2 \rightarrow R_2$ $\cdots \to R_m \to Y$ with $n, m \ge 0$ where no node along the path can be in W; otherwise, it would either be part of X, since we are conditioning on X, or in W', in which case all of its outgoing arrows would have been removed. Since Y is contained in T, the parent of Y, R_m , along the path must be either in T or W. However, as previously argued, no node along the path can be in W; therefore, it must be in T. This reasoning can be applied iteratively up to R_1 , implying that R_1 is also in T. Since T is closed under PC, the inclusion of R_1 in T implies that W_n must also be in T. Additionally, because T is closed under descendants, W_{n-1}, \dots, W_1 must also be in T. Consequently, W must be in T as well. However, this leads to a contradiction, since W is in W, and W and T are disjoint by definition. Therefore, the conditional independence statement $(Y \perp \!\!\! \perp \mathbf{W}' \mid \mathbf{X})$ must hold in $\mathcal{M}_{\overline{\mathbf{X}}\mathbf{W}'}$.

Claim 2.
$$(Y \perp \!\!\! \perp \mathbf{X}' \mid \mathbf{W})$$
 holds in $\mathcal{M}_{\overline{\mathbf{W}},\overline{\mathbf{X}'}}$ where $\mathbf{X}' \triangleq \mathbf{X} \setminus \mathbf{W}$.

Proof. Suppose this statement is *false*, i.e., $(Y \not\perp \mathbf{X}' \mid \mathbf{W})$ holds in $\mathcal{M}_{\overline{\mathbf{W}},\overline{\mathbf{X}'}}$. Then, there exists an m-connected path from some $X \in \mathbf{X}'$ to Y given \mathbf{W} in $\mathcal{M}_{\overline{\mathbf{W}},\overline{\mathbf{X}'}}$. Since all edges into \mathbf{X}' are removed, the path must begin with an edge going out of X. The path cannot contain any colliders, as no node can be an ancestor of a node in the conditioned set \mathbf{W} , given that all incoming edges to \mathbf{W} are cut. Thus, all edges along the path must be directed, pointing to Y: $X \to W_1 \to \cdots \to W_n \to Y (n \geq 0)$ where no node along the path can be in \mathbf{W} , since we are conditioning on \mathbf{W} . The parent of Y, W_n , along the path must be either in \mathbf{T} or \mathbf{W} , as Y in T. However, as previously argued, no node along the path can be included in \mathbf{W} , which means it must be in \mathbf{T} . This reasoning can be applied iteratively up to W_1 , implying that W_1 is also in \mathbf{T} . Therefore, X must be a parent of a node in \mathbf{T} , implying that X is in \mathbf{W} . This leads to a contradiction for $X \in \mathbf{X} \setminus \mathbf{W}$.

We are now ready to proceed to the main proof. We will show that X is *not* a POMIS by proving that $\mu_{X^*} \leq \mu_{W^*}$ in every SCM conforming to \mathcal{M} . We derive that the following holds:

$$\begin{split} \mu_{\mathbf{x}^*} &= \mathbb{E}[Y \mid do(\mathbf{x}^*)] \\ &= \sum_{\mathbf{w}'} \mathbb{E}[Y \mid do(\mathbf{x}^*), \mathbf{w}'] P(\mathbf{w}' \mid do(\mathbf{x}^*)) \\ &= \sum_{\mathbf{w}'} \mathbb{E}[Y \mid do(\mathbf{x}^*), do(\mathbf{w}')] P(\mathbf{w}' \mid do(\mathbf{x}^*)) \\ &= \sum_{\mathbf{w}'} \mathbb{E}[Y \mid do(\mathbf{x}^*[\mathbf{W}]), do(\mathbf{w}')] P(\mathbf{w}' \mid do(\mathbf{x}^*)) \\ &\leq \sum_{\mathbf{w}'} \mathbb{E}[Y \mid do(\mathbf{w}')] P(\mathbf{w}' \mid do(\mathbf{x}^*)) \\ &= \mathbb{E}[Y \mid do(\mathbf{w}^*)] \\ &= \mu_{\mathbf{w}^*}. \end{split}$$

Therefore, **X** is *not* a POMIS with respect to [M, Y], which completes the proof.

(If) To prove this direction, we will show that if $\mathbf{X} = \mathsf{IB}(\mathcal{M}, Y, \mathbf{X})$, then \mathbf{X} is a POMIS relative to $[\![\mathcal{M}, Y]\!]$. Suppose that $\mathbf{X} = \mathsf{IB}(\mathcal{M}, Y, \mathbf{X})$ holds. It suffices to show that there exists a causal diagram \mathcal{G} such that \mathbf{X} is a POMIS relative to $[\![\mathcal{G}, Y]\!]$. Consider the causal diagram \mathcal{G} constructed by the following lemma:

Lemma 34. Let \mathcal{M} be a MAG. Let \mathcal{G} be the graph resulting from the following procedure applied to \mathcal{M} .

Step 1. For each visible edge $A \to B$ in M, add $A \to B$ in G.

- Step 2. For each bidirected edge $A \leftrightarrow B$ in \mathcal{M} , add $A \leftrightarrow B$ in \mathcal{G} .
- Step 3. For each invisible directed edge $A \to B$ in M, if it is the unique invisible edge among directed edges outgoing from A in M, then add both a directed edge $A \to B$ and bidirected edge $A \leftrightarrow B$ to G.
- Step 4. Let $\mathbf{T}_{\mathcal{G}} \triangleq \mathsf{MUCT}(\mathcal{G}, Y)$. Consider all nodes A for which there are invisible edges outgoing from A in \mathcal{M} .
 - 1. If there exists $B \in Ch(A)_{\mathcal{M}}$ that is contained in $\mathbf{T}_{\mathcal{G}}$, add both a directed edge $A \to B$ and bidirected edge $A \leftrightarrow B$, and add directed edges $A \to C$ for all $C \in Ch(A)_{\mathcal{M}} \setminus \{B\}$.
 - 2. Otherwise, if there is no intersection with T_G , add directed edges $A \to C$ for all $C \in Ch(A)_M$.

This step is repeated with the updated $\mathbf{T}_{\mathcal{G}} \leftarrow \mathsf{MUCT}(\mathcal{G}, Y)$ as long as \mathcal{G} remains unchanged.

Then, the result graph G is a causal diagram conforming to M.

Proof. We need to show that \mathcal{G} and \mathcal{M} have the same ancestral relations, and the same conditional independence relations.

- (1) \mathcal{G} and \mathcal{M} have the same ancestral relations). This is evident, as each directed edge is added to \mathcal{G} if and only if it also exists in \mathcal{M} .
- (② \mathcal{G} and \mathcal{M} encode the same independence relations). The graphs \mathcal{G} and \mathcal{M} differ only in the bidirected edges added to \mathcal{G} corresponding to invisible edges in \mathcal{M} . Thus, it suffices to show that these additional bidirected edges added to \mathcal{G} do not encode any additional independence between variables. Therefore, we need to show that these edges do not create any new uncovered colliders.

Consider a bidirected edge $A \leftrightarrow B$ added to \mathcal{G} in **Step 3**. For this added edge to create a collider, there must be either a directed edge incoming to A (i.e., $C \to A \leftrightarrow B$), or bidirected edge incoming to A (i.e., $C \leftrightarrow A \leftrightarrow B$) in \mathcal{G} . In both cases, B and C are adjacent in \mathcal{M} , since $A \to B$ is invisible in \mathcal{M} by Lem. 19. Therefore, this collider at A does not introduce any new independence.

Now consider a bidirected edge $A \leftrightarrow B$ added to $\mathcal G$ in **Step 4**. The previous argument can be reused here to argue that this edge does not encode any new independence, since we add only one bidirected among outgoing directed edges from A. For clarity, suppose that we have a MAG $\mathcal M = \langle A \to B, A \to B, A \to D \rangle$ where B, C, and D are mutually not adjacent in $\mathcal M$. Adding at most one of $A \leftrightarrow C$, $A \leftrightarrow B$, or $A \leftrightarrow D$ does not introduce a new collider at A, thereby preserving conditional independence.

Let \mathcal{G} be the causal diagram constructed following Lem. 34. We will prove that \mathbf{X} is a POMIS with respect to $[\![\mathcal{G},Y]\!]$. Let X be any variable in \mathbf{X} . Then X is a parent of some $T \in \mathsf{MUCT}(\mathcal{M},Y,\mathbf{X})$ in \mathcal{M} . It suffices to show that $T \in \mathsf{MUCT}(\mathcal{G}_{\overline{\mathbf{X}}},Y)$ since this means that X is a parent of a member of $\mathsf{MUCT}(\mathcal{G}_{\overline{\mathbf{X}}},Y)$, and is therefore in $\mathsf{IB}(\mathcal{G}_{\overline{\mathbf{X}}},Y)$.

Let $\mathbf{T}_{\mathcal{G}} \triangleq \mathsf{MUCT}(\mathcal{G},Y)$ and $\mathbf{T}_{\mathcal{M}} \triangleq \mathsf{MUCT}(\mathcal{M},Y,\emptyset)$. We will show that $\mathbf{T}_{\mathcal{M}} \subseteq \mathbf{T}_{\mathcal{G}}$. Let T be a node in $\mathbf{T}_{\mathcal{M}}$. We know such a node always exists because Y is in both $\mathbf{T}_{\mathcal{G}}$ and $\mathbf{T}_{\mathcal{M}}$. Let $\mathcal{H} \triangleq \mathcal{G}[\mathsf{An}(Y)_{\mathcal{G}}]$ and $\mathcal{N} \triangleq \mathcal{M}[\mathsf{An}(Y)_{\mathcal{M}}]$. Since \mathcal{M} and \mathcal{G} share the same skeleton and the same ancestral relations among vertices, it follows that $\mathsf{An}(Y)_{\mathcal{M}} = \mathsf{An}(Y)_{\mathcal{G}}$, implying $\mathbf{V}(\mathcal{H}) = \mathbf{V}(\mathcal{N})$.

(① If $W \in PC(T)_{\mathcal{N}}$, then $W \in \mathbf{T}_{\mathcal{G}}$). Suppose that another node W is in the same pc-component of T in \mathcal{N} , i.e., $W \in PC(T)_{\mathcal{N}}$. This implies that there exists a path between T and W in \mathcal{N} such that (i) all non-endpoint nodes along the path are colliders, and (ii) none of the edges are visible.

For all directed edges $U \to V$ along this path, if there does not exist an edge $U \to Z (\neq V)$ in \mathcal{N} , a bidirected edge $U \leftrightarrow V$ is added to \mathcal{G} in Step 3. Consequently, T and W are in the same c-component in \mathcal{H} .

Otherwise, if there is some directed edge $U \to V$ along the path for which there exists $U \to Z (\neq V)$, then from Step 4, we know that one of these outgoing edges from U will have a corresponding bidirected edge in $\mathcal H$ which adds U to $\mathbf T_{\mathcal G}$. Since MUCT is closed under descendants, all descendants of U are also included in MUCT as well.

This logic applies along the entire path, ensuring that $T \in \mathbf{T}_{\mathcal{G}} \Rightarrow W \in \mathbf{T}_{\mathcal{G}}$.

- (② If $W \in De(T)_{\mathcal{N}}$, then $W \in \mathbf{T}_{\mathcal{G}}$). Now, suppose that W is a descendant of T in \mathcal{N} , i.e., $W \in De(T)_{\mathcal{N}}$. Then W is a descendant of T in \mathcal{H} as well, and so we have $T \in \mathbf{T}_{\mathcal{G}} \Rightarrow W \in \mathbf{T}_{\mathcal{G}}$.
- (① + ② implies $T_{\mathcal{M}} \subseteq T_{\mathcal{G}}$). Thus, we have shown that any node which can be shown to be in $T_{\mathcal{M}}$ can also be shown to be in $T_{\mathcal{G}}$, and therefore $T_{\mathcal{M}} \subseteq T_{\mathcal{G}}$.

It can be applied to show that $\mathsf{MUCT}(\mathcal{M},Y,\mathbf{X})\subseteq \mathsf{MUCT}(\mathcal{G}_{\overline{\mathbf{X}}},Y)$, as we can operate over $\mathcal{M}\setminus\mathbf{X}$ and $\mathcal{G}\setminus\mathbf{X}$ instead of \mathcal{M} and \mathcal{G} , respectively. Thus, we have that $T\in\mathsf{MUCT}(\mathcal{M},Y,\mathbf{X})$ implies $T\in\mathsf{MUCT}(\mathcal{G}_{\overline{\mathbf{X}}},Y)$. Therefore, we can conclude that $\mathsf{IB}(\mathcal{G}_{\overline{\mathbf{X}}},Y)=\mathbf{X}$ holds. \square

Proposition 6. Let \mathcal{P} be a PAG over \mathbf{V} . A set $\mathbf{X} \subseteq \mathbf{V} \setminus \{Y\}$ is a POMIS relative to $[\![\mathcal{P},Y]\!]$ if and only if there exists a MAG \mathcal{M} conforming to \mathcal{P} such that \mathbf{X} is a POMIS relative to $[\![\mathcal{M},Y]\!]$.

Proof. (If) Suppose **X** is a POMIS relative to $[\![\mathcal{M},Y]\!]$ for some \mathcal{M} conforming to \mathcal{P} . Then there exists an SCM \mathcal{S} conforming to \mathcal{M} such that $\mu_{\mathbf{x}^*} > \forall_{\mathbf{W} \in \mathbb{D}_{\mathcal{M},Y} \setminus \{\mathbf{X}\}} \mu_{\mathbf{w}^*}$. Since any SCM conforming to \mathcal{M} also conforms to \mathcal{P} , the SCM also conforms to \mathcal{P} , and thus **X** is a POMIS relative to $[\![\mathcal{P},Y]\!]$.

(**Only if**) Let X be a POMIS relative to $[\![\mathcal{P},Y]\!]$. Then there exists an SCM \mathcal{S} conforming to \mathcal{P} such that $\mu_{\mathbf{x}^*} > \forall_{\mathbf{W} \in \mathbb{D}_{\mathcal{P},Y} \setminus \{\mathbf{X}\}} \mu_{\mathbf{w}^*}$. Let \mathcal{G} be the causal diagram associated with the SCM \mathcal{S} . Then, there exists a MAG \mathcal{M} representing \mathcal{G} that corresponds to \mathcal{P} with \mathbf{X} as a POMIS relative to $[\![\mathcal{M},Y]\!]$, since $\mathbb{P}_{\mathcal{P},Y} \subseteq \mathbb{D}_{\mathcal{P},Y}$. This concludes the proof for this direction.

Proposition 7. Let $Q_{\mathbf{X}}$ be a PMG representing MAGs where \mathbf{X} is a POMIS with respect to Y. Then, the following properties hold in $Q_{\mathbf{X}}$, for every $X \in \mathbf{X}$:

- 1. Every uncovered proper possibly-directed path from X to Y relative to \mathbf{X} ends with an arrowhead (>).
- 2. If X is adjacent to Y, then the edge between X and Y is a directed edge $(X \to Y)$.

Proof. We will show that the conditions are necessary for X to be an MIS in the MAGs, which implies that they are also necessary for X to be a POMIS.

(**First condition**). For the sake of contradiction, suppose that there exists an uncovered path ending with a tail mark at Y in a MAG $\mathcal{M} \in [\mathcal{Q}_{\mathbf{X}}]$. This implies the path must take the form $X \leftarrow \cdots \leftarrow Y$ in \mathcal{M} . Since \mathbf{X} is an MIS relative to $[\![\mathcal{M},Y]\!]$, there exists a directed path from X to Y in \mathcal{M} , which would introduce a directed cycle, leading to a contradiction.

(Second condition). We will first show X * - *Y forms $X * \to Y$ in $\mathcal{Q}_{\mathbf{X}}$, and then demonstrate that it must be $X \to Y$ by proving that $X \leftrightarrow Y$ leads to a contradiction. For the sake of contradiction, assume that there exists $X \leftarrow Y$ in a MAG $\mathcal{M} \in [\mathcal{Q}_{\mathbf{X}}]$. In \mathcal{M} , any directed path from X to Y would violate the ancestral property, resulting in a contradiction. Similarly, assume that there exists $X \leftrightarrow Y$ in a MAG $\mathcal{M} \in [\mathcal{Q}_{\mathbf{X}}]$. This configuration would also violate the ancestral property by introducing an almost directed cycle, which leads to a contradiction.

Proposition 8. For every MAG $\mathcal{M} \in [\mathcal{Q}_{\mathbf{X}}]$, if \mathbf{X} is a POMIS relative to $[\![\mathcal{M}, Y]\!]$, then there exists a PMG $\mathcal{Q}^i_{\mathbf{X}}$ representing \mathcal{M} such that the following conditions are satisfied:

1. Every circle mark around $\mathbf{X} \cup \{Y\}$ in $\mathcal{Q}_{\mathbf{X}}$ is oriented as either a tail (-) or an arrowhead (>) in $\mathcal{Q}_{\mathbf{X}}^i$ according to valid local transformations.

- 2. Every $X \in \mathbf{X}$ is an ancestor of Y in $\mathcal{Q}_{\mathbf{X}}^i$.
- 3. $Q_{\mathbf{X}}^{i}$ is closed under orientation rules.

Proof. The first and third conditions are satisfied by the soundness and completeness of valid local transformations (Thm. 8). Furthermore, since X is a POMIS with respect to $[\![\mathcal{P},Y]\!]$ (thus, X is a DMIS), the second condition is also satisfied (see Lem. 22), which completes the proof.

Theorem 4 (Characterization of POMIS for PAGs). A set $X \subseteq V \setminus \{Y\}$ is a POMIS relative to [P, Y] if and only if there exists \mathcal{Q}_X^i satisfying Props. 7 and 8 such that $\mathsf{IB}(\mathcal{Q}_X^i, Y, X) = X$.

Proof. This follows from the result of Thm. 5.

Theorem 5 (Soundness and completeness). *The algorithm IsPOMIS* (Alg. 1) returns True if and only if there exists a MAG \mathcal{M} conforming to \mathcal{P} such that \mathbf{X} is a POMIS relative to $[\![\mathcal{M},Y]\!]$.

Proof. (IsPOMIS returns True $\Rightarrow \exists \mathcal{G}$ such that $\mathsf{IB}(\mathcal{M},Y,\mathbf{X})=\mathbf{X}$). Suppose that IsPOMIS returns True. Then, there is a PMG $\mathcal{Q}^i_{\mathbf{X}}$ satisfying $\mathsf{IB}(\mathcal{Q}^i_{\mathbf{X}},Y,\mathbf{X})=\mathbf{X}$. We will demonstrate that there exists a MAG $\mathcal{M} \in [\mathcal{Q}^i_{\mathbf{X}}]$ such that $\mathsf{IB}(\mathcal{M},Y,\mathbf{X})=\mathbf{X}$ by constructing such a MAG. To do so, consider the following lemma:

Lemma 35. Let $\mathcal{Q}_{\mathbf{X}}^{i}$ be a PMG in Alg. 1. Let \mathcal{M} be the graph resulting from the following procedure applied to $\mathcal{Q}_{\mathbf{X}}^{i}$.

- Step 1. Orient partial directed edges ($\diamond \rightarrow$) as directed edges (\rightarrow).
- Step 2. Consider $A * \to B$ in $\mathcal{Q}_{\mathbf{X}}^{i}$. Let $\mathbf{T}_{\mathcal{M}}^{\mathbf{X}} \triangleq \mathsf{MUCT}(\mathcal{M}, Y, \mathbf{X})$. If B is contained in $\mathbf{T}_{\mathcal{M}}^{\mathbf{X}}$, orient the circle component including A as a DAG where each circle edge involving A in $\mathcal{Q}_{\mathbf{X}}^{i}$ corresponds to a directed edge outgoing from A in \mathcal{M} (i.e., $A \circ \multimap V$ corresponds to $A \to V$).

This step is repeated with the updated $\mathbf{T}_{\mathcal{M}}^{\mathbf{X}} \leftarrow \mathsf{MUCT}(\mathcal{M}, Y, \mathbf{X})$ as long as \mathcal{M} remains unchanged.

Step 3. Orient remaining circle component into a DAG with no unshielded colliders.

Then, the resulting graph \mathcal{M} is a MAG conforming to $\mathcal{Q}_{\mathbf{X}}^i$.

Proof. The construction follows Lems 6 and 12, and the fact that every circle component can be oriented independently by Lem. 31.

Now, we will show that the MAG \mathcal{M} constructed according to Lem. 35 satisfies $\mathsf{IB}(\mathcal{M},Y,\mathbf{X})=\mathbf{X}$. Let X be any node in $\mathsf{IB}(\mathcal{Q}_{\mathbf{X}}^i,Y,\mathbf{X})$. Then, X is a parent of some $T_X\in\mathsf{MUCT}(\mathcal{Q}_{\mathbf{X}}^i,Y,\mathbf{X})$ in $\mathcal{Q}_{\mathbf{X}}^i$. By Lem. 24, there exists an uncovered possibly-directed path $T_X\circ -\circ \cdots \circ -\circ T_X^* \ ^?\to \cdot \to \cdots \to Y$. Due to the balanced property in Lem. 31 a path $X\to T_X^* \ ^?\to \cdot \to \cdots \to Y$ exists in $\mathcal{Q}_{\mathbf{X}}^i$, which corresponds to $X\to T_X^*\to \cdots \to Y$ in \mathcal{M} by construction (see Step 1). Therefore, we have that for any nodes $X\in\mathbf{X}$, X and T_X^* are included in $\mathsf{An}(Y)_{\mathcal{M}}$. Our goal is to show that $T_X^*\in\mathsf{MUCT}(\mathcal{M},Y,\mathbf{X})$ since this means $X\in\mathsf{IB}(\mathcal{M},Y,\mathbf{X})$.

For convenience, we denote $\mathbf{T}_{\mathcal{M}} = \mathsf{MUCT}(\mathcal{M}, Y, \mathbf{X})$ and $\mathbf{T}_{\mathcal{Q}_{\mathbf{X}}^i} = \mathsf{MUCT}(\mathcal{Q}_{\mathbf{X}}^i, Y, \mathbf{X})$. Let $\mathcal{N} \triangleq \mathcal{M}[\mathsf{An}(Y)_{\mathcal{M}}]$ and $\mathcal{H} \triangleq \mathcal{Q}_{\mathbf{X}}^i[\mathsf{PossAn}(Y)_{\mathcal{Q}_{\mathbf{X}}^i}]$. Suppose that T is a node such that $T \in \mathbf{T}_{\mathcal{Q}_{\mathbf{X}}^i} \cap \mathsf{An}(Y)_{\mathcal{M}}$ and $T \in \mathbf{T}_{\mathcal{M}}$. We know such a node exists, as Y is in both $\mathbf{T}_{\mathcal{M}}$ and $\mathbf{T}_{\mathcal{Q}_{\mathbf{X}}^i} \cap \mathsf{An}(Y)_{\mathcal{M}}$.

(① If $W \in PC(T)_{\mathcal{H}[An(Y)_{\mathcal{M}}]}$, then $W \in \mathbf{T}_{\mathcal{M}}$). Suppose that another node W is in the same pc-component of T in $\mathcal{H}[An(Y)_{\mathcal{M}}]$. This implies that there exists a path between T and W such that (i) all non-endpoint nodes along the path are colliders, and (ii) none of the edges are visible, i.e., $T*\to \cdots \leftrightarrow \cdots \leftrightarrow \cdots \leftrightarrow W$ in $\mathcal{H}[An(Y)_{\mathcal{M}}]$.

For all edges U
ightharpoonup V along this path, the edges correspond to directed edges $U \to V$ in \mathcal{N} . If there are no circle edges with U in \mathcal{H} , the edges remain invisible in \mathcal{N} since orienting a tail mark alone does not introduce any visible edges.

Otherwise, if there are any circle edges $U \circ \neg \circ Z$ in \mathcal{H} that correspond to $U \to Z$ in \mathcal{N} , no additional visible edges are introduced. When the edges correspond to $U \leftarrow Z$ in \mathcal{N} , U would already have been included in $T_{\mathcal{M}}$, which in turn ensures that V be included in $T_{\mathcal{M}}$.

(② If $W \in \mathsf{PossDe}(T)_{\mathcal{H}[\mathsf{An}(Y)_{\mathcal{M}}]}$, then $W \in \mathbf{T}_{\mathcal{M}}$). This means that there exists an uncovered possibly-directed path from T to W in $\mathcal{H}[\mathsf{An}(Y)_{\mathcal{M}}]$ by Lem. 28. According to our construction, there is a node $S \in \mathbf{T}_{\mathcal{M}}$ (it could be T) in the same bucket as T and W such that all nodes in the bucket are descendants of S in \mathcal{M} . Since $W \in \mathsf{De}(S)_{\mathcal{M}}$ and $S \in \mathbf{T}_{\mathcal{M}}$, we have $W \in \mathbf{T}_{\mathcal{M}}$.

(① + ②). Thus, we have shown that any node in $\mathbf{T}_{\mathcal{Q}_{\mathbf{X}}^i} \cap \operatorname{An}(Y)_{\mathcal{M}}$ can also be shown to be in $\mathbf{T}_{\mathcal{M}}$, and therefore we can get $T_X^* \in \mathbf{T}_{\mathcal{M}}$.

(IsPOMIS returns False $\Rightarrow \#\mathcal{M}$ such that $\mathsf{IB}(\mathcal{M},Y,\mathbf{X})=\mathbf{X}$). Suppose that \mathbf{X} is a POMIS relative to $[\![\mathcal{M},Y]\!]$. Then, we have $\mathbf{X}=\mathsf{IB}(\mathcal{M},Y,\mathbf{X})$. Let $\mathcal{Q}_{\mathbf{X}}^i$ be a PMG representing \mathcal{M} . Moreover, we have that $\mathsf{An}(Y)_{\mathcal{M}}\subseteq\mathsf{PossAn}(Y)_{\mathcal{Q}_{\mathbf{X}}^i}$ holds by Lem. 28.

Let X be any variable in $\mathsf{IB}(\mathcal{M},Y,\mathbf{X})$. Then, X is a parent of some $T_X\in\mathsf{MUCT}(\mathcal{M},Y,\mathbf{X})$ in \mathcal{M} . Furthermore, this appears in $\mathcal{Q}^i_{\mathbf{X}}$ by the construction of $\mathsf{IsPOMIS}$ in Alg. 1 (outgoing edges from X are determined in $\mathcal{Q}^i_{\mathbf{X}}$). By Lem. 24, there exists an uncovered possibly-directed path $T_X \circ - \circ \cdots T_X' \circ - \cdots \to Y$ in $\mathcal{Q}^i_{\mathbf{X}}$. Due to Lems 20 and 31, the path $X \to T_X^* \to \cdots \to Y$ exists in $\mathcal{Q}^i_{\mathbf{X}}$. Now we will show that $T_X^* \in \mathsf{MUCT}(\mathcal{Q}^i_{\mathbf{X}},Y,\mathbf{X})$ since this implies $X \in \mathsf{IB}(\mathcal{Q}^i_{\mathbf{X}},Y,\mathbf{X})$.

Let $\mathbf{T}_{\mathcal{M}} \triangleq \mathsf{MUCT}(\mathcal{M},Y,\mathbf{X})$ and $\mathbf{T}_{\mathcal{Q}_{\mathbf{X}}^{i}} \triangleq \mathsf{MUCT}(\mathcal{Q}_{\mathbf{X}}^{i},Y,\mathbf{X})$. Let $\mathcal{N} \triangleq \mathcal{M}[\mathsf{An}(Y)_{\mathcal{M}}]$ and $\mathcal{H} \triangleq \mathcal{Q}_{\mathbf{X}}^{i}[\mathsf{PossAn}(Y)_{\mathcal{Q}_{\mathbf{X}}^{i}}]$. Suppose that T is a node satisfying $T \in \mathbf{T}_{\mathcal{Q}_{\mathbf{X}}^{i}} \cap \mathsf{An}(Y)_{\mathcal{M}}$ and $T \in \mathbf{T}_{\mathcal{M}}$. We know such a node exists since Y is in both $\mathbf{T}_{\mathcal{M}}$ and $\mathbf{T}_{\mathcal{Q}_{\mathbf{X}}^{i}} \cap \mathsf{An}(Y)_{\mathcal{M}}$.

(If $W \in \mathbf{T}_{\mathcal{M}}$, then $W \in \mathbf{T}_{\mathcal{Q}_{\mathbf{X}}^i} \cap \operatorname{An}(Y)_{\mathcal{M}}$). Since any invisible edges in \mathcal{M} correspond to invisible ones in $\mathcal{Q}_{\mathbf{X}}^i$, we have $W \in \operatorname{PC}_{\mathcal{N}}(T)$ implies $W \in \mathbf{T}_{\mathcal{Q}_{\mathbf{X}}^i} \cap \operatorname{An}(Y)_{\mathcal{M}}$ according to Lem. 30. Furthermore, we know that $W \in \operatorname{De}(T)_{\mathcal{N}}$ implies $W \in \operatorname{PossDe}(T)_{\mathcal{H}[\operatorname{An}(Y)_{\mathcal{M}}]}$ by Lem. 28. Therefore, we get that $W \in \mathbf{T}_{\mathcal{Q}_{\mathbf{X}}^i} \cap \operatorname{An}(Y)_{\mathcal{M}}$. Thus, we have shown that any node in $\mathbf{T}_{\mathcal{M}}$ can also be shown to be in $\mathbf{T}_{\mathcal{Q}_{\mathbf{X}}^i} \cap \operatorname{An}(Y)_{\mathcal{M}}$, and therefore $T_X^* \in \mathbf{T}_{\mathcal{Q}_{\mathbf{X}}^i}$.

The remaining task is to prove that $\mathbf{W} \triangleq \mathsf{IB}(\mathcal{Q}_{\mathbf{X}}^i, Y, \mathbf{X}) \setminus \mathsf{IB}(\mathcal{M}, Y, \mathbf{X})$ is empty. For the sake of contradiction, consider any vertex $W \in \mathbf{W}$. Then, there exists a node $T_W \in \mathbf{T}_{\mathcal{Q}_{\mathbf{X}}^i}$ where $W \in \mathsf{Pa}(T_W)_{\mathcal{Q}_{\mathbf{X}}^i}$. If $W \to T_W$ is invisible in $\mathcal{Q}_{\mathbf{X}}^i$, then W is included in $\mathbf{T}_{\mathcal{Q}_{\mathbf{X}}^i}$, leading to a contradiction for $W \in \mathsf{IB}(\mathcal{Q}_{\mathbf{X}}^i, Y, \mathbf{X})$. If $W \to T_W$ is visible in $\mathcal{Q}_{\mathbf{X}}^i$, it is also visible in \mathcal{M} , and we can find a visible edge $W \to T_W^*$ satisfying $W \to T_W^* \to \cdots \to Y$ by Lems 24 and 27. This implies $W \in \mathsf{IB}(\mathcal{M}, Y, \mathbf{X})$, resulting in a contradiction. Therefore, we conclude the proof of the completeness of IsPOMIS.

Broader Impact Statement

This work addresses a structured causal bandit framework that leverages causal knowledge from a Markov equivalence class represented by a PAG. This approach has potential applications in practical settings such as personalized healthcare, adaptive education, and resource-constrained recommendation systems, where a decision-maker aims to make optimal decisions without assuming causal sufficiency (i.e., the absence of unobserved variables), an assumption that is often unrealistic in practice. Therefore, this study takes a step toward the practical application of the framework. However, improper specification of causal structures may lead to misleading conclusions and biased decisions; thus, careful validation and domain-specific causal modeling are essential prior to deployment in high-stakes environments.

NeurIPS Paper Checklist

1. Claims

Question: Do the main claims made in the abstract and introduction accurately reflect the paper's contributions and scope?

Answer: [Yes]

Justification: The main claims are clearly stated in the abstract. The contributions are explicitly stated in the introduction.

Guidelines:

- The answer NA means that the abstract and introduction do not include the claims made in the paper.
- The abstract and/or introduction should clearly state the claims made, including the
 contributions made in the paper and important assumptions and limitations. A No or
 NA answer to this question will not be perceived well by the reviewers.
- The claims made should match theoretical and experimental results, and reflect how much the results can be expected to generalize to other settings.
- It is fine to include aspirational goals as motivation as long as it is clear that these goals are not attained by the paper.

2. Limitations

Question: Does the paper discuss the limitations of the work performed by the authors?

Answer: [Yes]

Justification: The limitations are clearly stated in the "Limitations and Future works" section in the supplemental material (Appendix F).

- The answer NA means that the paper has no limitation while the answer No means that the paper has limitations, but those are not discussed in the paper.
- The authors are encouraged to create a separate "Limitations" section in their paper.
- The paper should point out any strong assumptions and how robust the results are to violations of these assumptions (e.g., independence assumptions, noiseless settings, model well-specification, asymptotic approximations only holding locally). The authors should reflect on how these assumptions might be violated in practice and what the implications would be.
- The authors should reflect on the scope of the claims made, e.g., if the approach was only tested on a few datasets or with a few runs. In general, empirical results often depend on implicit assumptions, which should be articulated.
- The authors should reflect on the factors that influence the performance of the approach. For example, a facial recognition algorithm may perform poorly when image resolution is low or images are taken in low lighting. Or a speech-to-text system might not be used reliably to provide closed captions for online lectures because it fails to handle technical jargon.

- The authors should discuss the computational efficiency of the proposed algorithms and how they scale with dataset size.
- If applicable, the authors should discuss possible limitations of their approach to address problems of privacy and fairness.
- While the authors might fear that complete honesty about limitations might be used by reviewers as grounds for rejection, a worse outcome might be that reviewers discover limitations that aren't acknowledged in the paper. The authors should use their best judgment and recognize that individual actions in favor of transparency play an important role in developing norms that preserve the integrity of the community. Reviewers will be specifically instructed to not penalize honesty concerning limitations.

3. Theory assumptions and proofs

Question: For each theoretical result, does the paper provide the full set of assumptions and a complete (and correct) proof?

Answer: [Yes]

Justification: Detailed proofs are provided in the "Proofs" section in the supplemental material (Appendix H).

Guidelines:

- The answer NA means that the paper does not include theoretical results.
- All the theorems, formulas, and proofs in the paper should be numbered and crossreferenced.
- All assumptions should be clearly stated or referenced in the statement of any theorems.
- The proofs can either appear in the main paper or the supplemental material, but if they appear in the supplemental material, the authors are encouraged to provide a short proof sketch to provide intuition.
- Inversely, any informal proof provided in the core of the paper should be complemented by formal proofs provided in appendix or supplemental material.
- Theorems and Lemmas that the proof relies upon should be properly referenced.

4. Experimental result reproducibility

Question: Does the paper fully disclose all the information needed to reproduce the main experimental results of the paper to the extent that it affects the main claims and/or conclusions of the paper (regardless of whether the code and data are provided or not)?

Answer: [Yes]

Justification: We clearly state the experimental settings and provide additional details in the "Experimental Details and Additional Results" section in the supplemental material (Appendix D).

- The answer NA means that the paper does not include experiments.
- If the paper includes experiments, a No answer to this question will not be perceived well by the reviewers: Making the paper reproducible is important, regardless of whether the code and data are provided or not.
- If the contribution is a dataset and/or model, the authors should describe the steps taken to make their results reproducible or verifiable.
- Depending on the contribution, reproducibility can be accomplished in various ways. For example, if the contribution is a novel architecture, describing the architecture fully might suffice, or if the contribution is a specific model and empirical evaluation, it may be necessary to either make it possible for others to replicate the model with the same dataset, or provide access to the model. In general, releasing code and data is often one good way to accomplish this, but reproducibility can also be provided via detailed instructions for how to replicate the results, access to a hosted model (e.g., in the case of a large language model), releasing of a model checkpoint, or other means that are appropriate to the research performed.

- While NeurIPS does not require releasing code, the conference does require all submissions to provide some reasonable avenue for reproducibility, which may depend on the nature of the contribution. For example
 - (a) If the contribution is primarily a new algorithm, the paper should make it clear how to reproduce that algorithm.
 - (b) If the contribution is primarily a new model architecture, the paper should describe the architecture clearly and fully.
 - (c) If the contribution is a new model (e.g., a large language model), then there should either be a way to access this model for reproducing the results or a way to reproduce the model (e.g., with an open-source dataset or instructions for how to construct the dataset).
 - (d) We recognize that reproducibility may be tricky in some cases, in which case authors are welcome to describe the particular way they provide for reproducibility. In the case of closed-source models, it may be that access to the model is limited in some way (e.g., to registered users), but it should be possible for other researchers to have some path to reproducing or verifying the results.

5. Open access to data and code

Question: Does the paper provide open access to the data and code, with sufficient instructions to faithfully reproduce the main experimental results, as described in supplemental material?

Answer: [Yes]

Justification: The provided code includes sufficient instructions to reproduce all of our results.

Guidelines:

- The answer NA means that paper does not include experiments requiring code.
- Please see the NeurIPS code and data submission guidelines (https://nips.cc/public/guides/CodeSubmissionPolicy) for more details.
- While we encourage the release of code and data, we understand that this might not be possible, so "No" is an acceptable answer. Papers cannot be rejected simply for not including code, unless this is central to the contribution (e.g., for a new open-source benchmark).
- The instructions should contain the exact command and environment needed to run to reproduce the results. See the NeurIPS code and data submission guidelines (https://nips.cc/public/guides/CodeSubmissionPolicy) for more details.
- The authors should provide instructions on data access and preparation, including how to access the raw data, preprocessed data, intermediate data, and generated data, etc.
- The authors should provide scripts to reproduce all experimental results for the new proposed method and baselines. If only a subset of experiments are reproducible, they should state which ones are omitted from the script and why.
- At submission time, to preserve anonymity, the authors should release anonymized versions (if applicable).
- Providing as much information as possible in supplemental material (appended to the paper) is recommended, but including URLs to data and code is permitted.

6. Experimental setting/details

Question: Does the paper specify all the training and test details (e.g., data splits, hyper-parameters, how they were chosen, type of optimizer, etc.) necessary to understand the results?

Answer: [Yes]

Justification: We clearly state the experimental settings and provide additional details in the "Experimental Details and Additional Results" section in the supplemental material (Appendix D).

Guidelines:

- The answer NA means that the paper does not include experiments.
- The experimental setting should be presented in the core of the paper to a level of detail that is necessary to appreciate the results and make sense of them.
- The full details can be provided either with the code, in appendix, or as supplemental
 material.

7. Experiment statistical significance

Question: Does the paper report error bars suitably and correctly defined or other appropriate information about the statistical significance of the experiments?

Answer: [Yes]

Justification: : Our experimental plot (Fig. 7 and Fig. 11) and table (Table 1) include standard deviations.

Guidelines:

- The answer NA means that the paper does not include experiments.
- The authors should answer "Yes" if the results are accompanied by error bars, confidence intervals, or statistical significance tests, at least for the experiments that support the main claims of the paper.
- The factors of variability that the error bars are capturing should be clearly stated (for example, train/test split, initialization, random drawing of some parameter, or overall run with given experimental conditions).
- The method for calculating the error bars should be explained (closed form formula, call to a library function, bootstrap, etc.)
- The assumptions made should be given (e.g., Normally distributed errors).
- It should be clear whether the error bar is the standard deviation or the standard error
 of the mean.
- It is OK to report 1-sigma error bars, but one should state it. The authors should preferably report a 2-sigma error bar than state that they have a 96% CI, if the hypothesis of Normality of errors is not verified.
- For asymmetric distributions, the authors should be careful not to show in tables or figures symmetric error bars that would yield results that are out of range (e.g. negative error rates).
- If error bars are reported in tables or plots, The authors should explain in the text how they were calculated and reference the corresponding figures or tables in the text.

8. Experiments compute resources

Question: For each experiment, does the paper provide sufficient information on the computer resources (type of compute workers, memory, time of execution) needed to reproduce the experiments?

Answer: [Yes]

Justification: We clearly state the computer resources in the "Experimental Details and Additional Results" section in the supplemental material (Appendix D).

Guidelines:

- The answer NA means that the paper does not include experiments.
- The paper should indicate the type of compute workers CPU or GPU, internal cluster, or cloud provider, including relevant memory and storage.
- The paper should provide the amount of compute required for each of the individual experimental runs as well as estimate the total compute.
- The paper should disclose whether the full research project required more compute than the experiments reported in the paper (e.g., preliminary or failed experiments that didn't make it into the paper).

9. Code of ethics

Question: Does the research conducted in the paper conform, in every respect, with the NeurIPS Code of Ethics https://neurips.cc/public/EthicsGuidelines?

Answer: [Yes]

Justification: We have reviewed the code of ethics.

Guidelines:

- The answer NA means that the authors have not reviewed the NeurIPS Code of Ethics.
- If the authors answer No, they should explain the special circumstances that require a deviation from the Code of Ethics.
- The authors should make sure to preserve anonymity (e.g., if there is a special consideration due to laws or regulations in their jurisdiction).

10. Broader impacts

Question: Does the paper discuss both potential positive societal impacts and negative societal impacts of the work performed?

Answer: [Yes]

Justification: We clearly state the broader impacts of our work.

Guidelines:

- The answer NA means that there is no societal impact of the work performed.
- If the authors answer NA or No, they should explain why their work has no societal impact or why the paper does not address societal impact.
- Examples of negative societal impacts include potential malicious or unintended uses (e.g., disinformation, generating fake profiles, surveillance), fairness considerations (e.g., deployment of technologies that could make decisions that unfairly impact specific groups), privacy considerations, and security considerations.
- The conference expects that many papers will be foundational research and not tied to particular applications, let alone deployments. However, if there is a direct path to any negative applications, the authors should point it out. For example, it is legitimate to point out that an improvement in the quality of generative models could be used to generate deepfakes for disinformation. On the other hand, it is not needed to point out that a generic algorithm for optimizing neural networks could enable people to train models that generate Deepfakes faster.
- The authors should consider possible harms that could arise when the technology is being used as intended and functioning correctly, harms that could arise when the technology is being used as intended but gives incorrect results, and harms following from (intentional or unintentional) misuse of the technology.
- If there are negative societal impacts, the authors could also discuss possible mitigation strategies (e.g., gated release of models, providing defenses in addition to attacks, mechanisms for monitoring misuse, mechanisms to monitor how a system learns from feedback over time, improving the efficiency and accessibility of ML).

11. Safeguards

Question: Does the paper describe safeguards that have been put in place for responsible release of data or models that have a high risk for misuse (e.g., pretrained language models, image generators, or scraped datasets)?

Answer: [NA]

Justification: This paper mainly deals with theoretical results that are unlikely misused.

- The answer NA means that the paper poses no such risks.
- Released models that have a high risk for misuse or dual-use should be released with
 necessary safeguards to allow for controlled use of the model, for example by requiring
 that users adhere to usage guidelines or restrictions to access the model or implementing
 safety filters.

- Datasets that have been scraped from the Internet could pose safety risks. The authors should describe how they avoided releasing unsafe images.
- We recognize that providing effective safeguards is challenging, and many papers do
 not require this, but we encourage authors to take this into account and make a best
 faith effort.

12. Licenses for existing assets

Question: Are the creators or original owners of assets (e.g., code, data, models), used in the paper, properly credited and are the license and terms of use explicitly mentioned and properly respected?

Answer: [Yes]

Justification: All related and used results are cited properly.

Guidelines:

- The answer NA means that the paper does not use existing assets.
- The authors should cite the original paper that produced the code package or dataset.
- The authors should state which version of the asset is used and, if possible, include a URL.
- The name of the license (e.g., CC-BY 4.0) should be included for each asset.
- For scraped data from a particular source (e.g., website), the copyright and terms of service of that source should be provided.
- If assets are released, the license, copyright information, and terms of use in the package should be provided. For popular datasets, paperswithcode.com/datasets has curated licenses for some datasets. Their licensing guide can help determine the license of a dataset.
- For existing datasets that are re-packaged, both the original license and the license of the derived asset (if it has changed) should be provided.
- If this information is not available online, the authors are encouraged to reach out to the asset's creators.

13. New assets

Question: Are new assets introduced in the paper well documented and is the documentation provided alongside the assets?

Answer: [NA]

Justification: The code is provided with annotated descriptions.

Guidelines:

- The answer NA means that the paper does not release new assets.
- Researchers should communicate the details of the dataset/code/model as part of their submissions via structured templates. This includes details about training, license, limitations, etc.
- The paper should discuss whether and how consent was obtained from people whose asset is used.
- At submission time, remember to anonymize your assets (if applicable). You can either create an anonymized URL or include an anonymized zip file.

14. Crowdsourcing and research with human subjects

Question: For crowdsourcing experiments and research with human subjects, does the paper include the full text of instructions given to participants and screenshots, if applicable, as well as details about compensation (if any)?

Answer: [NA]

Justification: Our work does not involve human subjects.

- The answer NA means that the paper does not involve crowdsourcing nor research with human subjects.
- Including this information in the supplemental material is fine, but if the main contribution of the paper involves human subjects, then as much detail as possible should be included in the main paper.
- According to the NeurIPS Code of Ethics, workers involved in data collection, curation, or other labor should be paid at least the minimum wage in the country of the data collector.

15. Institutional review board (IRB) approvals or equivalent for research with human subjects

Question: Does the paper describe potential risks incurred by study participants, whether such risks were disclosed to the subjects, and whether Institutional Review Board (IRB) approvals (or an equivalent approval/review based on the requirements of your country or institution) were obtained?

Answer: [NA]

Justification: Our work does not involve crowdsourcing or research with human subjects.

Guidelines:

- The answer NA means that the paper does not involve crowdsourcing nor research with human subjects.
- Depending on the country in which research is conducted, IRB approval (or equivalent) may be required for any human subjects research. If you obtained IRB approval, you should clearly state this in the paper.
- We recognize that the procedures for this may vary significantly between institutions and locations, and we expect authors to adhere to the NeurIPS Code of Ethics and the guidelines for their institution.
- For initial submissions, do not include any information that would break anonymity (if applicable), such as the institution conducting the review.

16. Declaration of LLM usage

Question: Does the paper describe the usage of LLMs if it is an important, original, or non-standard component of the core methods in this research? Note that if the LLM is used only for writing, editing, or formatting purposes and does not impact the core methodology, scientific rigorousness, or originality of the research, declaration is not required.

Answer: [NA]

Justification: Our work does not involve using LLMs.

- The answer NA means that the core method development in this research does not involve LLMs as any important, original, or non-standard components.
- Please refer to our LLM policy (https://neurips.cc/Conferences/2025/LLM) for what should or should not be described.